Characterization of the Role of Cyclin D1 and Ral GTPases in the Proliferation and Dissemination of Glioblastoma

Tània Cemeli Sánchez

Universitat de Lleida

TESI DOCTORAL

Characterization of the Role of Cyclin D1 and Ral GTPases in the Proliferation and Dissemination of Glioblastoma

Tània Cemeli Sánchez

Memòria presentada per optar al grau de Doctor per la Universitat de Lleida

Programa de Doctorat en Salut

Director/a

Dr. Eloi Garí Marsol

Dr. Francisco Ferrezuelo Muñoz

Tutor/a

Dr. Eloi Garí Marsol

2019

INDEX

INDEX

ABBREVIATIONS

Aa – Amino acid

ATP – Adenosine TriPhosphate

BrdU – Bromodeoxyuridine

BSA – Bovine Serum Albumin

CAAX – Farnesylation site of K-RAS protein

Ccnd1 – Cyclin D1

CDK – Cyclin Dependent Kinase

CEEA – Ethics Committee on Animal Experimentation

CEI – Ethical Committee

CKi – CDK inhibitor

CMV – Citomegalovirus

CNS – Central Nervous System

CSCs – Cancer Stem Cells

DMEM – Dulbecco's modified Eagle's Medium

DMSO – Dimethyl Sulfoxide

DTT – Dithiothreitol

ECM – ExtraCellular Matrix

EDTA – Ethylene diaminetetraacetic acid

EGF – human Epidermal Growth Factor

EGFR – human Epidermal Growth Factor Receptor

EMT – Epithelial Mesenchymal Transition

ERK – Extracellular signal-Regulated Kinase

FA – Focal Adhesion

FAK – Focal Adhesion Kinase

FBS – Fetal Bovine Serum

FDA – Food and Drug Administration

FGFR – Fibroblast Growth Factor Receptor

Fluc – Firefly Luciferase Gene

GAP – GTPase Activating Protein

GBM – Glioblastoma

GDP – Guanosine Diphosphate

GFP – Green Fluorescent Protein

GSCs – Glioblastoma Stem Cells

GSK-3β – Glycogen Synthase Kinase 3 beta

GTP – Guanine TriPhosphate

H&E – Hematoxylin & Eosin

HGF – Hepatocyte Growth Factor

HRP – Horseradish peroxidase

HUAV – Hospital Universitari Arnau de Vilanova

IDH1 – Isocitrate Dehydrogenase 1

IF – Immunofluorescence

IHC – ImmunoHistoChemistry

iMEF – Immortalized Mouse Embryonic Fibroblast

JNK – c-JUN n-terminal Kinase

kDa – Kilodalton

KO – Knock Out

KOD1 – Cyclin D1 Knock Out

MAPK – Mitogen-Activated Protein Kinase

MEF – Mouse Embryonic Fibroblast

Mm – *Mus* musculus

mTOR – Mammalian Target Of Rapamycin

MTT – 3-(4,5-Dimethylthiazol-2-yl)-2,5-Diphenyltetrazolium Bromide

NF1 – Neurofibromatosis type I

NFκB – Nuclear Factor Kappa-light-chain-enhancer of activated B cells

NSCs – Neural Stem Cells

p15 – CDKN2B

p16 – CDKN2A

p18 – CDKN2C

PAK1 – p21 Activated Kinase

PBD – p21 Binding Domain of PAK1

PBS – Phosphate Buffered Saline

PBST – Phosphate Buffered Saline with 0.1% Tween 20

PCR – Polymerase Chain Reaction

PDGFRα – Platelet Derived Growth Factor Receptor Alpha

PDGFα – Platelet Derived Growth Factor Alpha

PEI – Polyethilenimine

PFA – Paraformaldehyde

PI3K – Phosphatydil-Inositol 3-Kinase

PNS – Peripheral Nervous System

pRB – RetinoBlastoma

PTEN – Phosphatase and Tensin Homolog

PVDF – PolyViniliDene Fluoride

Pxn – Paxillin

Rac1 – Ras Related C3 botulinum toxin substrate 1

Ral A – Ras related protein A

Ral B – Ras related protein B

RB – Retinoblastoma

RB1 – Retinoblastoma gene

Rgl2 – Ral guanine nucleotide dissociation stimulator like 2

RhoA – Ras homolog gene family, member A

RNA – Ribonucleic Acid

Abbreviations

ROCK – Rho-associated protein kinase

RT – Room Temperature

RTK – Receptor Tyrosine Kinase

SCID – Severe Combined ImmunoDeficiency

SD – Standard Desviation

SDS – Sodium Dodecyl Sulfate

SDS-PAGE – Sodium Dodecyl Sulfate – Polyacrylamide gel electrophoresis

SEM – Standard Error of the Mean

shD1 – shRNA against cyclin D1

shRalA – shRNA against RalA

shRalB – shRNA against RalB

shRNA – Short Hairping RNA

TCGA – The Cancer Genome Atlas

TEMED – Tetramethylethylenediamine

TMA – Tissue MicroArray

Ubi – Ubiquitin

VEGF – Vascular Endothelial Growth Factor

WHO – World Health Organization

WT – Wildtype

YFP – Yellow Fluorescent Protein

ABSTRACTS

ENGLISH

Glioblastoma (GBM) is the most common tumor in the central nervous system in adults. This neoplasia shows an elevated capacity of evasion by migrating to surrounding tissues, which makes the complete surgical resection impossible. Therefore, new antitumor therapies are required for GBM treatment. In this context, the activity of the oncogenic complex Ccnd1-CDK4 and the small GTPases Ral A and Ral B are considered promising therapeutic targets. For instance, we have previously described that Ccnd1-CDK4 activates the small GTPases Rac1 and Ral which promotes carcinoma invasion. Thus, the main objectives of this thesis are to characterize the role of cyclin D1 and Ral GTPases in the proliferation and dissemination of glioblastomas, and to evaluate whether the inhibition of these targets is effective enough for GBM treatment.

Overall, this study resolves that Ccnd1 and Ral GTPases are indeed possible targets for GBM treatment. We show that Ccnd1-CDK4 promotes GBM invasion through the activation of the paxillin-Rac1 and Ral GTPases pathways. *In vivo*, the presence of cytoplasmic Ccnd1-CDK4 complexes induces GBM dissemination. The inhibition of Ccnd1-CDK4 activity hinders the invasion of GBM cells independently of the RB1 status. However, the inhibition of the complex only impedes the growth of RB1-positive GBM cells. Ccnd1-CDK4 inhibitor Palbociclib has already been approved by FDA as a treatment to reduce tumor proliferation in triple negative breast cancer. Conversely, our work proposes a new strategy in the use of Ccnd1-CDK4 inhibitors since the inhibition of Ccnd1-associated activity is particularly efficient in avoiding tumor cell dissemination, which is very relevant in tumors such as GBM. Concerning Ral GTPases, our results indicate that these small GTPases preserve the growth of GBM cells by avoiding a senescent response that may be stimulated by the excess of DNA damage in primary GBM cells (oncogenic stress). The inhibition of Ral GTPases promotes senescence, consequently arresting the proliferation of GBM cells. Unfortunately, there are no effective inhibitors available.

Finally, in this work, I have carried out the analysis of the kinoma induced by cytoplasmic expression of Ccnd1. These preliminary data added to the results obtained with primary GBM cells strongly suggest that cytoplasmic Ccnd1 plays a prominent role as cell signaling mediator. Furthermore, the understanding of this role of cytoplasmic Ccnd1 may be a powerful instrument for future cancer treatments.

CATALÀ

El glioblastoma (GBM) és el tumor més freqüent del sistema nerviós central en adults. Aquesta neoplàsia mostra una elevada capacitat d'evasió migrant cap als teixits circumdants que impossibilita la resecció quirúrgica completa. Per tant, es necessiten noves teràpies antitumorals per al tractament de GBM. En aquest context, l'activitat del complex oncogènic Ccnd1-CDK4 i de les GTPases Ral A i Ral B es consideren objectius terapèutics prometedors. Per exemple, hem descrit anteriorment que Ccnd1-CDK4 activa les GTPases Rac1 i Ral promovent la invasió dels carcinomes. Així, els principals objectius d'aquesta tesi són caracteritzar el paper de la ciclina D1 i les Ral GTPases en la proliferació i difusió dels glioblastomes, i avaluar si la inhibició d'aquestes proteïnes és suficient per al tractament de GBM.

En general, aquest estudi conclou que Ccnd1 i Ral GTPases poden ser possibles dianes per al tractament de GBM. Mostrem que Ccnd1-Cdk4 promou la invasió de GBM mitjançant l'activació de les vies de paxil·lina-Rac1 i Ral GTPases. *In vivo*, la presència de complexos citoplasmàtics Ccnd1-CDK4 indueix la difusió dels GBM. La inhibició de l'activitat Ccnd1-CDK4 dificulta la invasió de cèl·lules de GBM independentment de l'estat de RB1. No obstant això, la inhibició del complex només impedeix el creixement de cèl·lules de GBM RB1-positives. L'inhibidor de Ccnd1-CDK4, Palbociclib, ja ha estat aprovat per la FDA com a tractament per reduir la proliferació del càncer de mama triple negatiu. No obstant, el nostre treball proposa una nova estratègia en l'ús dels inhibidors de Ccnd1-CDK4, ja que la inhibició de l'activitat associada a Ccnd1 és especialment eficaç evitant la difusió de les cèl·lules tumorals, un punt molt rellevant en tumors com el GBM. Pel que fa a les Ral GTPases, els nostres resultats indiquen que aquestes GTPases conserven el creixement de cèl·lules GBM evitant una resposta senescent que pot ser estimulada per l'excés de danys a l'ADN present en les cèl·lules de GBM primàries (estrès oncogènic). La inhibició de Ral GTPases promou senescència, per la qual cosa frena la proliferació de cèl·lules de GBM. Malauradament, no hi ha inhibidors efectius disponibles.

Finalment, en aquest treball, vaig realitzar l'anàlisi del quinoma induït per l'expressió citoplasmàtica de Ccnd1. Les dades preliminars juntament amb els resultats obtinguts amb les cèl·lules primàries de GBM suggereixen que la Ccnd1 citoplasmàtica juga un paper destacat com a mediador de senyalització cel·lular. A més, el coneixement d'aquest rol associat a l'activitat citoplasmàtica de Ccnd1 pot ser un instrument poderós per a tractaments futurs contra el càncer.

CASTELLANO

El glioblastoma (GBM) es el tumor más común en el sistema nervioso central en adultos. Esta neoplasia muestra una capacidad elevada de evasión al migrar a los tejidos circundantes, lo que hace imposible la resección quirúrgica completa. Por este motivo se requieren nuevas terapias antitumorales para su tratamiento. En este contexto, la actividad del complejo oncogénico Ccnd1-CDK4 y las GTPasas Ral A y Ral B se consideran dianas terapéuticas prometedoras. Por ejemplo, anteriormente hemos descrito que Ccnd1-CDK4 activa las GTPasas Rac1 y Ral promoviendo la invasión de los carcinomas. Por lo tanto, los principales objetivos de esta tesis son caracterizar el papel de la ciclina D1 y las Ral GTPasas en la proliferación y diseminación de los GBM, y evaluar si la inhibición de estas proteínas es lo suficientemente efectiva para su tratamiento.

En general, este estudio caracteriza Ccnd1 y Ral GTPasas como posibles dianas para el tratamiento de GBM. Mostramos que Ccnd1-CDK4 promueve la invasión de GBM a través de la activación de las vías paxilina-Rac1 y Ral GTPasas. *In vivo*, la presencia de complejos citoplasmáticos Ccnd1-CDK4 induce la diseminación de los GBM. La inhibición de la actividad de Ccnd1-CDK4 dificulta la invasión de células de GBM independientemente del estado RB1. Sin embargo, la inhibición del complejo solo impide el crecimiento en células de GBM positivas para RB1. El inhibidor de Ccnd1-CDK4, Palbociclib, ya ha sido aprobado por la FDA como tratamiento para reducir la proliferación del cáncer de mama triple negativo. En cambio, nuestro trabajo propone una nueva estrategia para el uso de este inhibidor, ya que la inhibición de la actividad asociada a Ccnd1 es particularmente eficaz para evitar la diseminación de células tumorales, siendo muy relevante en tumores como el GBM. Con respecto a las Ral GTPasas, nuestros resultados indican que preservan el crecimiento de las células GBM al evitar una respuesta senescente que puede ser estimulada por el exceso de daño en el ADN presente en las células primarias de GBM (estrés oncogénico). La inhibición de las Ral GTPasas promueve senescencia y, en consecuencia, detiene la proliferación en las células GBM. Desafortunadamente, no hay inhibidores efectivos disponibles.

Finalmente, en este trabajo, he realizado el análisis del quinoma inducido por la expresión citoplasmática de Ccnd1. Los datos preliminares, junto con los resultados obtenidos con las células de GBM primarias, sugieren de manera clara que la Ccnd1 citoplasmática juega un papel prominente como mediador de señalización celular. Además, el conocimiento de este papel asociado con la actividad citoplasmática de Ccnd1 puede ser un poderoso instrumento para futuros tratamientos contra el cáncer.

INTRODUCTION

1 - ASTROCYTIC TUMORS

Cancer is a ubiquitous disease in human population that can be distinguished from a benign tumor by several characteristics. On the one hand, benign tumors are similar to the origin tissue; they are well differentiated, conserve original cell functions, grow slowly, and are circumscribed or encapsulated at the place of origin. On the other hand, malignant tumors have an atypical structure, can be completely dedifferentiated, grow quickly, contain cells with new functions, are not encapsulated, invade healthy surrounding tissue and can metastasize. Loss of differentiation (anaplasia) is a malignant characteristic whereby cells return to a primitive state, and it is associated with shape and size alterations (pleomorphism), such as change in nuclear shape, mitosis increase and loss of polarity, among others (Kumar, Abbas, Fausto 2010).

Cancer occurs after cells accumulate a number of somatic mutations in proto-oncogenes or tumor suppressor genes, which are generally involved in proliferation, apoptosis and other cellular processes. Oncogenes are over-expressed or mutated versions of proto-oncogenes that work autonomously, without dependence on external signals. They have multiple roles, but all participate in signaling pathways that lead to proliferation. They usually code for growth factors, growth factor receptors, signal transducers, transcription factors or cell cycle components. Tumor suppressor genes (p53 and pRB among others) are inhibitors of cell proliferation; they are part of a network of checkpoints that prevent uncontrolled growth, also involved in cell differentiation, apoptosis and DNA damage repair (Kumar, Abbas, Fausto 2010).

Over the years, a good deal of mutated genes in cancer has been discovered. These genes are involved in 10 essential physiological hallmarks of cancer that promote cellular transformation and the consequent progression of the tumor (Figure 1) (Hanahan and Weinberg 2011):

Sustaining proliferative signaling: tumors have the ability to proliferate in the absence of external stimuli as a consequence of the oncogene activation.

Evading growth suppressors: tumors do not respond to proliferation inhibitors as a consequence of tumor suppressor genes inactivation.

Avoiding immune destruction: in normal conditions the immune system recognizes and eliminates cells showing abnormal antigens. Tumor cells contain mutations that allow them to avoid the immune response.

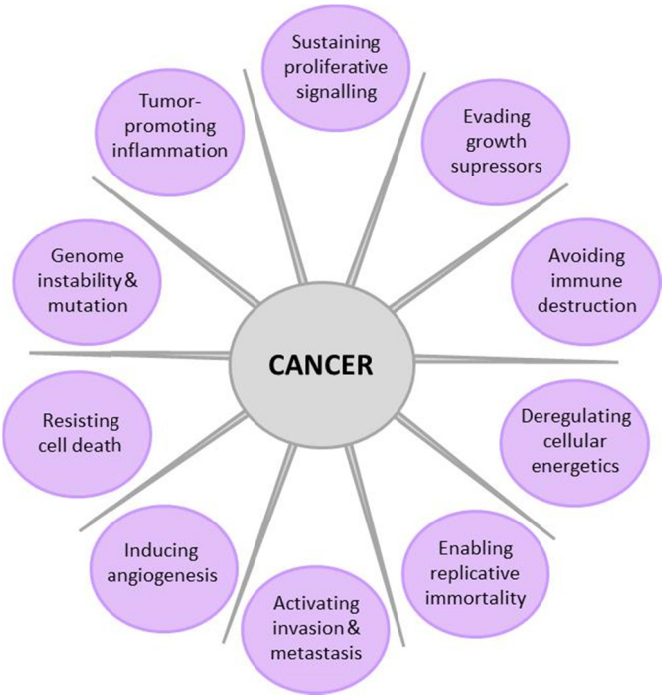

Figure 1. *The 10 hallmarks of cancer. Adapted from* (Hanahan and Weinberg 2011).

Deregulating cellular energetics: tumors are capable of performing "aerobic glycolysis" (Warburg effect), which requires a large amount of glucose entering the glycolytic pathway to give rise to ATP and lactate (lactic acid fermentation). Although this process is much less efficient that mitochondrial oxidative phosphorylation in generating cellular energy (ATP) it allows the production of intermediates for the synthesis of macromolecules and organelles necessary for rapid cell growth.

Enabling replicative immortality: tumors do not have restrictions in proliferation capacity; it is a property that allows them to avoid senescence.

Activating invasion and metastasis: tumor dissemination (metastasis) is the main cause of morbidity and mortality in most cancer patients.

Inducing angiogenesis: tumor cells are not able to grow without nutrients and oxygen, hence, they have the ability to induce angiogenesis. Tumor vascularization is essential for its growth and it is controlled by a balance between angiogenic and anti-angiogenic factors produced by the tumor. Hypoxia promotes angiogenesis through the transcription of the pro-angiogenic factor VEGF. The p53 protein induces the synthesis

of TSP-1, an angiogenesis inhibitory protein, while RAS increases the expression of VEGF and stimulates angiogenesis. VEGF inhibitors are used to treat advanced cancers, but they are not curative.

Resisting cell death: tumors are resistant to programmed cell death. Apoptosis is a protective response to many pathological conditions. Many signals induce apoptosis: DNA damage, expression of oncoproteins and loss of adhesion to the basement membrane among others. Apoptosis begins from an intrinsic or extrinsic pathway, either one leading to the activation of a proteolytic cascade of caspases that destroy the cell. In tumor cells, alterations have been found affecting both pathways, but intrinsic (mitochondrial) pathway mutations are the most common, such as those produced in the Bcl-2 family of proteins.

Finally, the acquisition of genetic and epigenetic alterations that confer these physiological characteristics can be accelerated through genomic instability and through inflammation caused by cancer.

Tumor's growth is accompanied by infiltration, invasion and destruction of the surrounding tissue while metastasis is the ability of the tumor to propagate to regions that are physically discontinuous with the primary tumor. In order to disseminate, invasiveness allows cancers to penetrate into blood and lymphatic vessels, as well as body cavities. All malignant tumors can metastasize, but occasionally metastatic behavior is unusual, such as in gliomas, central nervous system tumors, or in basal cell carcinomas of the skin. Therefore, the properties of invasion and metastasis can be separated.

Invasion and metastasis are the result of complex interactions between tumor cells and healthy stroma (Kumar, Abbas, Fausto 2010). Although millions of primary tumor cells are released into circulation, few are usually capable of producing metastasis. This indicates that the metastatic process is incredibly inefficient. Nonetheless this eventual spread of the tumor seriously reduces the possibility of cure; therefore, blocking this metastatic capacity would be greatly beneficial for patients.

Nervous system-derived neoplasias are considered cerebral tumors and can be classified in primary (they originate in the nervous system) or secondary tumors (metastasis of other types of tumor that invade the nervous system). Cerebral tumors can cause direct brain damage by compressing the brain areas due to growth or by the destruction of normal brain cells.

In vertebrates, the embryonic neural tube provides most cell types of the central nervous system (CNS), including neurons, astrocytes and oligodendrocytes. During embryonic development, the dorsal lip of the neural tube forms the neural crest, whose cells migrate giving rise to several tissues, including the peripheral nervous system (PNS) (Zhu and Parada 2002). Tumors of neuroectodermal origin (neurological) include all those derived from CNS and PNS cells. Once development is complete, neurons become post-mitotic (non-dividing) while glia cells still retain the ability to proliferate (Zhu and Parada 2002). It makes sense that most neurological tumors are considered to be of glial origin. Because the classical classification of neurological tumors is based on the cell type from which they originate, these tumors are called gliomas, and they are classified based on the type of cell they resemble and the markers they express: astrocytomas (astrocytes), oligodendrocytomas (oligodendrocytes) and ependymomas (ependymocytes) (Holland 2001). However, in recent years it has been proposed that these tumors may originate from glioma stem cells (GSCs).

Gliomas are tumors that cause high mortality and morbidity as a result of their location, being very aggressive and resistant to radiotherapy and chemotherapy (Weller et al. 2015; Zhu and Parada 2002). They have the ability to infiltrate the surrounding tissue, making complete surgical resection difficult. Otherwise, gliomas do not metastasize out of the brain (Zong, Verhaak, and Canolk 2012). They account for 30% of all brain tumors, and 80% of malignant brain neoplasms. Despite all the advances, survival rate 5 years after the detection of the tumor is only 5% (Chen, McKay, and Parada 2012) and for most patients survival does not exceed 14 months

1.1 CLASSIFICATION

Historically, the World Health Organization (WHO) has classified astrocytomas in different degrees of malignancy (grade I-IV) based on the presence of anaplastic aspects determined by histopathological criteria (Figure 2) (Louis et al. 2007).

Pilocytic astrocytomas (grade I) are tumors that mainly affect children and young people, are benign tumors with a slow and circumscribed growth and can be eliminated with a simple surgical resection. They mostly appear in the neuro axis, optic nerve, hypothalamus, thalamus and cerebral hemispheres. They represent 10% of astrocytic tumors and 85% of cerebellar tumors (Kleihues, Burger, and Scheithauer 1993).

Diffuse astrocytomas (grade II) are tumors with low malignancy and with a long clinical progression. They have a low proliferation rate but their capacity to infiltrate and invade the surrounding tissue makes their complete surgical resection difficult. Grade II astrocytomas are characterized by occasional nuclear atypia and non-visible mitotic activity (Furnari et al. 2007). They represent 35% of astrocytic tumors, mainly affect young adults and have a tendency to evolve into high-grade tumors. They can be located in any area of the CNS with a survival range of 5 to 15 years (Delgado-López et al. 2017).

Anaplastic astrocytomas (grade III) are considered malignant tumors with a high proliferation rate. They present anaplastic characteristics, specifically high cellularity rate, cellular pleomorphism, increased nuclear atypia and fast mitotic activity. These tumors are usually present in the two hemispheres and the survival of the patients is very low (less than three years) (Furnari et al. 2007).

Glioblastoma multiforme (GBM; grade IV) are the most malignant brain tumors with the worst prognostic. They have high rates of proliferation and high invasion capacity, presenting angiogenesis and necrosis. Necrotic areas are often surrounded by tumor cells in pseudo-symmetrical conformation. These tumors are usually very resistant to chemotherapy and radiotherapy and patient's survival does not usually exceed a year (Adamson et al. 2009). They may be classified as primary (or de novo) tumors, which appear without any type of previous injury, or as secondary tumors, which evolve from low-grade astrocytomas (Kleihues and Ohgaki 1999). Primary GBM make up to 90% of all GBM and affect adults (> 45 years old), while secondary GBM often affect younger patients, including adolescents and children. Most low-grade astrocytomas will evolve into secondary GBM. Although at the histopathological level primary and secondary GBM are indistinguishable, they present a very different genetic and molecular profile (Louis et al. 2007).

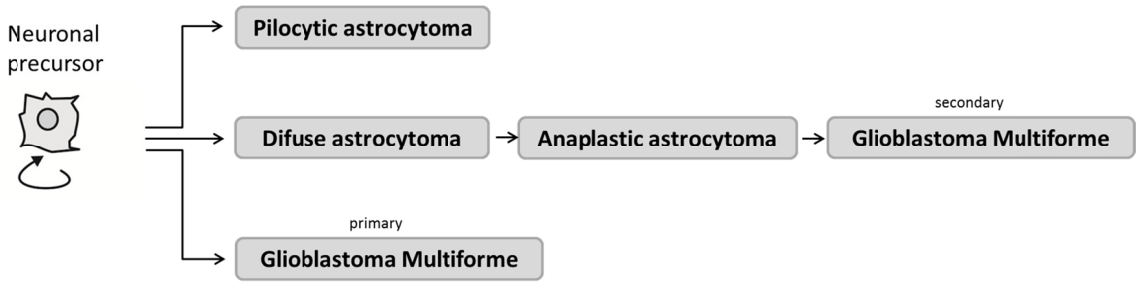

Figure 2. *Histopathological classification of glioblastoma*

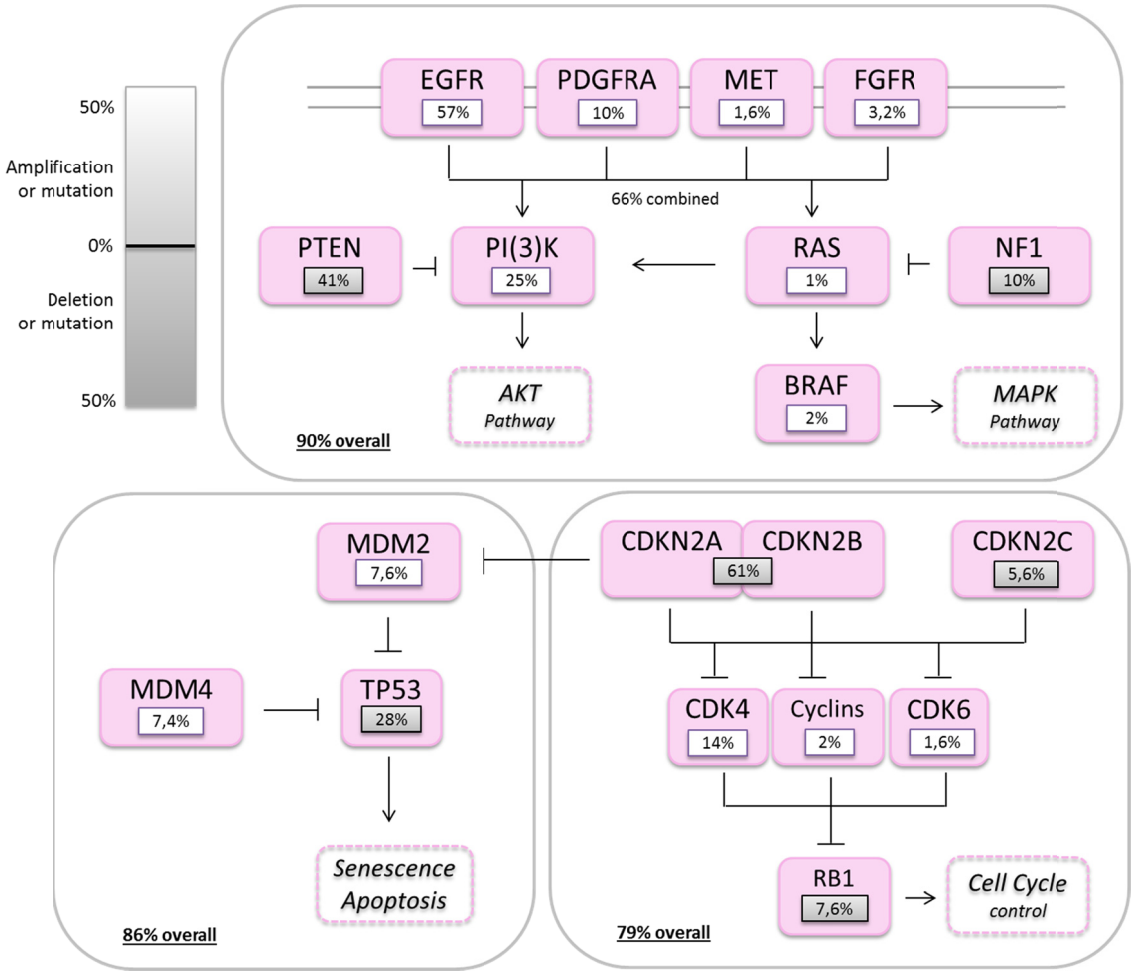

Figure 3. Glioblastoma's altered pathways. Adapted from (Brennan et al. 2013).

In recent years there have been multiple advances in the understanding of the molecular pathogenesis of gliomas and a new classification based on the patient's genetic profile has been developed. This complements the traditional histopathological classification (Blumenthal et al. 2016) and it is important to find new targets for effective and personalized treatments. Consequently, glioblastomas can also be classified by their genetic fingerprints. Sequencing data have extended the known somatic alterations that affect major cancer pathways in GBM (**Figure 3**) (Brennan et al. 2013). In **90%** of GBM there are mutations in the **MAPK pathway** with at least one RTK (*Receptor Tyrosine Kinase*) altered in 67.3% of GBM overall: EGFR (*Epidermal Growth Factor Receptor*) (57%), PDGFRα (*Platelet-Derived Growth Factor Receptor Alpha*) (10%), MET (1.6%) and FGFR3/2 (*Fibroblast Growth Factor Receptor*) (3.2%). PI3K mutations are found in 25% of GBM and are mutually exclusive with PTEN (*Phosphatase and Tensin Homolog*) (41%) mutations/deletions; also, NF1 (*Neurofibromatosis type I*) gene is deleted or mutated in 10% of the cases. The **p53 pathway** is dysregulated in **86%** of GBM through mutation or deletion of

TP53, amplification of MDM1/2/4 (15%) and/or deletion of CDKN2A (*Cyclin-Dependent Kinase Inhibitor 2A*) (61%). Most tumors (80%) have one or more alterations affecting RB (*Retinoblastoma*) function: direct mutation or deletion of RB1 (7.6%), amplification of CDK4/6 (15.6%), and the remainder via CDKN2A deletion.

The Cancer Genome Atlas (TCGA) Research Network generates a comprehensive catalogue of genomic abnormalities driving tumorigenesis. TCGA have provided a detailed view of the genomic changes in GBM, which can be classified in four groups depending on their molecular profile: Classical, Mesenchymal, Proneural and Neural (Verhaak et al. 2010).

In Classical GBM, chromosome 7 amplification is paired with chromosome 10 loss; these also present a high level of EGFR amplification and lack TP53 mutations. The EGFR amplification is usually accompanied by alterations in Rb pathway through CDKN2A deletion.

Mesenchymal GBM show a focal hemizygous deletion in chromosome 17 in the NF1 gene-encoding region. This subtype also expresses mesenchymal markers such as CHI3L1 and c-MET.

In Proneural GBM there are two major features: alterations of PDGFRα and point mutations in IDH1 (*Isocitrate DeHydrogenase 1)*. IDH1 mutations involve less production of α-ketoglutarate and NADH resulting in oxidative stress. These GBM usually present amplifications frequently accompanied by point mutations in the PDGFRα locus in chromosome 4. In addition, amplification of chromosome 7 and deletion of chromosome 10 (regions encoding EGFR and PTEN) are also typical. Secondary GBM derived from anaplastic and diffuse astrocytoma belong to this group.

Finally, Neural GBM are typified by the expression of neuron markers such as NEFL, GABRA1, SYT1 and SLC12A5.

There are studies of the temporal sequence of driver events during tumorigenesis. GBM subtypes are connected in an evolutionary framework that starts with the proneural type. The first event to happen is chromosome 7 gain and chromosome 10 loss. These two genetic alterations are very common in the early development of all subtypes of GBM. Additional copies of chromosome 7 lead to elevated expression of PDGFRα, and loss of chromosome 10 results in a reduced expression of PTEN (Zheng et al. 2008). Overexpression of PDGFRα is enough to induce gliomas that will be enhanced by PTEN loss to give the proneural subtype, but also heterozygous loss of PTEN is enough to induce gliomas in combination with other events such as TP53 loss with or without NF1 loss. The second event is the CDKN2A loss and/or p53 mutation. Mouse modelling shows that these events are enough to form a proneural-like GBM;

this type can be shifted to a mesenchymal subtype with the subsequent loss of NF1. Although it is possible that mesenchymal GBM can arise de novo only with mutations in NF1/TP53 and without alterations in PDGFRα and PTEN, most GBM are abnormal for chromosomes 7 and 10, and most likely they arise from a proneural GBM precursor lesion. PDGFRα is the gene that provides the strongest selection for the initial gain of chromosome 7, but there are others in this chromosome, such as *CUL1*, *CBLL1, ASNS*, that show similar but less robust effects (Ozawa et al. 2014).

1.2 TREATMENT

Standard treatment for GBM involves its complete surgical resection (almost impossible due to GBM dissemination), followed by chemo- and radiotherapy. GBM chemotherapy entails the use of the alkylating agent Temozolomide (TMZ), which produces DNA damage. In proneural GBM, chemotherapy and radiotherapy do not present an advantage and do not increase survival (Verhaak et al. 2010). Recurrences are present in all GBM groups due to the high invasion rate in this kind of tumors, but these recurrences belong to the same group as the primary tumor, even though there may be some molecular changes (Verhaak et al. 2010; Weller et al. 2013).

In relation to patient's treatment it is important to determine the methylation status of the O-6-methylguanine-DNA methyltransferase (MGMT) gene. This protein is capable of repairing DNA damages produced by alkylating agents (Wick et al. 2012). Hence, tumors with silenced MGMT are sensitive to TMZ because they are not able to repair DNA damages produced by TMZ. These patients will have better response to the treatment and consequently better prognosis (Weller et al. 2015).

1.3 ORIGIN AND EPIDEMIOLOGY

Before the discovery of adult stem cells, it was believed that gliomas derived from astrocytes (astrocytomas). It was thought that these cells underwent a process of malignant transformation, converting to dedifferentiated cells capable to mimic stem cells' properties. This concept was reinforced by the finding that it is possible to reprogram *in vitro* a differentiated cell (Chen, McKay, et al. 2012).

Discovery of neural stem cells (NSC) (Sanai, Alvarez-Buylla, and Berger 2005) in the postnatal brain opened the door to a new theory on the origin of gliomas. The ability to self-renewal of NSCs would make them more susceptible to accumulate mutations and develop tumors (Gilbertson and Rich 2007). The American Association for Cancer Research defines cancerous stem cells (CSCs) as a subpopulation of tumor cells with self-renewal capabilities, which can lead to a heterogeneous population of cancerous cells that make up the tumor (Chen, McKay, et al. 2012). In the case of gliomas, these cells present a persistent self-renewal capacity with the potential to give rise to cells of several differentiated lineages (glial and neuronal) and with the ability to form a new tumor when they are transplanted into model animals (Gilbertson and Rich 2007; Morokoff et al. 2015).

The relationship between glioma stem cells (GSCs) and the various molecular subtypes described (Verhaak et al. 2010) has not been well characterized, but based on their molecular characteristics these can be divided into two types (Morokoff et al. 2015): type I (Proneural) are cells that most resemble NSCs from foetus, being positive for markers CD133 and CD15, and with the ability to form floating neurospheres (Beier et al. 2007). By contrast, type II (mesenchymal) are more similar to adult NSCs, express CD44 and are negative for CD133, presenting more invasive behavior and growing as adhesive neurospheres.

Because these cells are responsible for the spread and maintenance of the tumor, they may be in principle good therapeutic targets for the treatment of gliomas. In addition, it has been described that GSCs, and in general CSCs, have a high invasion capacity and may be responsible for dispersal in another area of the brain, therefore for the recurrences. But GSCs are difficult targets for cancer therapeutics: they cycle slowly, express high levels of drug-export proteins and may not depend upon the oncoproteins that are targeted by the “smart drugs” (Stiles and Rowitch 2008).

The annual incidence of brain tumors in the United States between 2007 and 2011 was 21.4 per 100,000 people, of which 6.6 were gliomas, and half of these GBM. The incidence (for every 100,000) of the remaining gliomas is relatively low: 0.34 for pilocytic astrocytoma, 0.5 for diffuse astrocytoma and 0.37 for anaplastic astrocytoma. The incidence increases with age, being for GBM 0.15 in children, 0.41 in youth, 13.1 between 65 and 75 years and 15 in people between 75 and 85 years (Ostrom et al. 2015; Weller et al. 2015). In Spain, according to the Spanish Association Against Cancer (AECC), the incidence of brain tumors is 8.73 per 100,000 individuals in men and 5.41 in women. There are no conclusive data that support an increase in recent decades.

1.4 INVASIVE CAPACITY OF GLIOBLASTOMAS

GBM have a high infiltrating capacity at surrounding tissues; this is one of the main reasons for the incomplete resection of the tumor and the appearance of recurrences, which can arise near the resected area but also in distant zones or even at the other cerebral hemisphere (Paw et al. 2015). Glioma cells undergo biological changes such as gaining of mobility, stem cell phenotype and the ability to degrade extracellular matrix (ECM). This last property is present in all astrocytomas, including also the low grade ones, being a characteristic that appears at the first stages of oncogenic transformation (Louis et al. 2007). Moreover, the ECM also interacts chemically with glioma cells, and these, as other tumor cells do, influence stromal cells to produce a reorganization of the composition and structure of the ECM.

GBM do not metastasize outside the brain; they use extracellular spaces to invade brain regions. These tumors invade using the circulatory system composed by blood and lymphatic vessels. Specifically, they use the perivascular space present around blood vessels or the spaces present around neurons and glial cells, which compose the parenchyma and white substance. They can migrate using axons or nerve tracts as a road (Cuddapah et al. 2014; Furnari et al. 2007; Scherer 1938).

2 - CYCLIN D1

Cyclins were originally discovered by R. Timothy Hunt in 1982 while he was studying the cell cycle of sea urchins. He coined the name cyclin because the concentration of these proteins changes in a cyclical manner during the cell cycle. Cyclins regulate the progression of the different cell cycle stages by associating and forming complexes with cyclin dependent kinases (CDKs), the catalytic subunits. Until now, 29 cyclins and 20 CDKs have been identified in humans, although not all are related to the cell cycle (Malumbres 2014). In the cell cycle, the main role of CDKs is to make sure that an optimal control of the replication of DNA and correct chromosome segregation take place. CDK activity oscillates throughout the cell cycle by reversible phosphorylation and by transient association with specific cofactors such as cyclins and CKIs (CDK inhibitors). Cyclins perform a double function as CDK activators and as targeting agents toward specific substrates, whereas CKIs act both as architectural and as inhibitory components (Bendris, Lemmers, and Blanchard 2015). Cell cycle regulation is complex and results from the existence of checkpoints (quality controls) to ensure that each step of the cell cycle is completed before the next. Cyclins are generally different between them in primary structure, or amino acid sequence. However, all members of the cyclin family are similar in 100 amino acids that compose the cyclin box. There are several different cyclins that are active in different parts of the cell cycle and that cause the CDK to phosphorylate different substrates. Depending on the timing of their expression and functions in the cell cycle, cyclins are divided into four classes. Three of them, G1/S cyclins (cyclin E), S cyclins (cyclin A), and M cyclins (cyclin B), are directly involved in the control of cell cycle events. The fourth class, the G1 cyclins (cyclins D), controls the entry into the cell cycle in response to extracellular growth factors or mitogens.

In mammalian cells there are three different D-type cyclins: cyclin D1 (Ccnd1), cyclin D2 and cyclin D3. Although they are encoded by different genes, they are closely related. Overall, human cyclin D2 and cyclin D3 proteins are 62% and 51% identical to cyclin D1, respectively (Musgrove et al. 2011; Sherr and Roberts 1999). They are expressed in different manners depending on the tissue type, and they associate with CDK4 and CDK6 to form an active complex.

2.1 D-TYPE CYCLINS ARE ESSENTIAL

CCND1 Knock Out (KO) mice show retina abnormalities, a lack of development of breast epithelium during the gestational period, are smaller than normal, and present neurological impairment that so far has not been well characterized (Bienvenu et al. 2010; Sicinski et al. 1995). CCND2 and CCND3 single KO mice are also viable and have specific tissue defects. Loss of CCND2 produces female sterility, cerebellum abnormalities and errors in B lymphocyte proliferation (Sicinski et al. 1996). Mice lacking CCND3 fail to undergo normal expansion of immature T lymphocytes (Sicinska et al. 2003).

Embryos that lack all cyclins D are well developed until mid/late gestation, when most organs are well formed, showing that the loss of the three D-type cyclins does not affect cell division during early embryonic development. However, mice die due to anemia and coronary defects before gestation is complete (Kozar et al. 2004). Likewise, CDK4/6 KO mice show a phenotype similar to that of cyclin-D triple KO mice, with embryos dying before birth due to anemia. All cyclin-D elimination leads to proliferation failure in hematopoietic cells, also affecting the stem cell population in the liver. Hence, removal of the three D-type cyclins exacerbates any single KO phenotype, demonstrating that cyclins D must have some redundant functions. Nonetheless, some cell types proliferate fairly well without cyclins D. For instance, fibroblasts derived from triple KO embryos can proliferate similar to wild type, although they require higher mitogen concentrations and are resistant to cell cycle inhibition by p16 (CDK4/6 inhibitor). By contrast, Ccnd1-CDK4 activity is critical for specific tissues (Kozar et al. 2004), and Ccnd1 removal promotes specific defects in processes involving cell polarity, such as cell adhesion and migration (Liang et al. 2015; Neumeister et al. 2003), showing that there is no redundancy in the control of these functions.

2.2 CYCLIN D1 FUNCTION

Cyclin D1 is the best characterized and most studied cyclin since it is amplified in a number of different human tumors (Beroukhim et al. 2010). This cyclin acts as an essential ligand between the cellular environment and the cell cycle machinery (Sicinski et al. 1995). Unlike other cyclins that fluctuate periodically during the cell cycle, Ccnd1 expression is rapidly induced by extracellular mitogens, and it diminishes when these mitogenic agents disappear. Cyclin D-CDK4/6 complexes regulate the transition from G1 to S phase (Figure 4) where it operates a

checkpoint that monitors absence of DNA damage and attainment of a critical mass, among other cell statuses. Cyclin D-CDK4/6 complex performs two important functions in cell cycle initiation. One function is catalytic and involves pRB inactivation by phosphorylation (Kato et al. 1993), which releases the transcription factor E2F from pRB inhibition and consequently triggers a transcriptional program necessary for G1/S phase transition and for the S phase. However, recently this model has been questioned (Narasimha et al. 2014; Sanidas et al. 2019). One of the induced genes is cyclin E, which together with CDK2 hyperphosphorylates pRB and creates a positive feedback loop that reinforces cell cycle entry. Another function (non-catalytic) of cyclin D-CDK4/6 complexes is the sequestration of the CKIs p21 and p27, facilitating the activation of cyclin E-CDK2 complexes.

More recently, new Ccnd1 functions, both nuclear and cytoplasmic, outside the cell cycle have been described (**Figure 4**). Some of these functions are CDK-independent; for instance, Ccnd1 associates with a variety of chromatin modifying enzymes and it has been shown to modulate the activity of different transcription factors independently of CDK4; among these some members of the nuclear hormone receptors, regulating in this way cell proliferation, cell growth and differentiation. Also, Ccnd1 seems to participate in a number of biological processes such as migration, DNA damage response and gluconeogenesis (Musgrove et al. 2011; Qie and Diehl 2016).

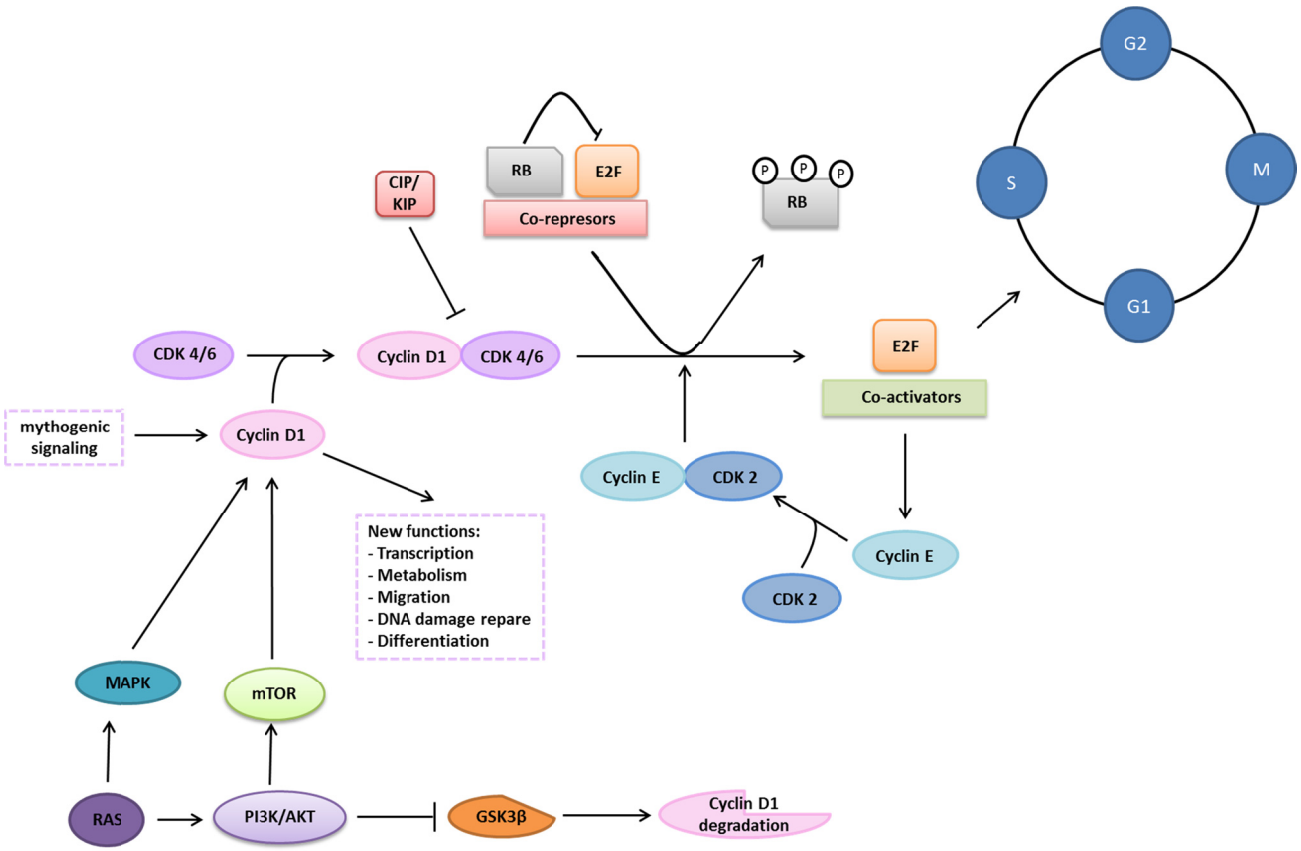

Figure 4. *Brief vision of the physiological regulation of cyclin D1 and its role in the cell cycle and beyond*. Extracellular factors activate cyclin D1 expression, which forms a complex with CDK4/6. In the nucleus, this complex initiates RB phosphorylation, releasing from its inhibition the E2F transcription factors, which induces the expression of cyclin E and other genes. Cyclin E-CDK2 complex hyperphosphorylates RB and inactivates it completely, promoting cell proliferation. The levels of cyclin D1 in the cell depend on CCND1 gene expression and cyclin D1 protein degradation. Expression is promoted by either the RAS-MAPK pathway or the PI3K/AKT/mTOR pathway, while inhibition of GSK-3β leads to Ccnd1 degradation. Other more recently described noncanonical functions of Ccnd1 are listed. These can be CDK dependent or independent.

2.3 CYCLIN D1 STRUCTURE AND EXPRESSION

Cyclin D1 is a protein of 36 kDa and 295 amino acids (aa) encoded by the CCND1 gene, which contains 5 exons and is located on human chromosome 11 at region 11q13.3. At the N-terminus (aa 5 to 9), it contains an LxCxE motif that mediates binding to RB. Between aa 56 to 145 there is a domain known as the cyclin box whereby CDK4/6 and CKIs (p21, p27 and p57) interact. At the C-terminus (aa 241-290) there is a PEST domain (rich in proline, glutamate, serine and threonine) that may be involved in protein degradation, and in particular a threonine residue at position 286 whose phosphorylation is necessary and sufficient to promote ubiquitin-dependent degradation of Ccnd1; thus, the C-terminal domain regulates protein stability. The region between the cyclin box and the C-terminus contains motifs responsible for the interaction with transcription factors. Transcriptional activation by Ccnd1 is associated with LLXXXL motif (between aa 251 to 255), this motif is an important site of coactivator recruitment. Transcriptional repression is associated to aa 142-253 (repressor domain) (**Figure 5**) (Qie and Diehl 2016).

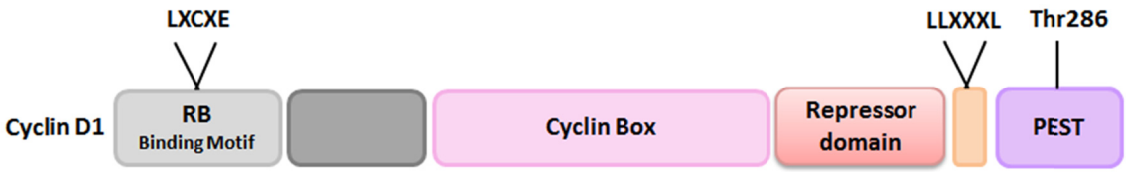

Figure 5. *Schematic structure of cyclin D1 protein.* RB binding motif is located at the N-terminus part followed by the cyclin box. Also, the repressor domain and the activator motif LLXXXL are featured. Finally, at the C-terminus part is located the PEST region and the Thr286. Modified from (Qie and Diehl 2016).

Cyclin D1 is a labile protein that has a median life of 10-30 minutes, depending its degradation on the specific cell cycle stage. Mitogenic factors and cell-ECM interactions collaborate in the induction of Ccnd1 expression through different signaling pathways. Anti-proliferative signals

can also contribute to determine Ccnd1 levels (Knudsen et al. 2006). This makes Ccnd1 to act as a proliferative sensor that may be induced rapidly by mitogens, but it may also be rapidly degraded in cells lacking growth factors or cells growing under anti-proliferative stimuli (Diehl, Zindy, and Sherr 1997). Both, the polyubiquitination and the nuclear export of Ccnd1 depend on Thr286 phosphorylation by glycogen synthase kinase 3β (GSK3β). GSK3β localization and modulation is performed by growth factors through the RAS/PI3K/Akt pathway (where RAS inhibits GSK3β activity). GSK3β is mostly cytoplasmic during G1, but at the G1/S transition it accumulates in the nucleus and phosphorylates Ccnd1 at Thr286 (Alao 2007; Alao et al. 2006; Qie and Diehl 2016). This phosphorylation facilitates the interaction with the nuclear exportin CRM1 promoting the exit of Ccnd1 from the nucleus. Once Ccnd1 is in the cytoplasm it is degraded by ubiquitination through the proteasome. AKT inactivates GSK3β by phosphorylation allowing Ccnd1 stabilization and nuclear accumulation (Alao 2007; Knudsen et al. 2006). In a tumor context and as a consequence of alternative splicing, a truncated form of Ccnd1, termed cyclin D1b, may be generated. Cyclin D1b lacks the C-terminus domain of the protein, including Thr286, and therefore it accumulates in the nucleus and it is more stable than the wild type protein. Furthermore, constitutive overexpression of a Ccnd1 T286A mutant version in mouse fibroblasts promotes cellular transformation and tumor growth in immunodeficient mice. Therefore, the elimination of Ccnd1 from the nucleus during the S phase of the cell cycle must be important to maintain a normal growth (Alao 2007).

2.4 CYTOPLASMIC FUNCTIONS OF CYCLIN D1

Cyclin D1 can also localize to the cytoplasm and interact functionally and physically with cytoplasmic and membrane-associated proteins that are involved in the regulation of cell migration. Some of these proteins are: filamin A, PACSIN2, RhoA, Ral GTPases and paxillin (Pxn), indicating that Ccnd1 might have an active role in cytoplasmic regulation of cellular adherence and migration (Fernández et al. 2011; Noel P. Fusté et al. 2016; Meng et al. 2011; Zhong et al. 2010). Cytoplasmic Ccnd1 has been associated with the invasive capacity of tumor cells. The analysis of the subcellular localization of Ccnd1 may be of interest to evaluate tumor malignancy and development, being a good biomarker of invasiveness (Noel P Fusté et al. 2016).

Cytoplasmic Ccnd1 has also been related to differentiation processes (Fernández-Hernández et al. 2013; Sumrejkanchanakij et al. 2003). During the first steps in brain differentiation, neuronal progenitors display some processes that require cell polarity such as loss of adherence,

migration and neurite formation (Singh and Solecki 2015). At this stage, Ccnd1 expression has not diminished and it is localized mostly in the cytoplasm. Cyclin D1 elimination in PC12 cell line promotes abnormalities in polarization, particularly affecting neurite formation (Marampon et al. 2008). Immunohistochemical studies reveal that Ccnd1 expression increases during cortical development and decreases during terminal differentiation. These observations suggest that cytoplasmic Ccnd1 may be important to coordinate those processes at early stages of cell differentiation. In consonance with this, it has been observed that CCND1 KO mice are viable but present neurological abnormalities (Sicinski et al. 1995).

2.5 CYTOPLASMIC CYCLIN D1 AND CELL MIGRATION

In addition to the canonical functions of cyclin D1 in cell cycle progression and tumorigenesis, new Ccnd1-associated functions have been described. These new functions include cell migration and invasion, increase of angiogenesis and inhibition of mitochondrial metabolism among others (Pestell 2013; Qie and Diehl 2016).

Cyclin D1 has been associated with tumor invasion and metastasis in different clinical studies and *in vivo* experiments. For instance, its overexpression has been related to bone metastasis of prostate cancer (Drobnjak et al. 2000). The regulation of adhesion and migration by Ccnd1 seems to be independent of its role in cellular proliferation (Velasco-Velázquez et al. 2011). Thus, Ccnd1 elimination in mouse macrophages and fibroblasts promotes specific defects in cell matrix adhesion, motility and invasion processes, stablishing that Ccnd1 improves cell migration and invasion (Li, Wang, et al. 2006; Z. Li et al. 2014; Neumeister et al. 2003). Cells lacking Ccnd1 also present a more extended morphology. Nonetheless, these phenotypes have been attributed to nuclear Ccnd1 acting as a transcriptional regulator of genes that control cell adhesion and migration (Z. Li et al. 2014).

Cyclin D1 negatively controls a group of genes that are involved in adhesion and migration processes such as ROCK (effector of RhoA GTPase) and TSP-1, a protein of the ECM that inhibits metastasis and tumor growth (Bendris et al. 2015; Li, Wang, et al. 2006; Z. Li et al. 2014). Ccnd1 deficient cells show an increase of RhoA activity that leads to an increase in adhesion foci and stress fibers; under this condition the cell is more spread and has poor motility. These cells also show an increase of TSP-1 production. Migration can be promoted in these cells either by Ccnd1 expression or by TSP-1 repression.

Moreover, there are post-transcriptional mechanisms involving Ccnd1 in the regulation of adhesion and migration. Ccnd1-CDK4 complex inhibits RhoA GTPase through p27 (CIP/KIP). This CKI interacts with and inhibits RhoA in the cytoplasm promoting cell migration (Besson et al. 2004; Li, Jiao, et al. 2006). Because p27 stability depends on Ccnd1-CDK4 complex activity (Li, Jiao, et al. 2006), fibroblasts lacking Ccnd1 show increased activity of RhoA that correlates with a significant reduction in p27 levels.

Several studies also suggest that Ccnd1 interacts with cytoplasmic proteins involved in the regulation of cell invasion and migration. Cyclin D1-CDK4 complex regulates filamin A phosphorylation, and Ccnd1 interacts and co-localizes with filamin A in membrane ruffles of migrating cells in a breast cancer cell line. Filamin A is an actin-binding protein involved in epithelial-mesenchymal transition. Inhibition of Ccnd1 in breast cancer cells diminishes cell migration and invasion (Zhong et al. 2010). Moreover, deficient Ccnd1 macrophages have fewer ruffles and less migratory capacity (Neumeister et al. 2003). On the other hand, Ccnd1 binds to Ral GTPases (Ral A and Ral B, which regulate exocist) and phosphorylates Rgl2 (Ral GEF) *in vitro*, stimulating the formation of active Ral (Fernández et al. 2011). Also, Ccnd1 interacts with PACSIN2 (Adaptor protein of adhesion foci) and regulates cell spreading and migration (Meng et al. 2011). More recently, our group has demonstrated that the Ccnd1-CDK4 complex phosphorylates a subpopulation of the focal adhesion component Pxn that is associated to the cell membrane, promoting Rac1 activation, and in this way triggering membrane ruffling and cell invasion (Noel P. Fusté et al. 2016).

2.6 CYTOPLASMIC CYCLIN D1 AND CELL SIGNALING

PAXILLIN-RAC1-FAK-SRC AXIS

The interactions of cells with the ECM provide chemical signals that influence different biological processes such as embryonic development, cicatrization, and tissue homeostasis. This influence can be achieved through the regulation of different cellular activities such as migration, differentiation and proliferation. The binding of cells to ECM components is mediated by cell-surface proteins called integrins (Figure 6). These are transmembrane proteins formed by two subunits (α and β) that bridge the ECM with intracellular signaling pathways and signalingthe actin cytoskeleton (Hynes 2002). Although the cytoplasmic domains of integrins do

not have enzymatic activity, ECM interaction promotes their dimerization which leads to the recruitment of structural and regulatory proteins to form a focal adhesion (FA), the macromolecular complexes through which cytoskeleton connects with ECM (Deakin and Turner 2008). Structural proteins mediate physical interaction with the cytoskeleton while regulatory proteins modulate cytoskeleton dynamics, foci formation and cell contraction by actin-myosin filaments. Proteins such as Pxn operate as scaffolds to facilitate functional integration of the multiple FA components.

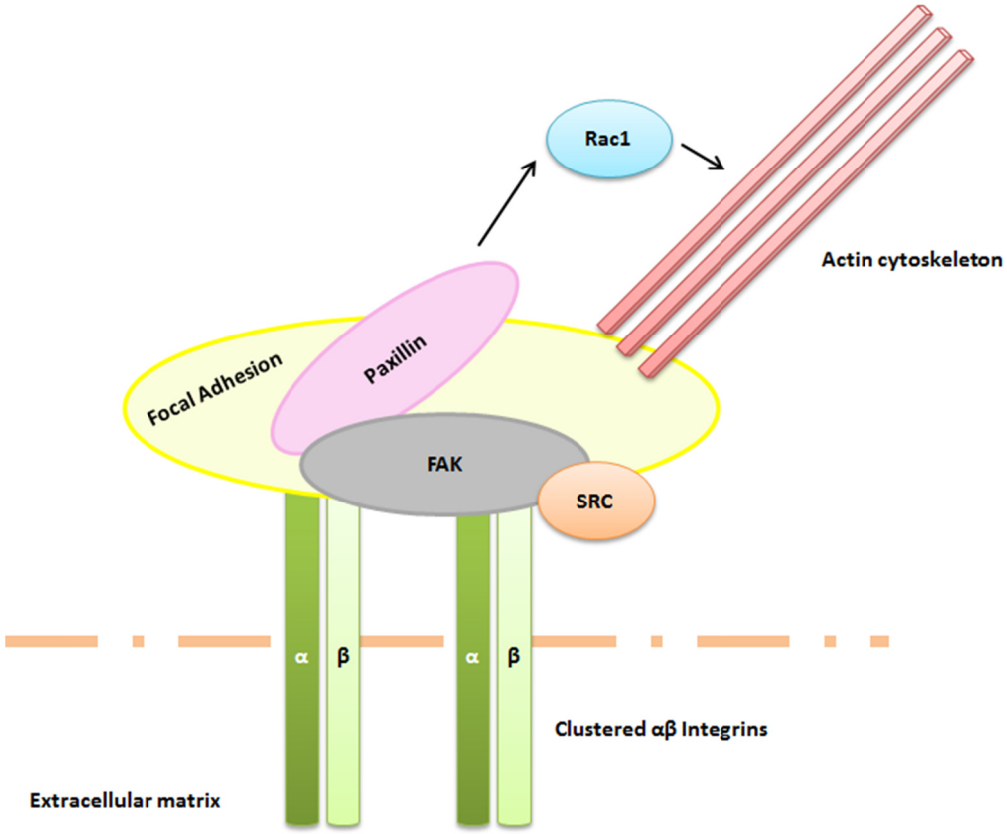

Figure 6. *Focal Adhesion structure*. Focal Adhesion allows a structural link between ECM and actin cytoskeleton. Cell interaction with the ECM through integrins leads to their activation and the recruitment of numerous intracellular proteins. Adapted from (Deakin and Turner 2008).

Paxillin is a 68 kDa protein with multiple domains that is a structural and regulatory component of FAs, and it is located at the end of FA actin fibers (Turner, Glenney, and Burridge 1990). Regulation of FA recycling is a key step in controlling cellular adhesion and motility. Many Pxn-interacting proteins are involved in the regulation of the actin cytoskeleton, which is necessary for cell motility in response to different biological events (Deakin and Turner 2008). Paxillin presents different tyrosines, serines and threonines as phosphorylation sites. It is a substrate of

multiple kinases that are activated in response to different stimuli like cell adhesion or growth factors. The elimination of Pxn in mouse fibroblasts leads to abnormal FA formation, structural abnormalities of the actin cytoskeleton, cell migration defects, focal adhesion kinase (FAK) inefficient distribution, reduction of fibronectin-dependent phosphorylation of FAK as well as loss of spreading (Hagel et al. 2002). Thus, Pxn is a key regulator of cell adhesion dynamics.

Fast assembly and disassembly of cell adhesion during migration is called turnover (Figure 7). This turnover is highly regulated and it is necessary for protrusion formation. FAs are dynamic structures that must assemble at the front part of the migrating cell and disassemble at the posterior part to allow the cell to move. Paxillin was one of the first proteins to be detected in FAs at the front of the cell (Digman et al. 2008). Upon integrin-ECM interaction, Pxn is phosphorylated by FAK and proto-oncogene tyrosine-protein kinase Src at tyrosines Y31 and Y118 (Deakin and Turner 2008). These tyrosine phosphorylations in Pxn induce the disassembly of FAs by Rac1 activation (Webb et al. 2004). Also, phosphorylation of Y31 and Y118 can modulate RhoA activity by sequestering a GAP of RhoA (Tsubouchi et al. 2002).

FAK is a critical intracellular mediator of extracellular changes such as ECM remodeling, nutrient availability or growth factor response. FAK is a non-receptor tyrosine kinase that localizes to FAs, is activated by integrin-ECM interactions, and is the center of multiple signaling pathways that promote tumor and metastasis development (Yoon et al. 2015) by controlling cell motility, invasion, survival, and epithelial mesenchymal transition (EMT). FAK regulates these functions in different ways. For instance, it participates in FA turnover (Zhao and Guan 2009), regulates the transcription of genes implicated in EMT, has an important role in angiogenesis by intracellular signaling in endothelial cells, regulates survival and tumor growth by kinase-dependent and -independent activities, and is implicated in proliferation by regulating different cell cycle stages (Frisch et al. 1996; Li et al. 2011; Veikkola et al. 2000; Zhao, Reiske, and Guan 1998).

Rac1 GTPase is the main inducer of membrane ruffles and stimulates a rapid accumulation of actin filaments at the plasma membrane (Ridley et al. 1992). Paxillin phosphorylation at tyrosines 31 and 118 can indirectly activate Rac1 and inhibit RhoA, both events necessary for protrusion and formation of membrane ruffles. The activation of JNK by EGF leads to the phosphorylation of Pxn at serine 178, a prerequisite for FAK interaction and its phosphorylation of Pxn (Huang, Yan, and Ge 2008). Overexpression of S178A mutant Pxn prevents cellular migration induced by EGF. In GBM, Pxn phosphorylation at serine 178 by JNK regulates cell migration through Rac1, and Rac1 inhibition diminishes S178 phosphorylation in FAs (Nomura et al. 2008). Another phosphorylation event occurs at S83 by ERK, which has an important role in

the turnover regulation of FAs. ERK phosphorylates Pxn at serine 83 upon HGF stimulation, which increases FAK association (Ishibe et al. 2004). Ccnd1-CDK4 complex also interacts with Pxn and phosphorylates serine 83. While ERK phosphorylation promotes cell spreading and migration, phosphorylation by Ccnd1-CDK4 at the same serine diminishes cell spreading. This discrepancy can be explained by the different subcellular localization of phosphorylated S83 Pxn. Ccnd1-CDK4 only co-localizes with Pxn at membrane ruffles and not at FAs. Hence, Pxn phosphorylation by ERK at FAs may lead to more efficient cell spreading while Pxn phosphorylation by Ccnd1-CDK4 at the cell membrane leads to an opposite effect (Noel P. Fusté et al. 2016).

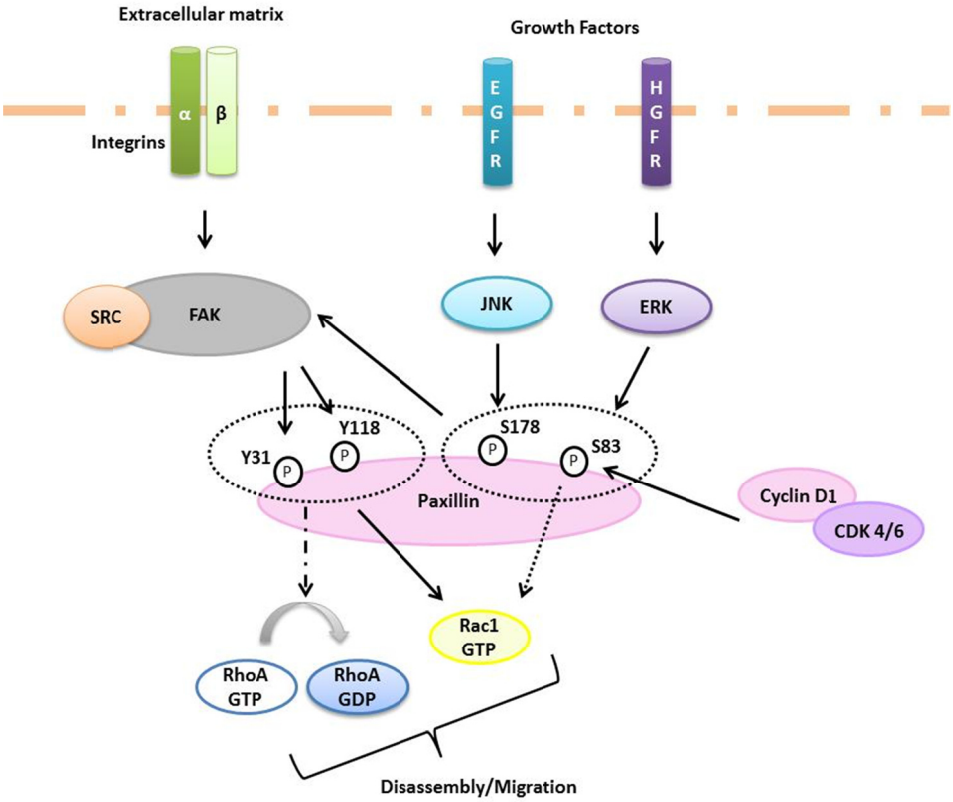

Figure 7. *Diagram of the signaling pathway of paxillin-dependent cell migration.*

RAL GTPASES

Ral GTPases are members of the superfamily of Ras-GTPases. They act as molecular switchers presenting two different conformational states: an active state bound to GTP, and an inactive state bound to GDP (Feig, Urano, and Cantor 1996). GDP/GTP exchange is regulated by Ral-specific Guanine nucleotide Exchange Factors (Ral-GEFs) and GTPase-Activating Proteins (Ral-

GAPs). Ral-GEFs activate Ral GTPases by promoting the exchange of GDP for GTP while Ral-GAPs are inhibitory proteins by promoting GTP hydrolysis.

The Ral GTPase family consists of two members: Ral A and Ral B, which have an 80% identity at amino acid level, and share essential functions during early development (Peschard et al. 2012). These proteins have the following domains: GTP/GDP binding domain, two effector regions whereby they interact with downstream proteins, and a hypervariable domain on the C-terminus part containing a highly conserved CAAX motif that can be isoprenylated and works as an anchorage site responsible for their correct localization at plasmatic or cytoplasmic membranes (Lim et al. 2005). Six Ral-GEFs have been identified, and are classified in two groups: the RalGDS family (RalGDS, Rgl, Rgl2 and Rgl3) whose members contain a Ras binding domain at their C-terminal part; and RalGPS1/RalGPS2 which lack this Ras binding domain (de Bruyn et al. 2000; Ceriani et al. 2007; Hofer et al. 1994; Kikuchi et al. 1994; Peterson et al. 1996; Shao and Andres 2000). Two Ral-GAPs have been described for Ral A and Ral B: Ral-GAP1 and Ral-GAP2 which consist of a catalytic (GAP) alpha 1 or 2 subunit and a common beta subunit (Shirakawa et al. 2009).

Ral GTPases are involved in the control of cell polarity including such processes as cell matrix adhesion, cell migration and cytokinesis (Chen et al. 2006; Rosse et al. 2006; Spiczka and Yeaman 2008). Of all the Ral GTPase effectors the most studied are Ral-BP1 (or RLIP76) and the members of the exocyst complex Sec5 and Exo84. Ral-BP1 is important in filopodia formation, actin dynamics and membrane ruffles. Sec5 and Exo84 are involved in targeting secretory vesicles to specific subcellular regions. Ral GTPases bind to different exocyst components and regulate vesicle trafficking (Guin and Theodorescu 2015; Kashatus 2013). Vesicle trafficking and recycling are essential for cell attachment and motility. This dual function of Ral GTPases — ability to assemble large protein machines and deliver them to specific subcellular locations — is ideal for membrane-altering events such as targeted exocytosis, receptor-mediated endocytosis, formation of filopodia and membrane ruffles.

Ral GTPases have been found to interact genetically with Ccnd1. Cytoplasmic Ccnd1-CDK4 co-localizes with Ral GTPases and modulates their activity. Moreover, Ccnd1 also interacts with the Ral-GEF Rgl2, which is phosphorylated by the complex *in vitro* (Fernández et al. 2011). Expression of Ccnd1 increases the levels of activated Ral B in a CDK4-kinase activity dependent manner (Pedraza et al. 2017). On the other hand, Ral pathway promotes proliferation through NFκB activation. In quiescent mouse fibroblasts a Ral hyperactive allele activates NFκB which in

turn induces Ccnd1, although the specific Ral effector involved remains unknown (Henry et al. 2000).

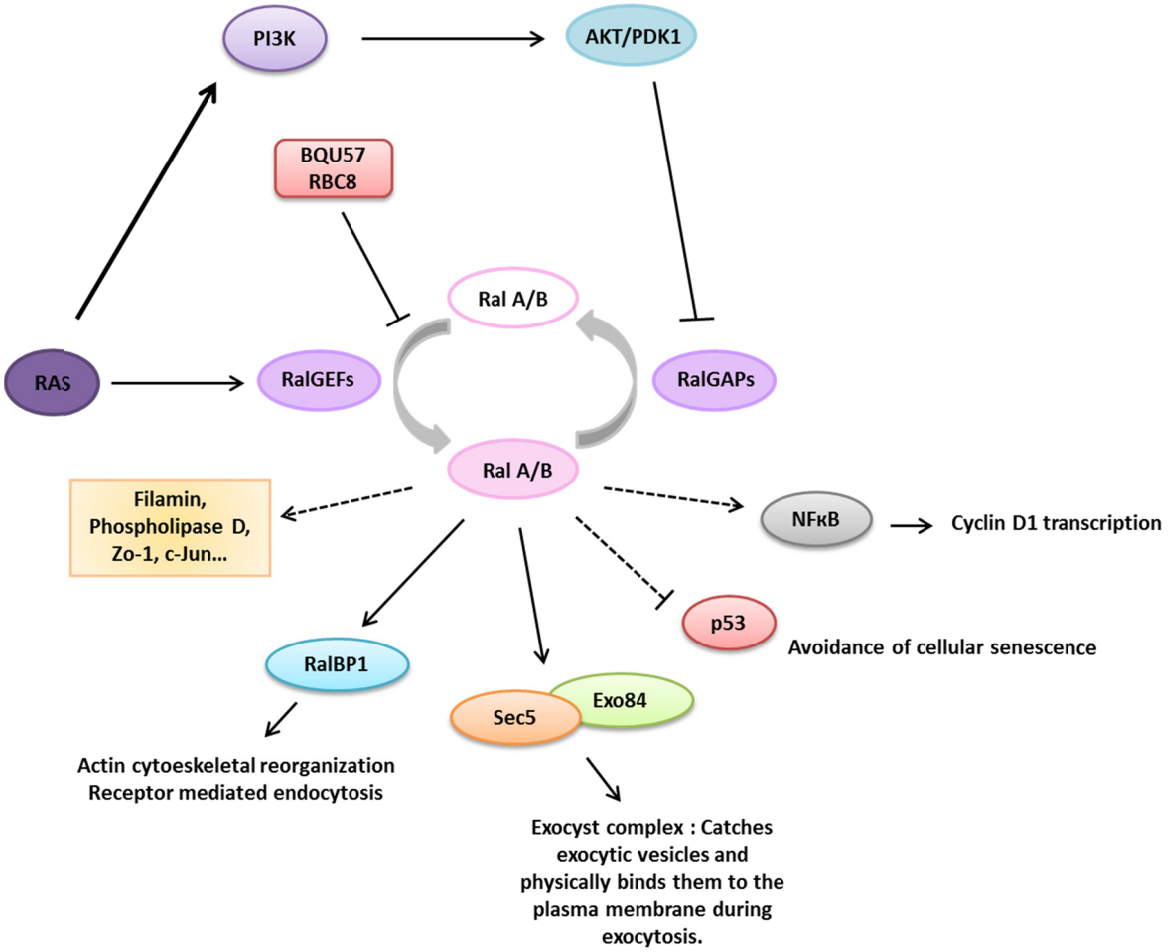

Figure 8. *Ral signaling*. Ral GTPases are activated by several mechanisms including Ras-mediated Ral-GEF activation. Recently characterized chemical compounds RBC8 and BQU57 bind directly to Ral and inhibit its activation. Activated Ral GTPases induce various downstream signalling pathways through NFκB, Sec5/Exo84 and Ral-BP1 among others. Adapted from (Shirakawa and Horiuchi 2015).

The activation of Ral GTPases is initiated by the Ras protein. Once Ras is activated, it associates with different molecular targets to perform its biological effects (**Figure 8**). There are three Ras effectors: phosphatidylinositol-3 kinase (PI3K), Raf and Ral-GEFs. Ral-GEFs promote Ral GTPase activation. These GTPases take part in oncogenesis through proliferation and survival regulation (Győrffy et al. 2015; Lim et al. 2005). Ral-GEF and Ral GTPase activation, in particular Ral A, are enough for promoting cell transformation. On the other hand, in human tumor cell lines there is a chronic Ral B activation that is related to apoptosis inhibition (Chien and White 2003; Gentry et al. 2014; Lim et al. 2006; Peschard et al. 2012; Shirakawa and Horiuchi 2015). Ral GTPases

regulate tumorigenesis and cancer progression through three different mechanisms: 1) activation of Ral effector proteins (RAL-BP1 and kinase Aurora A), 2) activation of different signaling pathways (SRC, JNK, NFκB and Ccnd1) and 3) direct Ral phosphorylation.

Ral GTPases are multifunctional proteins involved in the regulation of tumor initiation, invasion, migration and metastasis. Ral A plays a role in induced transformation by Ral-GEFs and tumorigenesis of human cells while Ral B seems to be more implicated and effective in the regulation of cell invasion and migration (Moghadam et al. 2017; Rosse et al. 2006). Oncogenic mutations in the guanine nucleotide region of Ral proteins can supress its GTPase activity giving rise to a constitutively active form of the protein that transmit survival signals continuously to the cell. Ral can be activated through multiple mechanisms including overexpression or mutations of tyrosine kinase receptors (Kashatus 2013). In most tumors, Ral A is the dominant Ral isoform. Ral-BP1 is the main Ral effector in many tumors; for instance, it has a role in the migration of bladder and prostate cancer cells. Sec5 and Exo84 are also effectors in different tumors (Camonis and White 2005; Guin and Theodorescu 2015).

The role of Ral GTPases in human malignant glioma is still unknown. Recent studies have shown the importance of geranylgeranyltransferase I (GGTase-I) in cancer progression and metastasis. GGTase-I can modify Rho, Rac and Ral, and via Ral B as a downstream effector has a role in invasion of gliomas (Song et al. 2015). Ral-BP1 overexpression is one of the most common changes in malignant cells. In GBM, this overexpression is associated with higher tumor grade and poor survival (Wang, Wang, et al. 2013), and Ral-BP1 knockdown supresses invasiveness, increases chemosensitivity to TMZ, and enhances the autophagic flux in these cells (Wang, Qian, et al. 2013; Zhang et al. 2017).

A

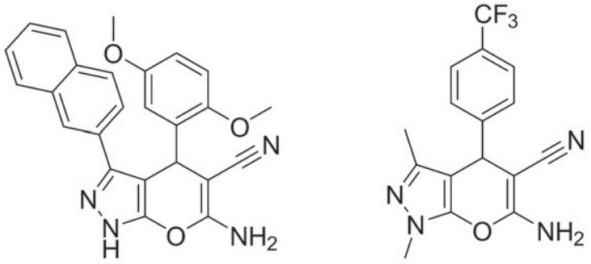

RBC8 **BQU57**

B

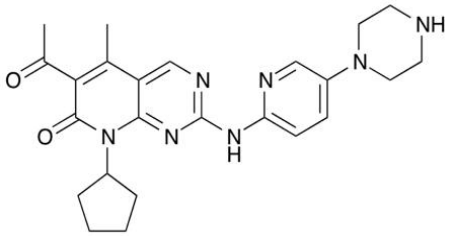

PALBOCICLIB

Figure 9. *Chemical structure of Ccnd1 and Ral GTPases inhibitors.*

Recently, the chemicals RBC8 and BQU57 have been described as Ral inhibitors (Figure 9A). These showed selectivity for Ral A and Ral B (Yan et al. 2014). RBC8 and BQU57 bind to a site on the GDP-bound form of Ral, its inactive state, inhibiting the binding of Ral-BP1. Both compounds inhibited growth in human lung cancer cell lines with IC_{50} values of 2 µM in H2122 cells and 1.3 µM in H358 cells, and also the growth of tumor xenografts. As they are new, little extra information is available.

2.7 CYCLIN D1 AND CANCER: GLIOBLASTOMAS

The role of cyclin D1 in cancer development has been associated to its cell cycle function. Genetic amplifications, reordering or overexpression of cyclins and CDKs have been reported. Particularly, *CCND1* amplification is one of the most frequent copy-number alterations in human cancers (Casimiro et al. 2014).

Ccnd1 is overexpressed in several tumors like lymphomas, lung, prostate, endometrium, breast and colon cancer among others (Casimiro et al. 2014; Cheung et al. 2001; Dickson et al. 1995). Ccnd1 overexpression correlates with tumor metastasis and poor prognosis (Musgrove et al. 2011). Accordingly, nuclear Ccnd1 overexpression has been detected by immunohistochemistry in different tumors; for example, in mantel cell lymphoma, Ccnd1 accumulation in the nucleus is used in diagnostic criteria (Musgrove et al. 2011).

In a study of 3000 tumor samples with 26 different histologic origins *CCND1* was detected as the second most common amplification while CDK4 was the fourth (Beroukhim et al. 2010). In fact, Ccnd1 was originally isolated as a gene amplified by a chromosomal inversion in parathyroid adenomas (PRAD1) and was also related to a chromosomal translocation t(11:14)(q13;q32) in B

cell lymphoma (BCL-1) (Motokura et al. 1991). Independently, Ccnd1 was also isolated from a GBM cell line cDNA library by complementation of G1 cyclin deficiency in yeast (Xiong et al. 1991).

The mechanisms whereby Ccnd1 can be overexpressed in a tumor context are multiple and varied. It is usual to detect genetic reordering in parathyroid adenoma and lymphomas (Casimiro et al. 2014; Motokura et al. 1991). Another mechanism is *CCND1* locus amplification, as in breast cancer wherein is associated with poor prognosis (Naidu et al. 2002). Some point mutations have been associated to some tumors; for example, mutations at Thr286 in endometrium and esophagus tumors (Benzeno et al. 2006) or P287S/P287T substitutions in endometrial cancer (Moreno-Bueno et al. 2003). Also, G/A870 polymorphism is associated with alternative splicing of Ccnd1 pre-mRNA. A870 allele gives rise to cyclin D1b, which lacks the C-terminal part of the protein and does not have neither the PEST sequence nor the Thr286 residue; hence this protein is almost exclusively located in the nucleus and it is a risk factor in cancer (Knudsen et al. 2006).

Although overexpression of nuclear Ccnd1 is critical in tumor formation, the presence of cytoplasmic Ccnd1 has also been described in different tumors. Ccnd1 is sequestered in the cytoplasm of several mammalian tumor cell lines (Alao et al. 2006). Ccnd1 has been associated with tumor invasion and metastasis in different clinical studies and *in vivo* experiments wherein microRNA-9 expression inhibits proliferation, invasion and metastasis of gastric cancer by Ccnd1 repression (Zheng et al. 2013), and overexpression of Ccnd1 is associated to bone metastasis of prostate cancer (Drobnjak et al. 2000). In neoplastic tissues, presence of cytoplasmic Ccnd1 has been recently correlated with invasiveness and metastatic potential (Noel P Fusté et al. 2016). These observations suggest that Ccnd1 may be a new therapeutic target against metastasis.

Increased expression of Ccnd1 contributes to the loss of cell cycle control in gliomas (W. Li et al. 2014). High expression of Ccnd1 is associated with the malignancy degree of astrocytomas, rapid cell proliferation and poor prognosis. CDK4/6 participate in one of the core pathways more frequently altered in GBM (Brennan et al. 2013; McLendon et al. 2008). The most frequent alterations leading to the activation of the CDK4/6 pathway in GBM are deletions of CDKN2A and CDKN2B loci (56%), amplification of CDK4 locus (14%) and deletion of RB1 locus (7.9%) (Brennan et al. 2013). In xenograft models, GBM growth is significantly reduced after treatment with pharmacological inhibitors of CDK4/6 activity (Fry et al. 2004; Michaud et al. 2010), although RB1-negative GBM are resistant to this treatment (Cen et al. 2012; Wiedemeyer et al. 2010). In addition to its role in cell proliferation, Ccnd1-Cdk4 can also

regulates cell-matrix attachment and invasion (Li, Wang, et al. 2006; Neumeister et al. 2003). The knockdown of Ccnd1 is enough to attenuate proliferation and invasiveness of GBM cells, emphasizing the relevance of Ccnd1-CDK4 activity in GBM dissemination (Arato-Ohshima and Sawa 1999; Wang et al. 2012).

2.8 CYCLIN D – CDK4/6 INHIBITION: PALBOCICLIB

Cyclin D1-CDK4 axis is often altered in human cancers and contributes to tumor proliferation and genome instability (Kato et al. 2015). This pathway can be altered by different mechanisms such as *CCND1* amplification or Ccnd1 overexpression (Bartkova et al. 1995; Dickson et al. 1995; Jiang et al. 1992; Knudsen et al. 2006; Motokura et al. 1991), CDK4/6 amplifications or activator mutations (Cheung et al. 2001; Khatib et al. 1993; Sheppard and McArthur 2013) or p16 loss (Xing et al. 2013).

For this reason, CDK inhibitors may be useful for cancer therapy. The first-generation of CDK inhibitors were not selective, not only blocking CDK4 but also several off-targets. These inhibitors showed limited efficacy because of their poor specificity and their secondary effects. Recently, specific CDK4/6 inhibitors have been developed and they are really promising; the most advanced drug in this field is PD0332991 (Palbociclib) (Figure 9B). Palbociclib has been the first CDK inhibitor that has demonstrated effectivity in different cancer treatments (Dickson 2014).

Palbociclib (PD0332991) is an oral inhibitor that specifically inhibits CDK4/6 with an IC_{50} between 10-20 nM. Other CDKs such as CDK1 or CDK2 are 1000-fold less sensitive to the inhibitor (Clark et al. 2016; Sherr 2016). Palbociclib is a small molecule of pyridopyrimidine that inhibits CDK4-6 activity by occupying the ATP binding site (Fry et al. 2004). Since its discovery, many preclinical studies have been carried out to determine its antitumor effects. Therapeutic activity of Palbociclib is based on its capacity to induce a strong but reversible cytostatic cell cycle arrest. In this way, there is a decrease in cell proliferation that leads to the diminishment of different subcutaneous tumors and in some cases even can promote regression (Bollard et al. 2017; Fry et al. 2004).

Several studies have proved the clinical therapeutic efficacy of Palbociclib. It has been approved by U.S. Food and Drug Administration (FDA). Due to the positive results from the phase II clinical trial PALOMA-1 (Finn et al. 2015), in March of 2015 Palbociclib received an accelerated

approbation by FDA for breast cancer treatment in combination with Letrozol. PALOMA-1 trial led to phase III clinical trial PALOMA-2, whose objective was to prove the results in a bigger population (Finn et al. 2016). This allowed that finally FDA granted the use of Palbociclib for this indication at March of 2017 (Schröder and McDonald 2015). Usage of Palbociclib as a therapeutic strategy alone or in combination has been evaluated in different clinical trials for tumor types other than breast cancer, such as lymphomas (Leonard et al. 2012), liposarcomas (Dickson et al. 2013), or prostate cancer, among others (Clark et al. 2016; de Dueñas et al. 2018; Parylo et al. 2018).

The fact that alterations in CCND1-CDK4/6-RB1 pathway are common in GBM makes Palbociclib a promising drug for the treatment of this tumor (Cen et al. 2012). Palbociclib can be also beneficial in the treatment of pediatric gliomas that have lost p16 (Barton et al. 2013). Some studies have shown that Palbociclib is capable of crossing the blood brain barrier (Schröder and McDonald 2015), a prerequisite in order to be effective for GBM treatment. Also, it acts as an effective antiproliferative intracranial drug against GBM xenografts in mice (Michaud et al. 2010). Investigators from The University of California in San Francisco carried out a phase II clinical trial in patients with RB1-positive recurrent glioblastoma to determine the efficacy of Palbociclib. They concluded that Palbociclib monotherapy is not an effective treatment for recurrent glioblastoma (NCT01227434). However, in combination with TMZ and radiotherapy, Palbociclib has shown significant efficacy (Raub et al. 2015; Schröder and McDonald 2015), which is encouraging to still consider Palbociclib for GBM treatment.

3 - HYPOTHESIS

Numerous observations and experimental results support the existence of cytoplasmic cyclin D1-CDK4 functions. In particular, previous results of our group demonstrate that cytoplasmic Ccnd1-CDK4 regulates cell invasion and adhesion through the activation of the small GTPases Rac1 and Ral. Ccnd1-CDK4 phosphorylates Pxn at serines 83 and 178 leading to the activation of Rac1. In addition, our results suggest that this cytoplasmic function of Ccnd1-CDK4 may be relevant to explain normal and pathological processes. For instance, Ccnd1 is accumulated in the cytoplasm of cancer cells arranged in the invasive front of different tumors. However, there are no available *in vivo* data regarding the relevance of the Ccnd1-CDK4-Pxn-Rac1 and Ccnd1-CDK4-Ral pathways on the dissemination of human tumors, although Ccnd1 expression is a poor prognosis marker and Ccnd1-CDK4 activity is frequently elevated in highly invasive tumors such as glioblastomas. Our first hypothesis is that the cytoplasmic Ccnd1-CDK4 pathways play a key role in the ability of those invasive tumors to disseminate. To test this proposal, we have used primary human glioblastoma cells as a model.

The role of Ral A and Ral B GTPases in glioblastoma formation and dissemination has been largely ignored. This is unexpected since these small GTPases are involved in survival, invasion and growth of other type of tumors. Moreover, there are several teams trying to obtain pharmacological inhibitors of Ral GTPases for future cancer treatment. At present, current treatments of glioblastoma are far from achieving complete tumor eradication. We hypothesize that Ral GTPases may be required for glioblastoma development. Therefore, we have undertaken the study of the role of these small GTPases in the formation and dissemination of glioblastoma.

Finally, based on preliminary results from our group, we also postulate that cytoplasmic Ccnd1-CDK4 may play a major role as cell signaling mediator, participating in different signal transduction pathways that regulate a broad spectrum of cellular processes.

4 - OBJECTIVES

1. Evaluation of the *in vivo* relevance of the Ccnd1-CDK4 cytoplasmic complex in human GBM dissemination, including the identification of downstream targets of the cytoplasmic complex.
2. Analysis of the functional implication of Ral GTPases in glioblastoma formation and progression as well as the study of the molecular mechanism that mediates Ral GTPase role in GBM.
3. Study of the role of cytoplasmic Ccnd1-CDK4 as signaling mediator by defining a number of transduction pathways regulated by cytoplasmic Ccnd1.

MATERIALS & METHODS

1 - CELL BIOLOGY TECHNIQUES

1.1 CELL CULTURES

All cell lines were grown in DMEM (GIBCO-Invitrogen) supplemented with 10% FBS, 2 nM glutamic acid and 100 μg/ml penicillin/streptomycin at 37°C. Cell passage was carried out every 3-4 days at 90% confluence. Primary cell cultures, due to their low proliferative rate, were passaged when they arrived at 90% confluence, but the medium was changed twice a week. The passage procedure was as follows: medium was sucked and cells washed with PBS to eliminate serum. Cells were detached with trypsin 5 min at 37°C 5% CO_2 in a humid chamber and then trypsin was inactivated by adding DMEM with 10% FBS. Cells were collected in a tube and centrifuged 5 min at 180 g. After removal of supernatant, the cell pellet was resuspended in 1 ml DMEM with 10% FBS and penicillin/streptomycin, and cells were counted in a Neubauer's Chamber or were directly seeded making a corresponding dilution depending on the cell type.

Cell lines and primary cell culture aliquots were stored in 90% FBS/10 % DMSO in liquid nitrogen. To thaw the cells, cryotubes were taken from the liquid nitrogen and incubated in a 37°C bath. Once the content was melted, it was transferred into a 15 ml tube and medium was added. Cells were centrifuged 5 min at 180 g and the supernatant removed. Cells were seeded on plates containing DMEM with 10% FBS and antibiotics.

293T CELLS

HEK 293T is a human cell line from embryonic kidney, and is a good system for protein overexpression. It is a variant of the human cell line of renal epithelium HEK 293 that expresses some adenovirus genes and the SV40 large T-antigen. This cell line grows fast, is easily transfected, and plasmids carrying the SV40 origin of replication can be transiently maintained at high copy number. For this reason, in this work I use this cell line for virus production. These cells were obtained from the *American Type Culture Collection* (ATCC).

IMMORTALIZED MOUSE EMBRYONIC FIBROBLASTS (IMEFS)

CCND1$^{-/-}$ and *CCND1*$^{+/+}$ immortalized mouse embryonic fibroblasts were kindly provided by P.Sicinski (growth conditions, morphology and chromosome number were authenticated following providers instructions).

GBM CELL LINES

GBM cell lines were kindly provided by Dr. Herreros, who obtained them originally from the *American Type Culture Collection* (ATCC).

U87-MG: This cell line comes from a 45-year-old woman, presents mutations in CDKN2A, PTEN and CDKN2C, grows in characteristic aggregates or spheroids, and has the ability to form tumors in immunosuppressed mice.

U251-MG: This cell line comes from a 75-year-old man, and presents mutations on PTEN and TP53.

GBM PRIMARY CELL CULTURES

Primary GBM were kindly provided by Dr. Herreros. Primary cell cultures were developed from patients' biopsies. These were obtained from surgical interventions of patients at Hospital Universitari Arnau de Vilanova (HUAV) in Lleida. The samples were kept in DMEM at 4°C before being processed. The manipulation of these samples was always carried out in Bio2A hoods.

1.2 TRANSFECTION

LIPOFECTAMINE

Lipofectamine 2000 (Invitrogen) was used for cells with a low transfection ratio. It is a mix of positively charged and neutral liposomes that interact with and facilitate DNA to cross the plasma membrane. Typically, the day before transfection cells are seeded so as to reach 70-90% confluence the following day. Lipofectamine and DNA are diluted separately in Opti-MEM medium, then mixed together and incubated 20 min at RT (Table 1). This mixture was added to cells and incubated 20-40 min at 37°C 5% CO_2 in a humid chamber. Finally, the transfection solution was exchanged by DMEM medium.

TRANS-IT X2 (MIRUS)

TransIT-X2 is an advanced, no liposomal polymeric system that enables high efficiency transfection. The day before transfection cells were seeded to reach 70-90% confluence the day after. DNA was diluted in Opti-MEM and was gently pipetted to be completely mixed (Table 1). Then TransIT-X2 was added to the diluted DNA mixture and incubated 15 min. The transfection solution was added drop-wise to different areas of the wells. Cells were incubated for 24-72 h.

ELECTROPORATION (NEON TRANSFECTION SYSTEM - THERMOFISHER)

The Neon Transfection System by Thermofisher is a device that employs an electroporation technology using the pipette tip as an electroporation chamber to transfect the cells. The transfection was performed with 2-4 x 10^5 cells per reaction in a sample volume of 100 µl. One or two days prior to electroporation, cells were transferred to a plate with fresh growth medium (cells had to be at 70-90% confluence the day of the experiment). After the trypsinization, cells were washed with PBS and re-suspended in R Buffer at a final desired density. In the meantime, a plate was prepared with medium without antibiotics and pre-incubated at 37°C 5% CO_2 in a humid chamber. To electroporate cells, an appropriated number of cells needed to be prepared with the plasmidic DNA at the suggested concentrations (20 µg in our case). The Neon Tube was set up with 3 ml of Electrolytic Buffer into the Neon Pipette

station. The cells were added to the tube containing DNA and gently mixed and inserted into the Neon Tip without any air bubbles. For our experiments, the desired conditions were 1350 V; 30 ms; 1 pulse. After delivering the electric pulse, cells were seeded in the previous pre-incubated plates and incubated for 48 h.

POLYETHILAMINE

Polyethylenimine (PEI) is a cationic lipid that condensates plasmidic DNA neutralizing its negative charges and preventing the action of nucleases. The resulting aggregates have a high affinity for negatively charged cell membranes, which leads to a high transfection efficiency. PEI (sigma-aldrich) does not required a high confluence in the cell culture and it is inexpensive. The transfection procedure (see table 1) is similar to that for lipofectamine with longer incubation periods. Due to its low cost, PEI is frequently used for 100 mm-plate transfections.

Table 1. Amounts of DNA, Lipofectamine, PEI and TransIT-X2 added according to plate size.

	LIPOFECTAMINE		**Trans-ITx2**		**PEI**	
Culture vessel	**DNA + Opti-MEM**	**Lipofectamine + Opti-MEM**	**DNA + Opti -MEM**	**Trans-ITx2**	**DNA + Opti-MEM**	**PEI + Opti-MEM**
24 well plate (16mm Ø)	0.8 µg + 50 µl OPT	2 µg + 50 µl OPT	0.5 µg + 50 µl OPT	1 µl	-	-
12 well plate (23 mm Ø)	1.6 µg + 100 µl OPT	4 µl + 100 µl OPT	1 µg + 100 µl OPT	2 µl	-	-
6 well plate (35mm Ø)	4 µg + 250µl OPT	10 µl + 250 µl OPT	2.5 µg + 250 µl	5 µl	-	-
60 mm Ø	8 µg + 500 µL OPT	20 µg + 500 µl	5 µg + 500 µl	10 µl	-	-
100 mm Ø	-	-	15 µg + 1.5 ml OPT	30 µl	24 µg + 1.5 ml OPT	240 µl + 1.26 ml OPT

1.3 VIRUS PRODUCTION AND INFECTION

VIRUS PRODUCTION

For lentivirus production, 293T cells were transfected with lentiviral expression vectors, together with wrapping vector pVSV.G and packaging vector pHR'82ΔR (encoding gag and pol viral proteins) in a 2:1:1 proportion. Cells were seeded 24 h before transfection in collagen-coated plates (100 μg/ml in 0.02 M acetic acid; two plates for each condition) and were transfected using the PEI protocol described above.

Three days after transfection the medium was collected. This medium contained viral particles and was filtered with a 0.45 μm nitrocellulose membrane. Virus collection and manipulation were performed in a Bio IIA hood. To concentrate viruses, the supernatant was filtered at 2200 g for 30 min in VIVASPIN 20 concentrators (Sartorius Stedim Biotech). Lentiviruses were kept at -80 °C. In general, non-concentrated viruses were used.

CELL TRANSDUCTION

In a BioIIA hood, cells were seeded in 6-well plates in 1 ml medium, and 1 ml virus solution containing 8 μg/ml polybrene (Hexadimethrine Bromide, a cationic polymer that increases infection efficiency from Sigma-Aldrich) was added. Cells were in contact with viruses for 24 h and then medium was changed. I usually wait 3-4 days for the cells to incorporate DNA before performing any treatment or processing.

1.4 CELL PROLIFERATION

PROLIFERATION ASSESSMENT BY TRYPAN BLUE

Trypan blue is an azo dye that selectively colours dead tissues or cells in blue. Live cells do not incorporate trypan blue because they have an intact cell membrane. Hence, only dead cells are blue stained. This assay was used to assess cell viability and proliferation. About 15000 cells/well were seeded in triplicate on a 24-well plate. After 24 h cells were counted after desired treatment. They were counted at 24, 48, 72 and 96 h. Cells were washed with PBS, trypsinized, resuspended in 300 μl medium, and finally trypan blue was added (10 μl 0.4% trypan blue to 10 μl cells). I used 10 μl of this mix in a Neubauer's chamber to count live and dead cells.

PROLIFERATION ASSESSMENT BY BRDU INCORPORATION

BrdU (Bromodeoxyuridine or 5-bromo-2'-deoxyuridine) (Sigma-Aldrich) is a synthetic nucleotide analog that can be incorporated into new chains of replicating DNA instead of thymidine during the S phase of the cell cycle.

For these assays, BrdU was added overnight into the media at a final concentration of 8 μg/ml. Then cells were fixed 15 min with 4% paraformaldehyde (PFA) at RT, and permeabilized 2 min with 0.2% Triton X-100 followed by 3 washes with PBS. Next, 2 M HCl was added for 30 min at 37°C to denature and produce double strand breaks in DNA. This step facilitates the recognition of BrdU by the primary antibody. To neutralize HCl, 0.1 M sodium tetraborate (pH 8.5) was added for 2 min. Subsequently, cells were blocked with 3% BSA for 1 h, followed by 3 washes with PBS before adding the primary antibody for overnight incubation. The next day cells were washed again with PBS and the secondary antibody and Hoechst, which binds to DNA and allows detection of all nuclei (Sigma-Aldrich), were added at a final concentration of 0.5 μg/ml in blocking solution for 1 h at RT. After 3 final washes with PBS, cells were counted under the microscope (positive cells for BrdU as well as total cells).

1.5 CELL VIABILITY

MTT ASSAY

MTT (3-(4,5-Dimethylthiazol-2-yl)-2,5-Diphenyltetrazodium Bromide) is used in a colorimetric assay whereby the activity of succinate dehydrogenase is measured. This enzyme is localized in mitochondria and catalyzes the reduction of the soluble yellow MTT solution to an insoluble purple product called formazan. This reaction only occurs in cells metabolically active, therefore the quantity of formazan produced is proportional to the number of living cells in the culture (viability).

MTT assays were carried out as follows: cells were incubated at 37°C 5% CO_2 in a humid chamber for 30 min with MTT reagent at 1 mg/ml in darkness. Medium was taken out and DMSO was added to the wells to dissolve formazan crystals produced by active cells. After 5 min incubation at RT in darkness, it was read in a spectrophotometer (Bio-Rad) at 595 nm wavelength. Each condition was performed in triplicate and the experiment was repeated at least three times to perform a statistical analysis.

CLONOGENIC ASSAY

Clonogenic ability is the capacity of a single cell to form a colony. The purpose of this assay is determining the effect of different proteins in cell proliferation.

Adherent: To perform this assay cells were seeded in 6-well plates at a density of 1000 cells/well. Cells were incubated 15 days, stained with violet crystal 30 min and washed with PBS. The number of colonies was counted using the digital image processing program *Image J*.

Non-adherent: For non-adherent conditions cells were resuspended at a concentration of 3000 cells/ml in 0.3% agar diluted in culture medium. A 1-ml aliquot of this cell suspension was added to a 6-well plate that was previously covered with a 0.6% agar layer. Cell plate was incubated 15 days at 37°C 5% CO_2 in a humid chamber. After this time, cells were treated with MTT 1h at 37°C 5% CO_2 in a humid chamber in darkness (in these experiments it was not needed to add DMSO to solubilize the crystals because cells were in suspension). The number of colonies was counted using the digital image processing program Image J.

1.6 OTHER CELL BIOLOGY METHODS

SPREAD ASSAY

One way to study the capacity of cells to adhere to the ECM is to measure the number of cells showing spread morphology after a given time. Generally, low adhesion is associated with high invasion.

For this assay, glioma cells were treated or transfected with a DNA plasmid 48 h before the procedure was started. Then cells were trypsinized and seeded in plates containing culture medium without serum. Previously, plates had been treated overnight with 5 μg/ml fibronectin (Invitrogen) at 4°C. Cells were incubated 30-45 min at 37°C 5% CO_2 in a humid chamber until approximately 50% of control cells presented spread morphology. Hereafter, cells were fixed 10 min with 2% PFA on ice. Pictures were taken with a 10x objective in an Olympus IX71 microscope. I counted both spread and unspread green cells.

MIGRATION AND INVASION ASSAY

Invasion assays are performed in *Transwells* (Corning) with 6.5 mm diameter and 8 μm pore size. Cells are required to migrate through a porous membrane and then degrade an ECM of Matrigel (BD Bioscience) in order to invade. Hence, this assay probes both migration and invasion. The procedure I employed is as follows: first, *Transwells* were covered with Matrigel (BD Bioscence) with growth factors in a dilution 1:3 in culture medium. For this, 30 μl of diluted Matrigel were placed at the bottom part of the *Transwell* and allowed to dry in the incubator for 30 min. During this time, cells were trypsinized and prepared in 2 x 10^4 cells/100 μl of media per condition. Once Matrigel was dried, *Transwells* were placed in 24-well plates, 500 μl medium was added between the *Transwell* and well, and 100 μl of cell suspension to the upper part, inside the *Transwell*. Cells were allowed to invade for 8 h, and thereafter they were fixed with PFA. Cells not able to invade remained inside the *Transwell* and they were removed with a cotton stick. Cells able to migrate and invade remained inside the Matrigel. These cells were stained with Hoechst and counted under the microscope. All experiments were done in duplicate or triplicate. The number of stained nuclei was counted using ImageJ.

SENESCENCE ASSAY

The most used biomarker for senescent cells is the senescence-associated β-galactosidase (SA-β-gal) which is the β-galactosidase activity detectable at pH 6 in cultured cells. This activity is encoded by the lysosomal β-galactosidase gene that catalyzes the hydrolysis of β-galactosides into monosaccharides and is induced in senescent cells (Lee et al. 2006).

For the analysis of SA-β-gal cells were incubated 10 min in PBS with 1 mM $MgCl_2$ followed by incubation in X-gal solution – 20 mg/ml X-gal (Sigma Aldrich), 5 mM $K_3Fe(CN)_6$, 5 mM $K_4Fe(CN)_6$, 2 mM $MgCl_2$ in PBS at pH=6. This incubation was carried out for 4 h (cell lines) or overnight (primary cell cultures). Finally, cells were fixed with 0.5% glutaraldehyde in PBS. To better compare different samples, this assay was performed with all samples at the same time.

1.7 TUMORSPHERES

Tumorspheres are solid, spherical formations developed from the proliferation of a single tumor stem cell. They can be obtained by culturing cells in serum-free media and in an Ultra-Low Attachment surface plate in order to enrich the cancer stem cell population, the only cells that can survive and proliferate under these conditions. These tumorspheres are easily distinguishable from aggregated cells.

The protocol to obtain tumorspheres was as follows: cells in 2D cultures were trypsinized, centrifuged 5 min at 180 g washed with neurobasal media (GIBCO), resuspended in tumorsphere media (50 ml neurobasal media + 1 ml B27 supplement + 500 µl Glutamax + 100 µl of penicillin/streptomycin + 100 µg FGF + 100 µg EGF), and seeded in Ultra-Low Attachment surface plates. Floating cells were transferred into new Ultra-Low Attachment surface plates where tumorspheres would grow.

When they reach an appropriate size, tumorspheres were concentrated by gravity in a 15-ml tube for 15 min. Then media was aspirated and tumorspheres washed in PBS with trypan blue, centrifuged 2 min at 5 g, resuspended in 500 µl PBS with a cut pipette tip, and moved into a 4-well plate. Photos were taken under the microscope and analyzed with Image J.

1.8 *IN VITRO* PHARMACOLOGICAL TREATMENTS

PALBOCICLIB

Palbociclib is an ATP-competitive inhibitor with a high selectivity towards the cyclin-dependent kinases CDK4 and CDK6. It has been the first CDK4/6-specific inhibitor approved as a cancer therapy. I obtained Palbociclib or PD-332991 as a powder from Selleckchem. For *in vitro* treatments Palbociclib was dissolved in sterile DMSO at 2.5 mM stock concentration and it was kept at -80°C in dark conditions. For experiments Palbociclib was diluted in culture media to final concentrations ranging from 1 to 5 µM depending on the experiment.

BQU57

BQU57 is a selective inhibitor of the RAS-like small GTPases Ral A and Ral B, which are downstream mediators of Ras signaling. It shows selectivity for Ral relative to the GTPases Ras and RhoA. BQU57 binds to a site of the GDP-bound form to its effector (RAL-BP1; also known as RLIP760) which are involved in proliferation, metastasis and survival of several human cancers. BQU57 was obtained as a powder from Sigma-Aldrich. For *in vitro* treatments it was dissolved in sterile DMSO at 3 mM stock concentration and kept at -80°C. For experiments BQU57 was diluted in culture media and used at working concentrations ranging from 10 to 20 µM depending on the experiment.

2 - MOLECULAR BIOLOGY TECHNIQUES

2.1 PLASMID CONSTRUCTIONS

All plasmids were obtained with QIAGEN MAXI KIT or SIGMA MINIPREP KIT, following the manufacturer's instructions. Quality of DNA was checked by electrophoresis in agarose gels with ethidium bromide staining. Concentration of DNA was measured in the NanoDrop ND-1000 (NanoDrop Technologies) spectrophotometer. I have followed *Current Protocols in Molecular Biology* (Ausubel 1987) for manipulating and analyzing DNA constructs. Plasmids were checked by restriction enzyme digestions. In table 2 the plasmid vectors used in this work are shown.

In pcDNA3 or pCMV-SPORT6, coding sequences were under control of the strong serum-dependent CMV promoter. In some vectors this promoter was substituted by the constitutive serum-independent Ubiquitin promoter (Ubip). To create point mutations or deletions the PCR-SDM method (Weiner et al. 1994) was used. Lentiviral constructions were done in pDSL-hpUG vector (ATCC) after eliminating the GFP coding sequence. In some cases the CMV promoter was substituted by the Ubi promoter using the recombination *Gateway technology* (Invitrogen). For RNA interference of CCND1, RALA and RALB we used shRNA pLKO.1-puro from Sigma

Table 2. Plasmidic and lentiviral vectors.

Name	Plasmidic Vector	Description
pCDNA3	CMVp-3 FLAG	Control vector
pEGFP-N1	CMVp-EGFP	Control vector with GFP (green fluorescence)
pCYC2111	shRNA SCR (Scramble)	Control vector shRNA SCR pLKO.1-puro (Sigma)
pCYC291	CMVp-3FLAG-Ccnd1	EGFP was amplified by PCR of pEGFP-N1 vector and cloned in CMVp-Ccnd1 in BamHI site
pCYC801	Ubip-3HA-CBP-Ccnd1 in pDSL (ΔUbip-GFP) (lentiviral vector)	2.3 kb fragment amplified from pCYC794a vector (Ubip-3HA-CBP-Ccnd1) was inserted in pDSLΔGFP-UbiC vector by recombination with pDONR
pCYC2057	3HA-Ccnd1-CAAX	0.9 kb fragment amplified by PCR that contained BamHI-Ccnd1-CAAX-EcoRI was cloned in pNBM470 vector

pCYC2058	Ubip-3HA-Ccnd1-CAAX in lentivirus (pDSL)	0.9 kb fragment amplified by PCR from pCYC2057 vector that contains BamHI-Ccnd1-CAAX-EcoRI has been cloned in lentiviral pDSL-hpUG vector (ΔUbip and ΔGFP) fromlpCYC 801, in the 9 kb fragment opened with BamH1-EcoRI
pCYC2066	EGFP-MmPaxillin	Paxillin mouse DNA has been inserted BglII and/o BamHI of pEGFP-C1. (Gift from J. Yamauchi)
pCYC2084	3HA-CBP-MmPaxillin in lentivirus (pDSL)	1.7 kb amplified fragment by PCR from pCYC2064 (GST-MmPaxillin) that contains EcoRI-Paxillin-XhoI, has been cloned in pDSL-hpUG vector (ΔUbip ΔGFP) from pCYC 801, in the 9 kb fragment opened with EcoRI-XhoI
pCYC2103	EGFP-MmPaxillin (S83E;S178E)	To change Serine 83 and Serine 178 to glutamic acids in la EGFP-Mm Paxillin (pCYC2066)
pCYC2105	EGFP-MmPaxillin (S83A;S178A)	Site directed mutaganesi to change Serine 83 and Serine 178 in to Alanin in EGFP-Mm Paxillin (pCYC2066)
pCYC2133 (FSV)	FSV in lentivirus	FSPsi without puromicin and with GFP. For cloning some gene it has to be opened with 5'AgeI i 3'BamHI. (Gift from Mario Encinas lab)
pCYC2140	627 - packaging helper (ΔR)	Packaging helper pHR'82ΔR that codifies for gag and pol proteins (Gift from Xavier Dolcet lab)
pCYC2141	628 - envelope helper (VSV)	Vector pMD2G that codifies for the virus envelope pVSV.G. (Gift from Xavier Dolcet lab)
pCYC2175	YFP-PBD	The PAK1 binding domain (155 bp) cloned in the pEYFP-C1 vector (4733 bp, Clontech) in the BamHI and BglII sites. Used for locating Rac1-GTP. Acquired of Addgene
ShD1 (human)	Human Cyclin D1 shRNA	shRNA against human Cyclin D1 in pLKO.1-puro vector TRCN0000040038 (Sigma)
ShRalA (human)	Human Ral A shRNA	shRNA against human Ral A in pLKO.1-puro vector TRCN0000004865 (Sigma)
ShRalB (human)	Human Ral B shRNA	shRNA against human Ral B in pLKO.1-puro vector TRCN0000072957 (Sigma)

3 - BIOCHEMICAL TECHNIQUES

3.1 ANTIBODIES

Table 3. Antibodies

Antibody	Reference	IHC	IF	IB
Anti-Ccnd1	Rabbit monoclonal clone EP12, Dako #M3642	Ready to use	1/200[2]	-
Anti-Ccnd1	Mouse monoclonal DCS-6, BD Pharmigen #556470	-	-	1/500
Anti-Paxillin	Mouse monoclonal 349, BD Biosciences #610051	-	1/200	-
Anti-Ral A	Mouse monoclonal 8, BD Pharmigen #610222	-	1/200	1/2000
Anti-Ral B	Rabbit polyclonal, Cell Signaling #3523	-	-	
Anti-HA	Rat polyclonal clone 3F10, Roche 11867423001	1/400	1/200[2]	-
Anti-BrdU	Rat monoclonal BU1/75 (ICR1), Bio-Rad #MCA2060	-		-
Anti-Glut1	Mouse monoclonal SPM498, Thermofisher #MA-11315	-	1/200[2]	-
Anti-GFP	Rabbit polyclonal, Invitrogen A21311	-	1/200[2]	-
Anti-Ki67	Mouse monoclonal, clone MIB-1, Agilent-DAKO.	Ready to use	-	-
Anti-phosphoFAK (Tyr397)	Rabbit monoclonal, clone 31H5L17, Thermofisher #700255	1/100	-	1/500[3]
Anti-CDK4	Rabbit polyclonal C-22, SantaCruz #sc-260	-	-	1/250
Anti-RB	Mouse monoclonal G3-245, BD Pharmigen #554136	-	-	1/500
Anti-Actin	Mouse monoclonal Clone C4, Millipore #MAB1501R	-	-	1/1000
Anti-Rac1	Mouse monoclonal 102, BD Pharmigen #610222	-	-	1/2000
Anti-p21	Mouse monoclonal, Millipore #05-345	-	-	1/500
Anti-p27	Mouse monoclonal, BD Biosciences #610242	-	-	1/500
Anti-MGMT	Mouse monoclonal MT3.1, Millipore #MAB16200	-	-	1/1000
Anti-Tubulin	Mouse monoclonal Clone B-5-1-2, Sigma #T5168	-	-	1/1000
Anti-phosphohistone H2A-X (Ser139)	Mouse monoclonal JBW301, Millipore #05-636	-	1/200	-
Anti-PDGFRα	Rabbit monoclonal D1E1), Cell Signaling #3174	1/100	-	-

IHC: Immunohistochemistry; IF: Immunofluorescence; IB: Immunoblot

1- If not specified, antibodies were used in 0.3% BSA
2- Antibodies used in 4% BSA + 0.04% Tween-20
3- Antibodies used in 3% BSA

3.2 PROTEIN EXTRACTION AND WESTERN BLOT

SDS PROTEIN EXTRACTION

Protein extracts were obtained from cell cultures growing on plates. Culture plates were washed with cold PBS and cells were scrapped in 1xSR (2% SDS and 0.125 M Tris-HCl at pH 6.8). This buffer allows an efficient extraction because it breaks protein interactions and allows the detachment of proteins. Also, SDS denatures and inactivates most enzymes present in the sample, including proteases that could degrade the extract. The volume of buffer used depends on plate size. For example, in a 6-well plate (35-mm diameter) 100 µl 1xSR were added or in a 4-well plate (16-mm diameter) 60 µl were added. They were collected with a scrapper or with a pipette tip. Cells were sonicated twice 10 s at power 8 with an MSE Soniprep 150 sonicator.

SAMPLE QUANTIFICATION BY LOWRY METHOD

The Lowry method was used to determine total protein quantity in the extracts. Bio-Rad reagents were used and calibration was done with BSA. Briefly, 5 µl BSA or 3 µl experimental samples were added per well in a 96-well plate. Next 25 µl reagent A and 200 µl reagent B (fluorogenic substrate) were added to each well and incubated 15 min in darkness at RT. Afterwards; absorbance was read at 595 nm wavelength. For each sample, absorbance values were extrapolated using the calibration curve into protein concentrations.

SDS-POLYACRYLAMIDE GEL ELECTROPHORESIS

Once extracts were quantified, loading samples were prepared by taking a volume corresponding to the same protein amount for each sample and adding 4xSS (20% sucrose, 0.02% bromophenol blue) to a final concentration of 1xSS, as well as 1% ß-mercaptoethanol. In order to achieve complete protein denaturation, samples were boiled 5 min at 95 °C before loading in SDS-PAGE gels. These were prepared from a solution of 30% acrylamide and 2% bis-acrylamide. Polymerization was induced by adding 0.1% TEMED (Sigma-Aldrich) as an initiator of the reaction and 0.05% ammonium persulfate as a catalyst. Discontinuous gels were used formed by two parts with different percentages of acrylamide. At the upper part or stacking gel samples were loaded, and served to concentrate different-sized proteins in a front so that all entered the separating gel (lower part) at the same time. Stacking gel consisted of 5% acrylamide in 125 µM Tris-HCl at neutral pH (6.8). Separating gel was prepared in a basic buffer (375 µM Tris-HCl pH 8.8) with various amounts of acrylamide depending on the molecular weight of the proteins to be detected, ranging from 7.5 to 15%. Gels were subject to a constant current of 20 mA in an electrophoretic solution containing 25 mM Tris, 1.44% glycine and 0.1% SDS. A MiniProtean system from Bio-Rad was used. As a molecular weight marker I loaded an aliquot of the PageRuler™ Prestained Protein Ladder from ThermoFisher (#26616).

PROTEIN TRANSFER

After electrophoresis, proteins were transferred to a PVDF membrane (Immobilon-P, Millipore). Membranes were activated with methanol, hydrated with water and equilibrated in transfer buffer (25 mM Tris, 192 mM glycine, 10 or 20% methanol). A semi-dry system with a 60 mA constant current for 1 h was used. After this, membrane was blocked with 3% BSA in PBST buffer (PBS + 0.1% Tween-20) for at least 1 h at RT.

PROTEIN IMMUNODETECTION

After blocking, several PBST washes were done and a primary antibody of interest was added. In general, primary antibody incubation was carried out overnight at 4°C. Antibody dilutions are shown in table 3. Three PBST washes were done after primary antibody incubation, and then secondary antibody in 0.3% BSA in PBST was added. This was conjugated with HRP peroxidase

(GE Healthcare UK Ltd) and it was normally used at a 1:10000 dilution. Membrane was incubated for 1 h at RT and finally was washed three more times with PBST.

For detection, membrane was incubated 5 min with HRP chemiluminescent substrate (Immobilon Western, Millipore). Finally, signal was visualized with the *Chemidoc™ MP Imaging System* (BioRad) and protein band quantification was performed with the associated software, *Image Lab*.

3.3 RAL ACTIVITY ASSAY

Ral activity was analyzed by measuring the Ral active form, i.e. Ral bound to GTP (van Triest and Bos 2004). To perform this assay Ral-BP1 agarose beads were used (Upstate, cat# 14-415) following manufacturer's instructions. GBM cell lysates were obtained from a 100-mm diameter plate. Pellets were resuspended in 600 µl cold lysis buffer (Tris-HCl 50 mM pH 7.5, NaCl 200 mM, $MgCl_2$ 2.5 mM, DTT 2.5 mM, 1% Triton-X100, and a mix of protease and phosphatase inhibitors). Cells were broken with a Douncer homogenizer and lysates were centrifuged 5 min at 300 g at 4°C. An aliquot from supernatant was collected as "soluble extract" and the rest was incubated 30 min at 4°C with 10 µg Ral-BP1 beads on a roller. After three washes with cold lysis buffer, agarose beads were eluted with 2xSSR (4% SDS, 0.25 M Tris-HCl pH 6.8, 10% sucrose, 2% β-mercaptoethanol, 0.01% bromophenol blue) and boiled 5 min at 95°C. Samples were analyzed by western blotting with a primary antibody against Ral A or Ral B (Table 3). Ral A and Ral B activities were calculated as the ratios between the quantity of Ral A or B from the affinity purification (GTP-bound Ral A or B) and the quantity of Ral A or B from the soluble extract (total Ral A or B).

3.4 YFP-PBD

The YFP-PBD vector encodes the p21-binding domain (PBD) of human PAK1 fused to the yellow (citrine) fluorescent protein. Because PBD binds only to Rac-GTP, the fusion YFP-PBD serves as a probe to monitor localization of activated Rac inside the cell.

Briefly, 48 h after transfection with the YFP-PBD vector cells were seeded on fibronectin for 2 h and then fixed. Photos were taken under the microscope and analyzed with Image J.

3.5 PEPTIDE ARRAY

PamGene's PamChip arrays were used to measure the activity of kinases in lysates from cell lines, xenografts and tumor biopsies. These are based on measuring peptide phosphorylation by protein kinases. The PamChip®4 disposable consists of 4 identical arrays, each array containing 144 (STK; serine/threonine kinase) or 196 (PTK; phosphotyrosine kinase) peptides immobilized on a porous ceramic membrane. The peptide sequences (13 amino acids long) harbor phosphorylation sites derived from literature or computational predictions and are correlated with one or multiple upstream kinases. Fluorescently labelled anti-phospho antibodies are used to detect the phosphorylation level of each peptide in the array. The PamChip® kinase assay workflow consists of three steps: (1) Sample preparation (cell or tissue lysis) with a protein concentration between 0.5 and 2 µg/µl. First, a quick wash with ice cold PBS was done, and cells were lysed by scrapping in 200-300 µl lysis buffer (MPER Buffer 1/100 Halt protease, 1/100 Halt phosphatase, all from PIERCE). Lysates were recovered in an ice cold Eppendorf tube and were incubated 20 min on ice, without vortexing or sonication. Afterwards, samples were centrifuged 20 min at 4°C and supernatant was recovered and aliquoted in different tubes; (2) PamChip® assay. During the assay, the sample solution was pumped through the porous membrane, allowing for faster kinetics and real-time measurements. When the solution was underneath the array, images of each array were taken at several exposure times by the CCD camera in the workstation. Kinase(s) in the sample readily phosphorylate substrates on the PamChip® in the presence of ATP. A FITC-conjugated PY20 antibody, present in the reaction mix, was used to detect phosphorylated serines, threonines and tyrosines. Images were taken every 5 minutes to generate real time kinetics data. (3) Data analysis and knowledge integration. Images were used to generate kinetic data curves for each peptide. The data workflow consisting of image quantification, quality control, statistical analysis, visualization and interpretation was performed using the BioNavigator® software.

3.6 PROTEOME PROFILER

Phospho-Kinase Array is a rapid and sensitive tool to simultaneously detect the relative levels of phosphorylation of 43 kinase phosphorylation sites and two related total proteins without performing numerous immunoprecipitations and western blots. First, cells were rinsed with PBS and resuspended at a density of $1x10^7$ cells/ml in Lysis Buffer. These lysates were rocked gently 30 min at 2-8 °C and then centrifuged at 14000 g for 5 min. Supernatant was transferred into a

clean tube. The maximum lysate volume allowed was 334 µl per array set (A and B). Lysates were used immediately or aliquoted and stored at less than -70 °C. Membranes were blocked 1 h at RT (manufacturer's instructions) and then incubated with cell lysates overnight at 4°C in a rocking platform. Next day membranes were washed three times with washing buffer. Membranes were incubated 2 h at RT on a rocking platform with 1 ml Detection Antibody Cocktail A or B and then washed three times with Wash Buffer. Diluted Streptavidin-HRP was added and incubated 30 min on a rocking platform and washed with Wash Buffer. Finally, Chemi Reagent Mix was applied to membranes and signal detected with Chemidoc (Bio-Rad) and analyzed with Chemidoc software ImageLab.

4 - MICROSCOPY TECHNIQUES

4.1 IMMUNOHISTOCHEMISTRY & HISTOLOGY

BASIC HISTOLOGY

Once animals were sacrificed, brains were extracted and fixed immediately in 2% PFA for 2 h for cryofrozen samples or 4% PFA overnight for paraffin blocks. Cryofrozen brains were photographed under a magnifying glass (Nikon SMZ18) and then placed in a 30% sucrose buffer overnight to get dehydrated. Afterwards, they were placed in cassettes with Optimum Cutting Temperature reagent (OCT) (Tissue-Tek O.C.T. Compound, VWR Cat#25608-930) and were kept at -80°C until cut in the cryostat in 20 µm sections. For embedding in paraffin, PFA fixed brains were placed in cassettes, dehydrated with a series of alcohols and included in paraffin. To study the histology of each sample, 5 µm paraffin block sections were stained with hematoxylin-eosin (H-E) and checked by pathologists.

TISSUE MICRO ARRAYS

Tissue microarrays (TMA) are paraffin blocks produced by placing paraffin samples from different donors in a single microarray block. They allow the simultaneous analysis of different molecular aspects in identical and standardized conditions in a single slide, providing maximum preservation and the use of limited, irreplaceable tissue samples.

Astrocytoma/Glioblastoma TMA 324 was obtained from CNIO Biobank. The use of these samples was approved by the Ethical Committee (CEI) of CNIO.

In addition, two TMAs were constructed using the manual arrayer from Beecher instruments TM. The TMAs contained fixed paraffin-embedded (FFPE) tissue from 17 astrocytoma samples (7 grade II, 10 grade III) and 57 GBM samples. Tumors were classified following the most recent WHO criteria. Samples were obtained from the HUAV surgical pathology files. The study was approved by the local ethics committee and informed consent was obtained from each patient.

Briefly, all tissue samples were histologically examined by two members of the team, and representative tumor or non tumor areas were marked in the corresponding paraffin blocks. Tissue cylinders with a diameter of 0.6 mm were punched from two different tumor areas from each “donor” tissue block and brought into a recipient paraffin block.

IMMUNOHISTOCHEMISTRY

Paraffin blocks of human tumor tissue and mouse tissue samples were sectioned at a thickness of 3 µm, and were dried for 1 h at 65°C before deparaffinization and rehydration of the tissue. Next, an epitope retrieval step was carried out by incubation with a commercial buffer that contains Tris/EDTA 50x at pH 9 in a Pre-Treatment Module, PT LINK (Dako, Glostrup, Denmark) at 95°C for 20 min. Before staining the sections, endogenous peroxidase was blocked by incubating the slides in a 3% H_2O_2 solution. Afterwards, three washes with PBS were done and samples were incubated with primary antibody (Table 3) for 30 min at RT. Next, three more washes with PBS were done and samples were incubated with secondary antibody. If the signal was strong enough, a peroxidase-conjugated secondary antibody for 30 min was used. If necessary, to increase the signal a biotin-conjugated secondary antibody (1:200 dilution, Jackson, 11-065-144) for 30 min was used, followed by incubation with peroxidase-conjugated streptavidin (1:400 dilution, Jackson, 016-030-084) for 15 min at RT. Samples were visualized with the EnVision FLEX Detection Kit (Dako, Glostrup, Denmark) using diaminobenzidine chromogen as a substrate. Slides were counterstained with hematoxylin. Background controls were obtained without the addition of the primary antibody. The immunohistochemical analysis was conducted by pathologists and a researcher to ensure pre-established histological criteria.

Results of immunohistochemical analysis were evaluated using an image automated system ACIS III (Dako). In this work intensities of Ccnd1 and P-FAK were measured. Samples were scanned and the system offered an automatically a value of intensity in each case. Results were evaluated with an image automated system ACIS III (Dako). In this work intensities of Ccnd1 and P-FAK were measured.

CELL PROLIFERATION ANALYSIS

In immunohistochemical analyses, proliferation was evaluated by quantifying Ki-67, a marker that only proliferative cells express. For this, five photos of each tumor were taken and cell proliferation was calculated as Ki-67 positive nuclei versus total nuclei of the image. Photos were taken with a stereomicroscope (Nikon SMZ18) and were manually quantified with Image J program.

4.2 IMMUNOFLUORESCENCE

CELL IMMUNOFLUORESCENCE

For immunofluorescence, cells were seeded in an 8-well glass-bottom plate that allows to take photos in a confocal microscope. Cells were washed with PBS and fixed with 4% PFA for 15 min at RT. Afterwards, each well was washed twice with PBS, cells permeabilized with 0.2% Triton-X100 for 3 min at RT and blocked with 3% BSA (Sigma) for 30 min. Primary antibodies (Table 3) were diluted (1:200) in 0.3% BSA and incubated overnight at 4°C. Next day wells were washed three times with PBS and a corresponding secondary antibody labeled with Alexa 488 or Alexa 594 (Molecular Probes) at a 1:1000 dilution was added in 0.3% BSA in darkness at RT together with Hoechst (Sigma) to stain cell nuclei. *SlowFade* antifade reagent (Molecular Probes) was added to prevent photobleaching. Epifluorescence images were acquired with 10x or 20x objectives in an inverted Olympus IX71 microscope whereas confocal images were obtained with 40x or 60x objectives in an Olympus FV1000i confocal microscope. Finally, to quantify Rac1 accumulation in ruffles Image J was used.

TISSUE IMMUNOFLUORESCENCE

For tissue immunofluorescence, fixed mouse brains were included in OCT (Optimal cutting temperature compound) and cut in the cryostat at 20 μm thickness. Samples were taken to RT

and after being fixed with 4% PFA and washed with PBS, they were permeabilized with methanol-acetone 2 min at -20°C, washed with PBS and blocked with 4% BSA 0.2% Tween-20.

Primary antibodies (Table 3) at a working dilution of 1:200 in 0.8% BSA were added and samples were incubated overnight at 4°C. The next day, after three washes, appropriate secondary antibodies (Alexa 488 or Alexa 594 from Molecular Probes) were added and incubated 1 h at 4°C. Nuclei were stained with Hoechst during this incubation.

For GFP staining a combination of two secondary antibodies was used to increase the signal. First, sample was incubated with an anti-rabbit goat antibody Alexa 488 (or with anti-mouse donkey antibody Alexa 594 if necessary), then washed three times with PBS, and incubated with an anti-goat rabbit antibody Alexa 488 and Hoechst one more hour. Photos were taken with an EVOS FL fluorescence microscope.

5 - EXPERIMENTAL ANIMALS

5.1 PREVIOUS CONSIDERATIONS

The experimental methods used with laboratory animals have been developed according to the recommendations contained in the following legal provisions:

- European Community: Directive 2010/63/EU on protecting animals used for scientific purposes.
  http://europa.eu/legislation_summaries/environment/nature_and_biodiversity/sa0027_es.htm
- Spain: Royal Decree 53/2013, of 1 February, which refers to the applicable rules for the protection of animals used in experimentation and other scientific purposes. https://www.boe.es/diario_boe/txt.php?id=BOE-A-2013-1337
- Spain: Order ECC / 566/2015 where the training requirements that must be met by personnel handling animals used, bred or supplied for experimental purposes and other scientific purposes, including teaching, are established.
  https://www.boe.es/diario_boe/txt.php?id=BOE-A-2015-3564

All the procedures for the manipulation of experimental animals were carried out under the supervision of the relevant personnel at our institution, respecting all legal and ethical regulations in force. In addition, this work has been approved by the Ethical Committee of Animal Experimentation of the University of Lleida.

5.2 SCID MICE

SCID (*Severe Combined ImmunoDeficiency*) mice are characterized by their inability to provide an adequate immune response due to the absence or defect of T and B lymphocytes, as a consequence of a recessive mutation in chromosome 16. At a functional level, this mutation prevents the maturation of the immune system; hence SCID mice cannot fight infections or reject tumors or transplants. These mice are used as an animal model for the study of subcutaneous or xenografted tumors.

5.3 INTRACRANIAL INJECTION

SCID hr/hr mice (12-week-old; 20–25 g) were maintained in specific pathogen-free conditions. Infected cells (5×10^5) were injected by intracranial injection at the right hemisphere (2 mm left to Bregma, 1 mm anterior to Coronal suture, 3 mm depth) (**Figure 10**). Animals were euthanized 21 days later (or 28 in the case of long metastasis assays), brains analyzed by bioluminescence and fluorescence, and finally recovered and fixed with PFA; a sample was included in paraffin for hematoxylin-eosin staining and immunohistochemistry analysis and others were included in tissue freezing medium.

To enable non-invasive monitoring of intracranial tumor growth, cells were transduced with HIV1-based lentiviral vectors expressing firefly luciferase (Fluc). Luciferine was injected in the animals and the signal was recorded twice a week with a PhotonIMAGER and the software Photo-Acquisition. Image analysis was carried out in M3VisionTM.

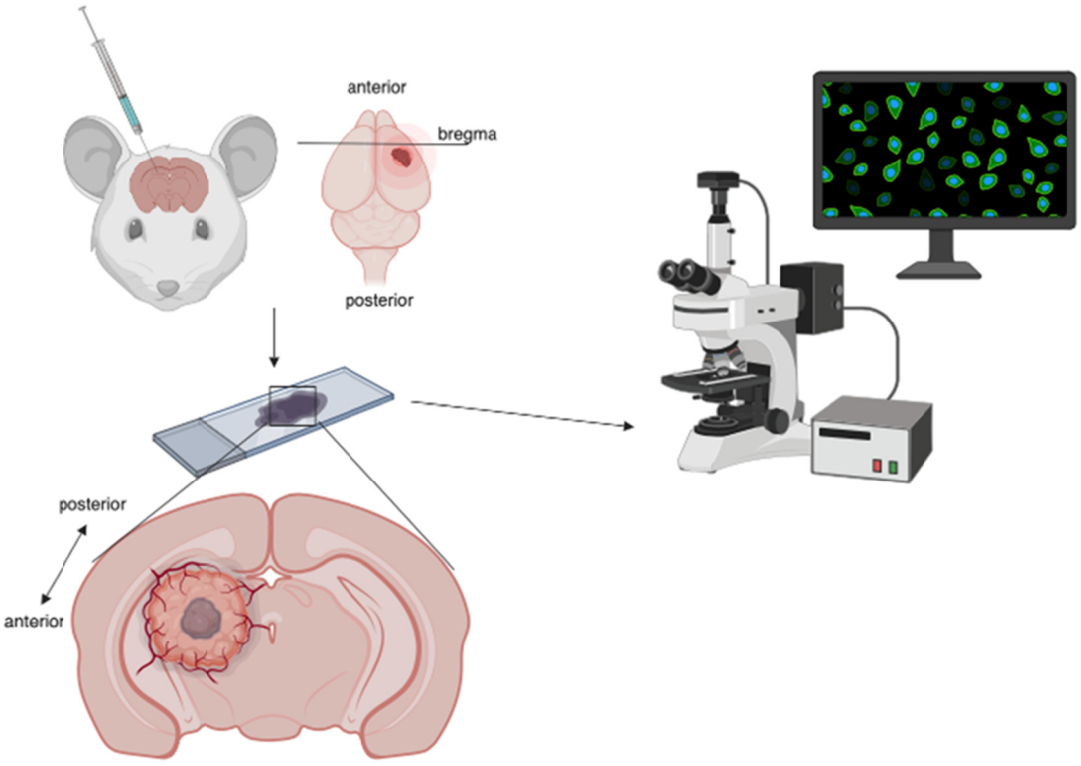

Figure 10. *Representative scheme of intracranial injection followed by cryostat sections and posterior analysis.*

6 - BIOINFORMATIC TOOLS

6.1 IMAGEJ

ImageJ is a program of digital image processing of public domain programmed in Java. This application allows you to view and manage images obtained from any microscope. It is very useful because it allows you to edit or color any image, quantify intensities, count points, select regions of interest, develop co-location analysis, among many other functions.

http://rsb.info.nih.gov/ij/

6.2 GLIOVIS

Gliovis is a platform for the processing of existing databases in glioma. This tool allows the analysis in a very easy and intuitive way of gene expressions, survival curves, and correlations among others.

https://gliovis.shinyapps.io/GlioVis/

6.3 GENE ONTOLOGY

To evaluate the enrichment pattern of the identified peptides in Kinoma, we have used the Gene Ontology platform. The Gene Ontology resource provides a computational representation of our current scientific knowledge about the functions of genes (or, more properly, the protein and non-coding RNA molecules produced by genes) from many different organisms, from humans to bacteria. It is widely used to support scientific research, and has been cited in tens of thousands of publications.

http://geneontology.org/.

RESULTS

CHAPTER 1 - CYTOPLASMIC CYCLIN D1 REGULATES GLIOBLASTOMA INVASION

RETINOBLASTOMA-INDEPENDENT FUNCTIONS OF CYCLIN D1 REGULATE THE INVASION EFFICIENCY OF GLIOBLASTOMA CELLS

To address the importance of the Ccnd1-CDK4-RB1 regulatory pathway in GBM, first we analyzed the expression levels of Ccnd1, CDK4 and RB1 in primary cultures from human GBM and grade II astrocytoma biopsies (Figure 11A). All the GBM samples showed expression of Ccnd1 and CDK4, most displaying higher levels than the low grade astrocytoma samples (see below). In contrast, RB1 expression exhibited different levels among GBM samples and was not detected in two (GBM65 and GBM66). In order to confirm the absence of RB1 expression in GBM65, we tested the growth rate of these cells after inhibition of the CDK4 activity with Palbociclib as compared to the RB1-positive strain GBM6. As expected, Palbociclib brought down the growth rate of the GBM6 strain (Figure 11B) but had no effect on the growth of GBM65 (Figure 11C). This result is in agreement with previous works that showed that the effect of Palbociclib on the proliferation rate of GBM cells depends on RB1 status (Cen et al. 2012; Michaud et al. 2010; Wiedemeyer et al. 2010).

To test the importance of Ccnd1-CDK4 activity on GBM invasiveness, GBM cells expressing different levels of RB1 were pre-incubated either with or without Palbociclib and then transferred to a matrigel-coated transwell. The invasion capacity of GBM cells was clearly reduced by Palbociclib independently of RB1 status (Figure 11D; Figure 12A and 12C), whereas cell viability was not affected by the treatment with the inhibitor (Figure 11E; Figure 12B and 12D). Similarly, after the knockdown of Ccnd1, the invasion efficiency was reduced in the RB1-negative GBM65 cells as well as in the RB1-positive GBM6, U251-MG and U87-MG cells (Figure 11F; Figure 12E, 12G and 12H). Also, the efficiency of spreading on fibronectin was increased in Ccnd1-defective cells (Figure 11G; Figure 12I and 12J). We conclude that Ccnd1-associated activity promotes cell invasion and reduces adhesion in primary GBM cells independently of RB1.

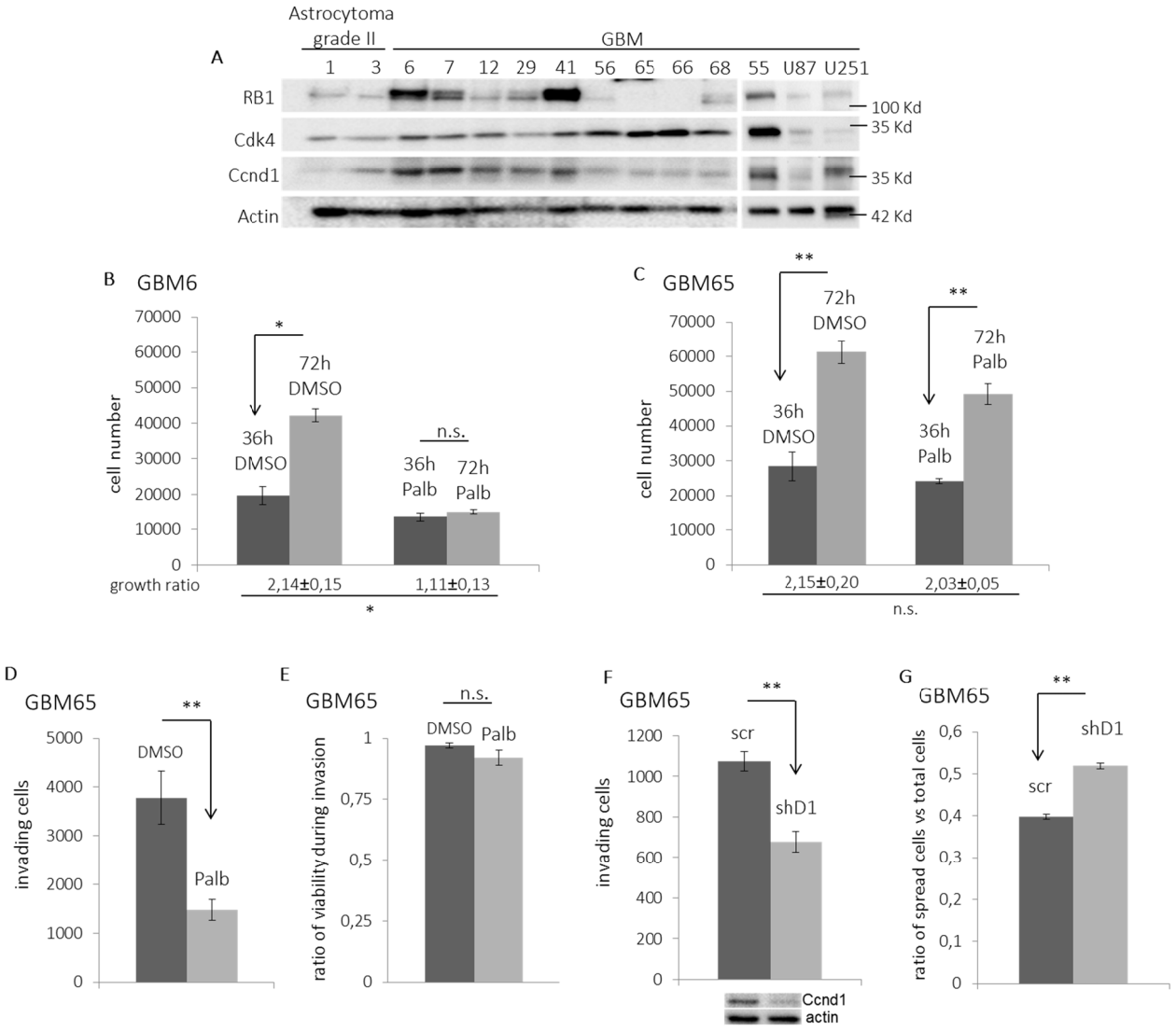

Figure 11. *Cyclin D1 regulates the efficiency of cell invasion and adhesion independently of retinoblastoma.* **A)** Immunoblot to detect the levels of Ccnd1, CDK4 and RB1 in different primary glioblastoma cells (GBM), low grade gliomas and glioblastoma cell lines. Actin staining was used as loading control. **B** and **C)** Respectively, the same number of RB1-positive (GBM6) and RB1-negative (GBM65) cells were treated with the Ccnd1-CDK4 inhibitor Palbociclib (time 0) and cell number was determined at 36 and 72 hours after Palbociclib addition. The experiment was repeated three times (n=3). **D)** RB1-negative GBM65 cells were incubated in the presence of Palbociclib (5 µM) in a transwell device coated with matrigel at 37°C and 5% CO_2. After eight hours of incubation, invading cells were counted (n=3). **E)** Cells in D were incubated with Palbociclib (5 µM) for eight hours, and after this time, viable and total cells were counted (n=3). The ratio of viable (trypan-blue negative) cells versus total cells is drawn. **F)** GBM65 cells were infected with scramble (scr) or shRNA anti-Ccnd1 (shD1) and the invasion efficiency tested as in D (n=5). The lower panel shows the levels of Ccnd1 and actin as a loading control. **G)** RB1-negative GBM65 cells infected with scramble (scr) or shRNA anti-Ccnd1 (shD1) were seeded in fibronectin plates and incubated for 30 minutes at 37°C and 5% CO_2. After this incubation, spread and total cells were counted (n=3). For all the experiments, data are the mean ± SEM and statistical significance was determined by student-t test. *($p \leq 0.05$) ** ($p \leq 0.01$). ns = not significant.

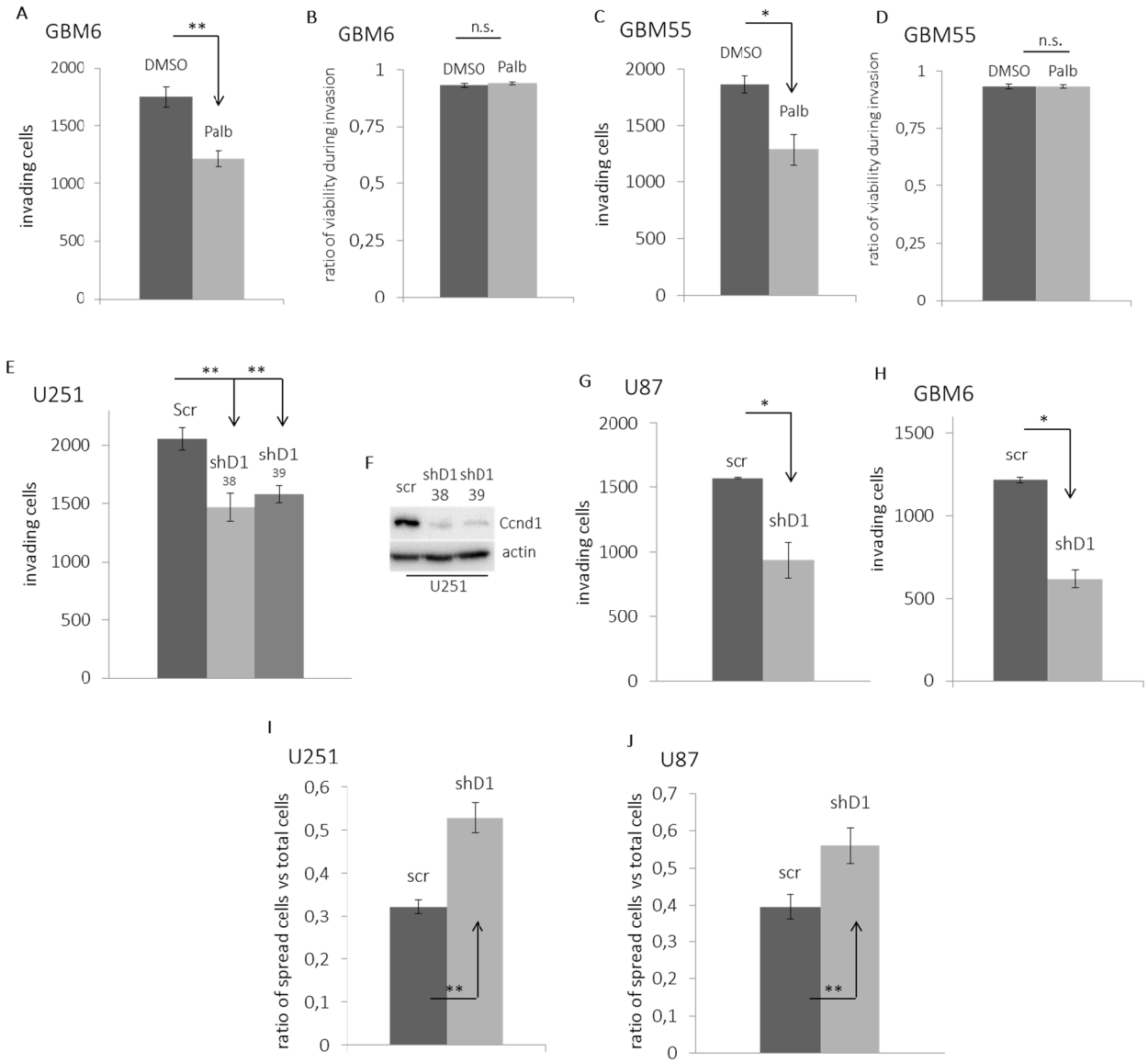

Figure 12. *Cyclin D1-CDK4 activity regulates the efficiency of cell invasion in glioblastoma cells*. **A** and **C)** GBM cells were incubated in the presence of Palbociclib (2 µM) in a transwell device coated with matrigel at 37ºC and 5% CO_2. After eight hours of incubation, invading cells were counted (n=3). **B** and **D)** Cells in **A** and **C** were incubated with Palbociclib (2 µM) for eight hours, and after this time, viable and total cells were counted (n=3). The ratio of viable (trypan-blue negative) cells versus total cells is drawn. **E)** U251-MG cells were infected with scramble (scr) or with two different shRNAs anti-Ccnd1 (shD138 and shD139) and the invasion efficiency tested as in A (n=4). **F)** The downregulation of Ccnd1 in E was tested by immunoblot. Actin was used as a loading control. **G** and **H)** U87-MG and GBM6 cells were respectively infected with scramble (scr) or with the shRNA anti-Ccnd1 shD138 and the invasion efficiency tested as in **A** (n=3). **I** and **J)** U251-MG and U87-MG cells were infected with shD138 or with a scramble shRNA as a control. To test spreading, cells were seeded in serum-free medium in fibronectin-coated plates. Thirty minutes later, the proportion of spread cells was determined and plotted (n=4). For all the experiments, data are the mean ± SEM and statistical significance was determined by student-t test. *($p \leq 0.05$) ** ($p \leq 0.01$). ns = not significant.

LOCALIZATION OF THE CYCLIN D1-CDK4 ACTIVITY IN GLIOBLASTOMA CELLS

Previous data suggest that Ccnd1-CDK4 regulates invasiveness in tumor cells by cytoplasmic mechanisms (Noel P. Fusté et al. 2016; Zhong et al. 2010). Since GBM is a highly invasive tumor, we have studied in depth the localization of Ccnd1 in GBM cells. By using tissue microarrays (TMA), we have confirmed that Ccnd1 expression is higher in GBM versus grade I and II astrocytoma cells (Figure 13A and 13B) (Chakrabarty, Bridges, and Gray 1996; Martínez-Sáez et al. 2016). However, in all those samples only a small proportion of cells showed clear cytoplasmic signal for Ccnd1 (Figure 13C). This result was not completely unexpected since in other solid tumors Ccnd1 is preferentially accumulated in the cytoplasm of cells located at the invasive fronts (Noel P Fusté et al. 2016). Then, to better analyze Ccnd1 localization during GBM invasion, we have used a mouse model of gliomagenesis, which allows us to visualize the tumor dissemination along the entire brain (Ozawa et al. 2014). We infected neonatal *Nestin/tv-a CDKN2A-/-* mice with an RCAS retroviral vector expressing human PDGFα. At four month of age, these mice showed human-like proneural GBM (Figure 13D). We found a strong nuclear signal for Ccnd1 in these tumors, but interestingly we also detected GBM cells containing cytoplasmic Ccnd1 that were escaping outside the tumor (Figure 13D). These cells also showed positive PDGFα receptor staining, a marker of proneural-like tumor cells (Ozawa et al. 2014). This result agrees with the possibility that cytoplasmic Ccnd1 plays a role in GBM cells during the invasion of the surrounding brain tissue.

To further characterize the subcellular localization of Ccnd1 in the invasive GBM cells, we have used a xenograft model wherein human GBM cells (U87-MG) were injected into the brains of SCID mice. To determine the localization of Ccnd1, U87-MG cells were infected with lentiviral particles harboring an HA-Ccnd1 construct (Figure 15B). Three weeks after the injection, mice developed intracranial tumors. We have observed that a high proportion of cells in the tumor mass showed HA-Ccnd1 accumulated in the nucleus (Figure 14A and 14C). In contrast, most evaded cells exhibited a sharp cytoplasmic signal for HA-Ccnd1 (Figure 14B; Figure 15A). This result agrees with the possibility that cytoplasmic Ccnd1 plays a role in GBM cells during the invasion of the surrounding brain tissue. Moreover, we have observed that Ccnd1 also co-localizes with cytoplasmic targets such as Pxn (Noel P. Fusté et al. 2016) and Ral A (Fernández et al. 2011) in the cytoplasm and membranes of primary GBM cells (Figure 14D and 14E; Figure 15C). These results reinforce the idea that cytoplasmic Ccnd1 could promote the invasion capacity of human GBM cells through the regulation of Pxn and Ral GTP activity.

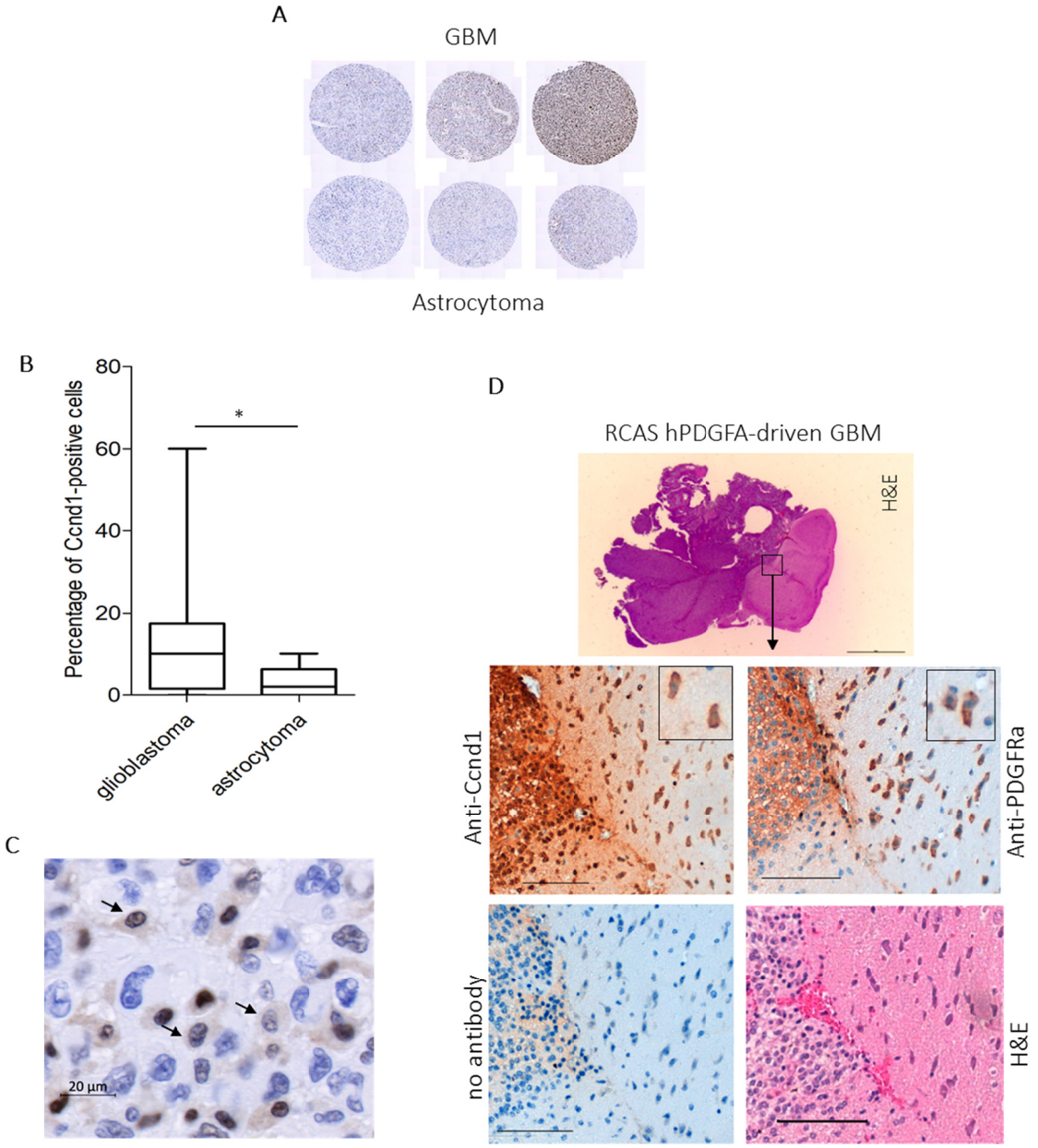

Figure 13. *The expression and localization of cyclin D1 in glioblastoma*. **A)** Representative Ccnd1 staining of glioma samples from the Tissue MicroArray (TMA). **B)** Boxplot representing the proportion of Ccnd1-positive cells in the samples of low-grade astrocytoma versus GBM. Mann–Whitney U test demonstrated a significant difference between the Ccnd1 percentages in lower grade glioma and GBM (p=0.022). **C)** Representative image of GBM cells expressing cytoplasmic Ccnd1. Arrows indicate cells with cytoplasmic localization. **D)** Tumors were generated by the injection of RCAS-hPDGFα viruses in neonatal mice (Nestin/tv-a;CDKN2A-/-). Images from the immunohistochemical analysis with the indicated antibodies and H&E from the selected region. The images correspond to consecutive slices. Boxes show an enlarged region. Scale bars, 100 µm.

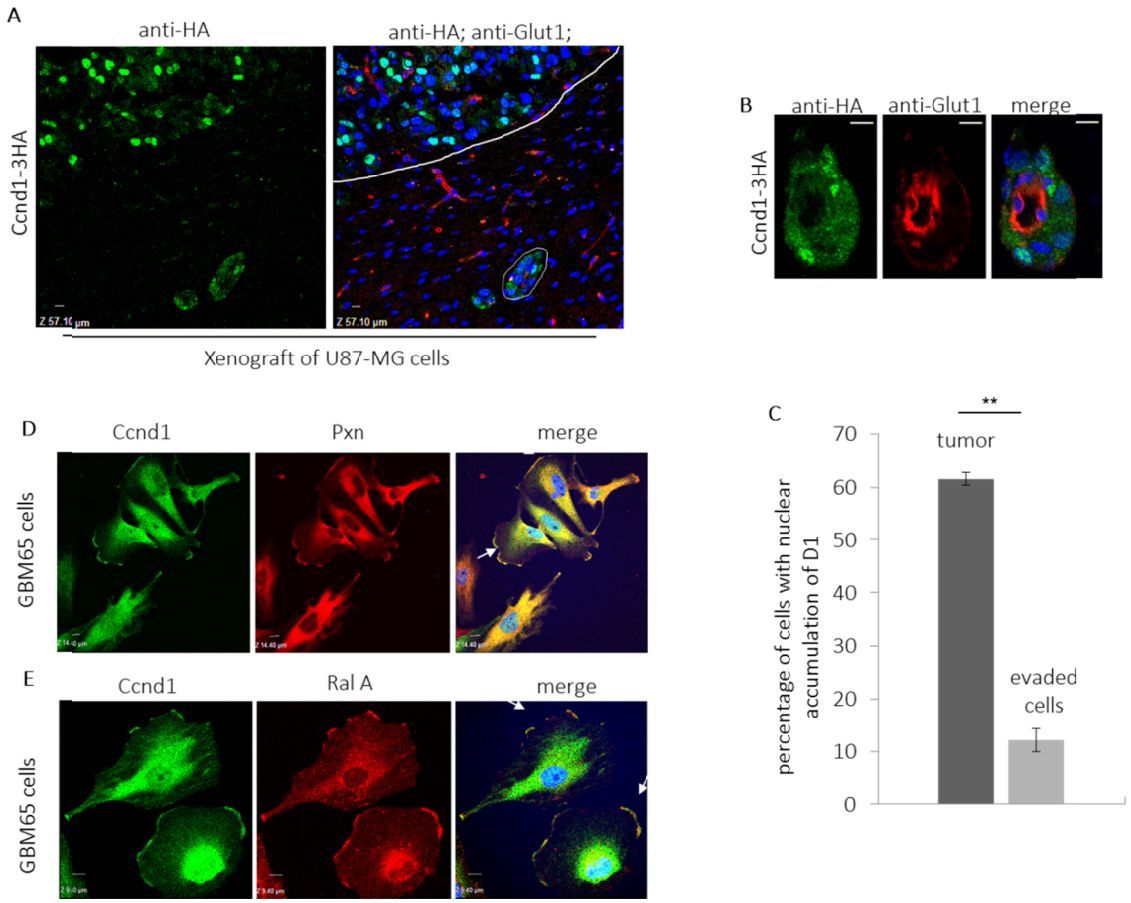

Figure 14. *Cyclin D1 localizes in the cytoplasm of glioblastoma cells and co-localizes with paxillin and Ral A (Part 1).* **A)** U87-MG cells infected with lentiviral particles containing a 3HA-Ccnd1 were injected into the brains of SCID mice to establish intracranial tumors. Three weeks after injection, brains were cryopreserved and processed for IF. The antibodies used were anti-HA (green) and anti-Glut1 for the detection of blood vessels (red). Images were acquired by confocal microscopy (10 µm bar). Nuclei were stained with Hoechst (blue). The white contour designates regions with tumor cells. **B)** Representative image of evaded cells in A. **C)** From three different brains, we have counted the number of infected cells (green cells) showing nuclear accumulation of HA-Ccnd1. Data are the mean ± SEM and statistical significance (n=3) was determined by student-t test (** p≤0.01). **D** and **E)** Cells were seeded in fibronectin plates for two hours, then fixed in 4% PFA and permeabilized with 0.2% Triton X-100. Images were acquired by confocal microscopy (10 µm bar). Nuclei were stained with Hoechst (blue). The antibodies used were Anti-Ccnd1 (green), anti-Pxn (red) in C and anti-Ral A (red) in D.

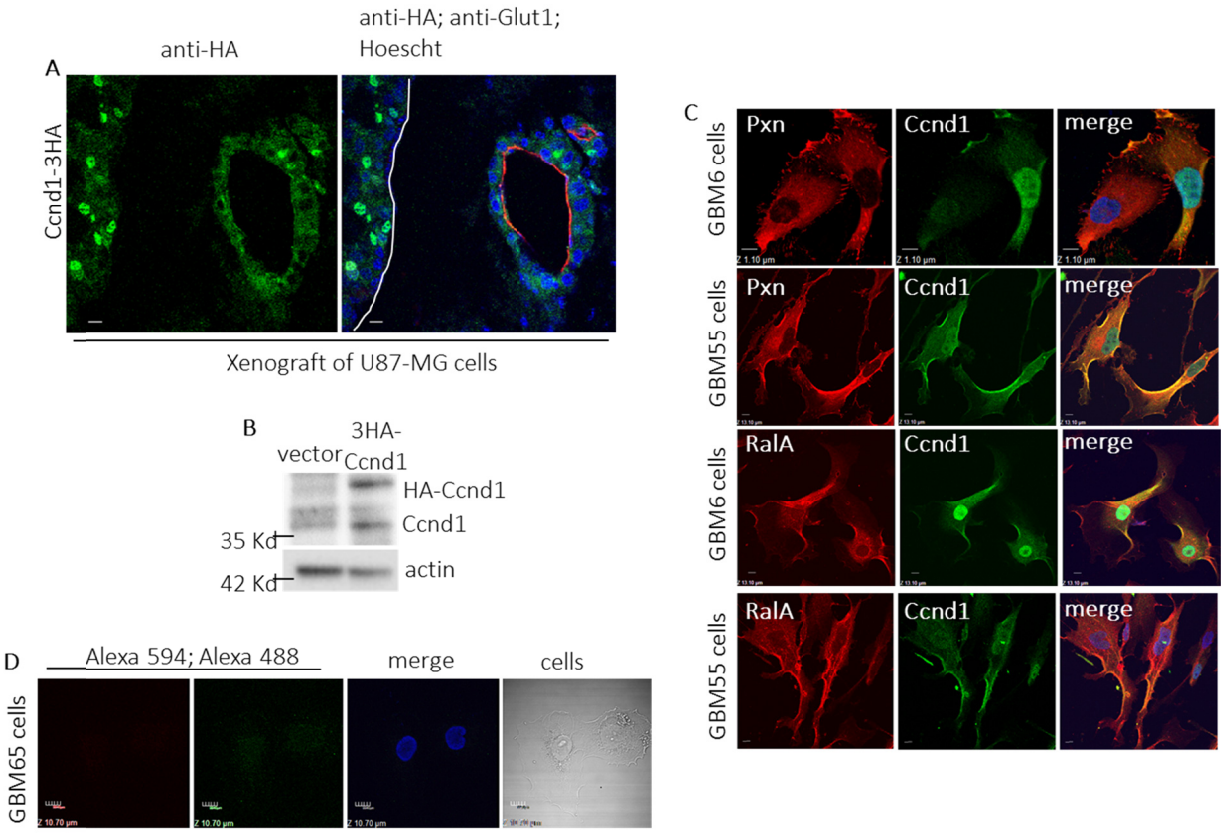

Figure 15. *Cyclin D1 is localized in the cytoplasm of glioblastoma cells and co-localizes with paxillin and Ral A (Part 2).* **A)** Intracranial tumors were established injecting U87-MG cells infected with lentiviral particles containing a 3HA-Ccnd1 into the brains of SCID mice. Three weeks after injection, brains were cryopreserved and processed for IF. The antibodies used were anti-HA (green) and anti-Glut1 for the detection of blood vessels (red). Images were acquired by confocal microscopy (10 µm bar). Nuclei were stained with Hoechst (blue). The white contour designates the tumor mass perimeter. **B)** The expression of 3HA-Ccnd1 in the U87-MG cells was determined by immunoblot (DCS6 antibody). Actin was used as a loading control. **C)** Cells were seeded in fibronectin plates for 24 hours, then fixed in 4% PFA and permeabilized with 0.2% Triton X-100. Images were acquired by confocal microscopy (10 µm bar). Nuclei were stained with Hoechst (blue). The antibodies used were Anti-Ccnd1 (green), anti-Pxn (red) and anti-Ral A (red). **D)** GBM65 cells incubated only in the presence of secondary antibodies were used as a control.

CYCLIN D1 PROMOTES INVASION BY HUMAN GLIOBLASTOMA CELLS THROUGH THE STIMULATION OF RAC1, FAK AND RAL A ACTIVITIES

We have analyzed the levels of Rac1 activation in GBM cells with YFP-PBD, a construct that is a fluorescent biosensor of Rac1 activity (Hoppe and Swanson 2004). The p21-binding domain of PAK1 (PBD) specifically binds to Rac1-GTP forms. GBM65 cells were infected with interference RNA against *CCND1* or with a scramble RNA as a control. Once Ccnd1 was downregulated, cells were transfected with the YFP-PBD construct. Two days after transfection, we seeded the cells

on fibronectin for 2 h before fixation and processing. The number of cells with accumulation of YFP signal in the membrane or protrusion tips was lower in GBM cells knocked down for Ccnd1 (**Figure 16A and 16B**). This was indicative of lesser Rac1 activity associated to the membranes in the absence of Ccnd1.

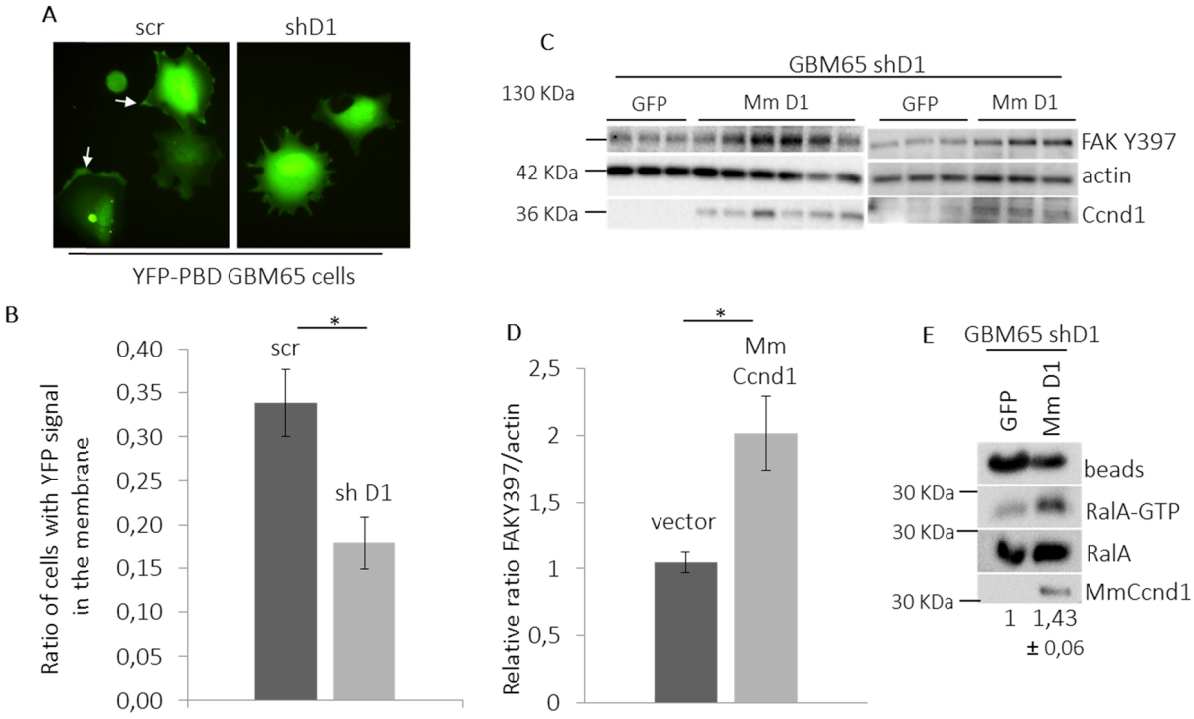

Figure 16. *Cyclin D1 stimulates Rac1 and Ral A activities in human glioblastoma cells.* **A)** GBM65 cells were infected with a scramble (scr) or an anti-Ccnd1 (shD1) shRNA, and 48 hours later, transfected with YFP-PBD. Transfected cells were seeded in fibronectin-coated plates for two hours and next fixed for ten minutes on ice in 2% PFA to avoid YFP-signal loss (10 µm bar). Two representative images are shown. Arrows indicate membrane regions with YFP accumulation. **B)** YFP signal was measured with ImageJ. Mean values and confidence limits of the ratio of cells displaying YFP-signal accumulation in membrane (α=0.05; Cells counted: n≥ 50) are represented. **C)** Knockdown GBM65 cells (shD1) were transfected with a mouse Ccnd1-expression vector (Mm D1, n=9) or a control vector (GFP, n=6). Cells were maintained with low serum for 16 hours before collecting samples. The amount of FAK Y397, β-actin and Ccnd1 was determined by immunoblot. **D)** The levels of protein were determined by densitometry with the Image-Lab 4.0.1 software from BioRad. β-actin was used as a loading control. Data are expressed as mean ± SEM. Significance was determined by a t-test. **E)** Knockdown GBM65 cells (shD1) were transfected with a mouse Ccnd1-expression vector (Mm D1) or a control vector (GFP), and incubated in 10%-serum medium for 24 hours. Then, active Ral A-GTP was affinity purified with Ral BP-beads from cell lysates. Ral A-GTP and total Ral A were detected by immunoblotting. RalBP-beads were used as loading controls. Mm Ccnd1 amount is also shown. The experiment was independently repeated twice. Relative mean values ± SD for the Ral A-GTP/total Ral A ratios are shown.

In order to determine the impact of Ccnd1 expression on FAK and Ral GTPase activation, we stably downregulated human Ccnd1 in GBM65 cells by RNA interference, and then transfected with a mouse Ccnd1-expression vector or a control vector. First we determined the level of FAK phosphorylation at tyrosine 397 by immunoblot. Consistent with the Rac1 results obtained above, the immunoblot revealed that phosphorylation of FAK at Y397 is stimulated by the expression of Ccnd1 (Figures 16C and 16D). We have also observed an increase of the Ral GTP amount in GBM65 cells expressing mouse Ccnd1 (Figure 16E). The overall data lead us to think that Ccnd1 could regulate invasiveness in GBM cells through the Pxn-FAK-Rac1 and Ral activation pathways.

To test this possibility, we first infected GBM65 cells either with an allele of Pxn (Pxn S83A S178A) that cannot be phosphorylated by Ccnd1-CDK4 or with a dominant negative allele of Ral A (Ral AS31N) (Figure 17B). Infected cells were incubated in a transwell device coated with matrigel. The GBM cells expressing the non-phosphorylatable Pxn or the Ral A dominant negative alleles showed a decrease in their efficiency of invasion, suggesting that active Pxn and Ral pathways are required for GBM invasion (Figure 17A). In a second experiment, we infected GBM65 cells with a phosphomimetic allele of Pxn (S83E S178E), with Rgl2-CAAX (Ral GTPase activator), or with an empty vector (Figure 17D). Then, we tested the invasion capacity of these cells after inhibition of Ccnd1-CDK4 activity with Palbociclib. In the presence of the phosphomimetic or the hyperactive allele of Rgl2, the inhibition of Ccnd1-dependent activity did not reduce invasion to the same extend as the control (Figure 17C). This result is consistent with the interpretation that Ccnd1-CDK4 regulates invasion of GBM65 cells through Pxn and Ral pathways.

Finally, we also tested the dependence of GBM-cell adhesion on Ccnd1, Pxn and Ral activities. U251-MG cells stably expressing the interfering RNA against Ccnd1 were co-transfected with mouse Ccnd1 fused to GFP, the non-phosphorylatable Pxn allele (S83A S178A), a dominant negative allele of Ral B (Ral BS28N), or an empty vector. Cells expressing Ccnd1-GFP required more time to spread on fibronectin, but this delay was not observed in the presence of non-active alleles of Pxn or Ral GTPase (Figure 17E). This result suggests that ccdn1 also regulates the adhesion of GBM cells through Pxn and Ral pathways.

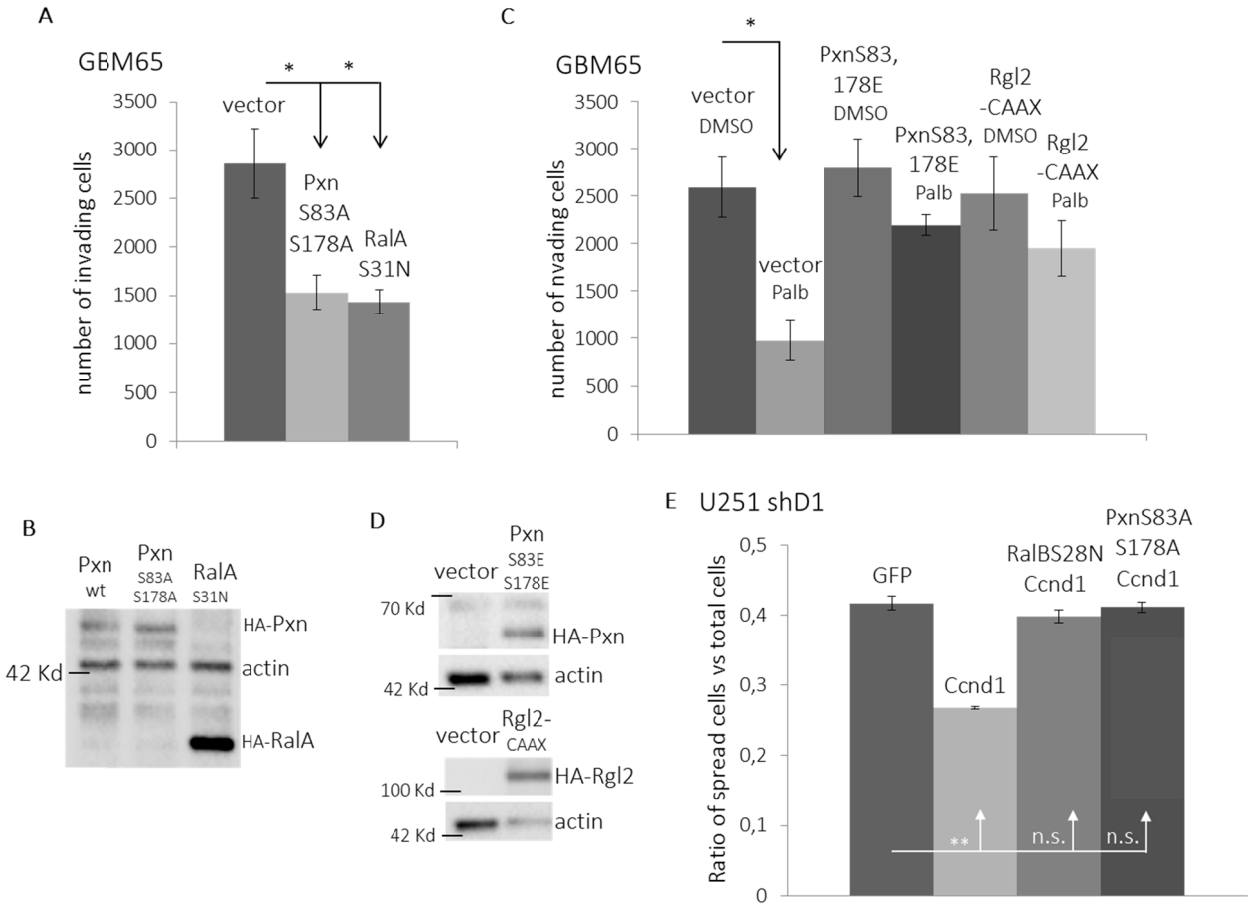

Figure 17. *Cyclin D1 promotes invasion of human glioblastoma cells through paxillin phosphorylation and Ral activation.* **A)** GBM65 cells were infected with the non-phosphorylatable Pxn allele, the dominant negative allele Ral A S31N, or with an empty vector. Forty eight hours later, cells were seeded in 24-well transwell filters previously coated with matrigel, and allowed to invade for seven hours. Relative values are expressed as mean ± SEM (n=3). Significance was determined by one way ANOVA and Tukey-HSD post-test (*p<0.05). **B)** Immunoblots showing the expression of Pxn and Ral alleles (rat anti-HA) in the infected cells in A. Actin was used as a loading control. **C)** GBM65 cells were infected with the phosphomimetic Pxn allele, with Rgl2-CAAX, or with an empty vector. The invasion efficiency was tested as in A but cells were treated with palbociclib, or DMSO as a control. **D)** Immunoblots showing the expression of Pxn and Ral alleles (rat anti-HA) in the infected cells in C. Actin was used as a loading control. **E)** U251 cells stably expressing shD1 were transfected with GFP vector as a control or with Ccnd1-GFP, and then co-transfected with the non-phosphorylatable Pxn allele (S83A S178A) or with the hyperactive allele Ral BS28N. Percentage of spreading was determined as in **Figure 11G**. Values are expressed as mean ± SEM (n=3). Significance was determined by one way ANOVA and Tukey-HSD post-test (**p<0.01)

ACCUMULATION OF CYCLIN D1 IN THE MEMBRANE PROMOTES GLIOBLASTOMA SPREAD *IN VIVO*

In a previous work, we fused the farnesylation site of K-Ras protein (CAAX) to the C-terminus of Ccnd1, generating a cyclin that associates to the membrane and promotes Ral activation and cell invasion in prostate and endometrium tumor cell lines (Noel P Fusté et al. 2016). To apply a similar approach to GBM cells, luciferase-expressing U87-MG cells were co-infected with a lentiviral-GFP vector and Ccnd1-CAAX, wt Ccnd1, or an empty vector. Then, cells were inoculated in mice by intracranial injection, and the animals were euthanized four weeks later. The localization and size of the tumors were analyzed by luminescence (Figure 18A). Tumors harboring Ccnd1-CAAX exhibited distant nodes from the original tumor (Figure 18B and 18C) and showed disseminated groups of tumor cells (cell foci) into the surrounding brain tissue (Figure 18F and 18G). Conversely, control tumors remained for the most part encapsulated (Figure 18H and 18I). By ki67 staining, we determined that the proliferative status of the induced tumors was not significantly different independently of the Ccnd1 allele expressed (Figure 18D and 18E). To evaluate the tumor dissemination, we defined three areas (proximal, intermediate and distal) around the tumor mass (Figure 18K and 18L). We calculated the number of cell foci in each area (Figure 18M). Those tumors that showed intermediate and distal cell foci were considered disseminated tumors. The total number of dispersed tumors was significantly increased in Ccnd1-CAAX samples (Figure 18J). Finally, we confirmed that Ccnd1-CAAX was localized in the cell membrane of evaded tumor cells (Figure 19). In Figure 20 we can observe all the analyzed brains. Overall, these results indicate that the accumulation of Ccnd1 in the membrane of GBM cells promotes GBM dissemination *in vivo*.

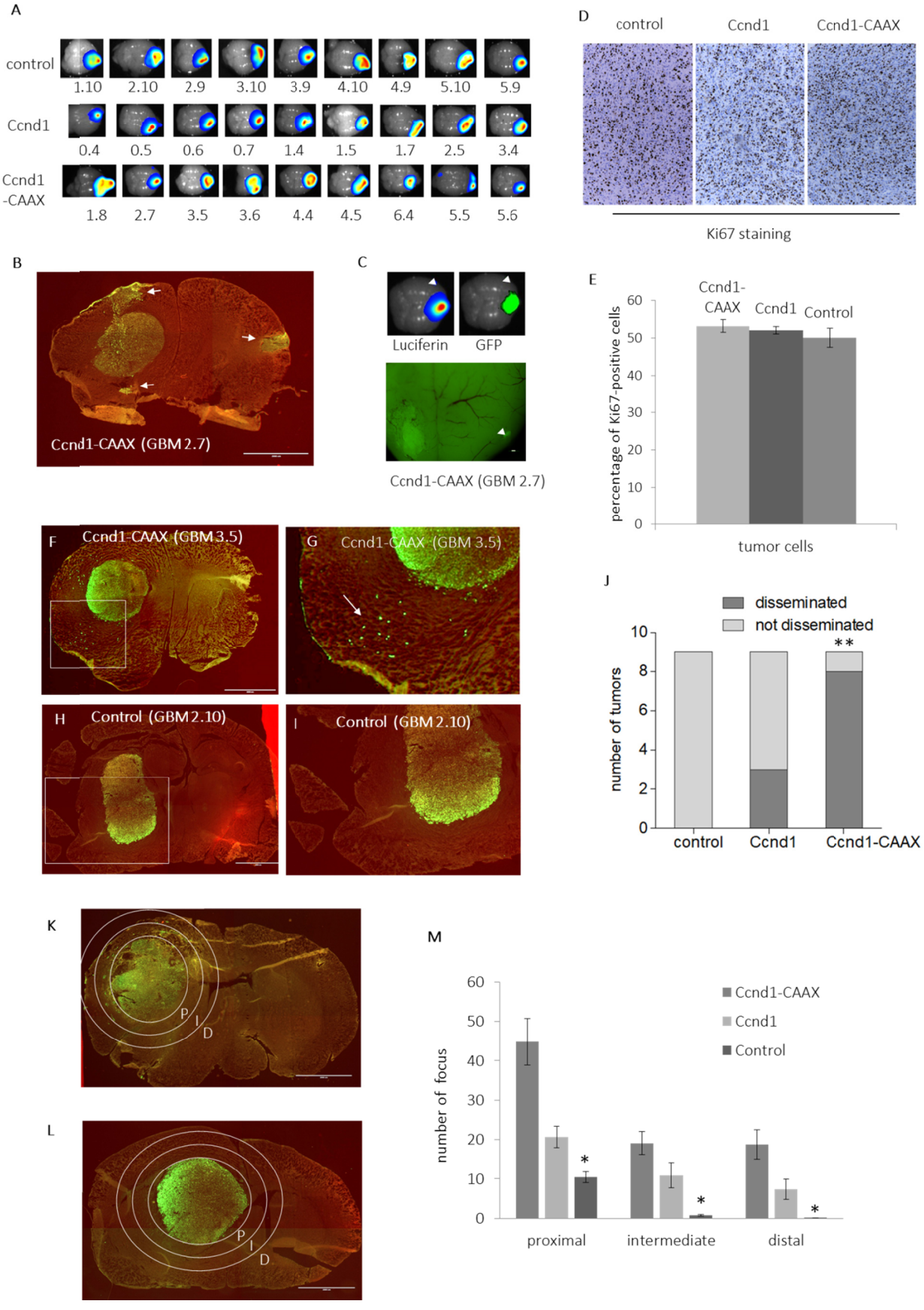
A
control
1.10 2.10 2.9 3.10 3.9 4.10 4.9 5.10 5.9
Ccnd1
0.4 0.5 0.6 0.7 1.4 1.5 1.7 2.5 3.4
Ccnd1 -CAAX
1.8 2.7 3.5 3.6 4.4 4.5 6.4 5.5 5.6
D
control
Ccnd1
Ccnd1-CAAX
Ki67 staining
B
Ccnd1-CAAX (GBM2.7)
C
Luciferin
GFP
Ccnd1-CAAX (GBM 2.7)
E
Ccnd1-CAAX
Ccnd1
Control
percentage of Ki67-positive cells
tumor cells
F
Ccnd1-CAAX (GBM3.5)
G
Ccnd1-CAAX (GBM 3.5)
H
Control (GBM2.10)
I
Control (GBM2.10)
J
disseminated
not disseminated
number of tumors
control
Ccnd1
Ccnd1-CAAX
K
P
I
D
L
P
I
D
M
Ccnd1-CAAX
Ccnd1
Control
number of focus
proximal
intermediate
distal

Figure 18. *Expression of cyclin D1 in the membrane induces glioblastoma dissemination in vivo.* **A)** Tumor location and size were determined by luciferine-mediated luminescence. **B)** Representative image of a tumor expressing Ccnd1-CAAX showing disseminated nodules (arrows). **C)** Luminescence and GFP pictures showing a contralateral nodule in the sample 2.7. **D)** Representative pictures of Ki67staining. **E)** The percentages of Ki67-positive cells in the tumors were plotted. Human U87-MG cells stably expressing luciferase were co-infected with lentiviruses harboring GFP and Ccnd1-CAAX, wt Ccnd1, or an empty vector. Tumors were induced in mice by intracranial injection of these cells, and four weeks after injection mice were euthanized. Brains were processed for cryopreservation. To detect tumor cells (green), serial slides of the brain were immunostained with a rabbit anti-GFP antibody conjugated with Alexa Fluor-488 (from Invitrogen). The mouse brain (red) was contrasted with a secondary anti-mouse Alexa Fluor-594 antibody (from Invitrogen). **F** and **G)** Representative images of a tumor expressing Ccnd1-CAAX showing evaded tumor cells (arrow). **H** and **I)** Representative images showing an encapsulated control tumor. **J)** Plot showing the number of disseminated tumors versus total (n=9). The statistical significance was calculated with a Fisher's exact test (**p<0.01). Quantification of GBM dissemination *in vivo*. **K** and **L)** we have defined three areas (P-proximal, I-intermediate and D-distal) around the tumor mass to estimate the extent of tumor dissemination. **M)** Plot showing the number of cells foci at different distances of the tumor mass. The statistical significance was calculated with a Kruskal-Wallis test (* p<0.05).

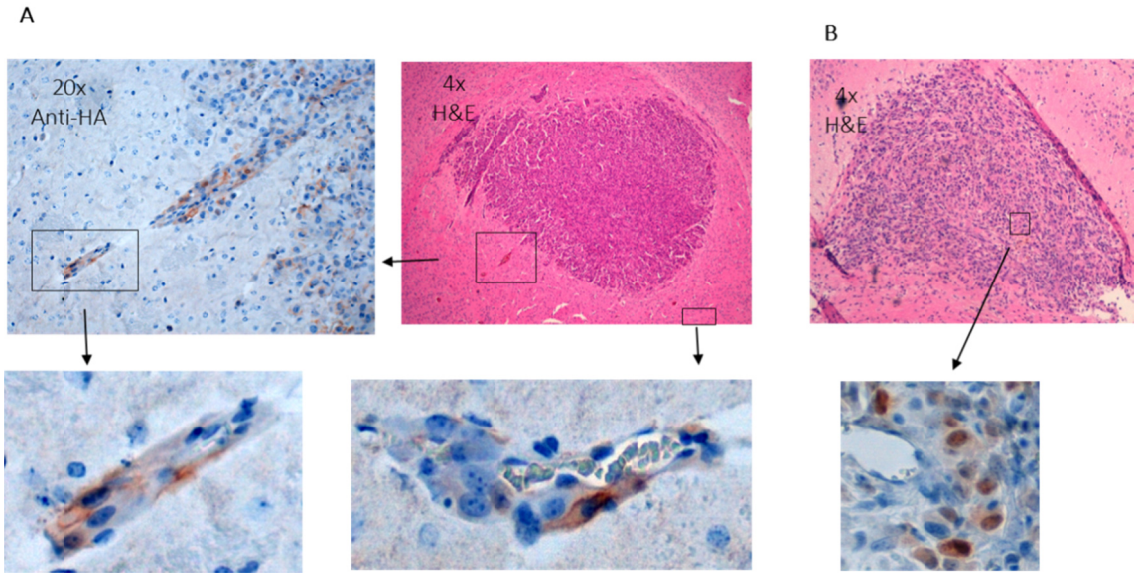

Figure 19. *Cyclin D1-CAAX localizes in the membrane of human U87-MG cells in intracranial induced tumors.* Human U87-MG cells were infected with lentiviruses harboring HA-Ccnd1-CAAX **A)** or HA-Ccnd1 **B)**. These cells were inoculated by intracranial injection in nude mice, and three weeks later mice were sacrificed. Brains were obtained and included in paraffin for IHC detection. H&E staining was used to visualize the induced tumor. Ccnd1 localization was detected with a rat monoclonal anti-HA antibody and nuclei were stained with hematoxylin.

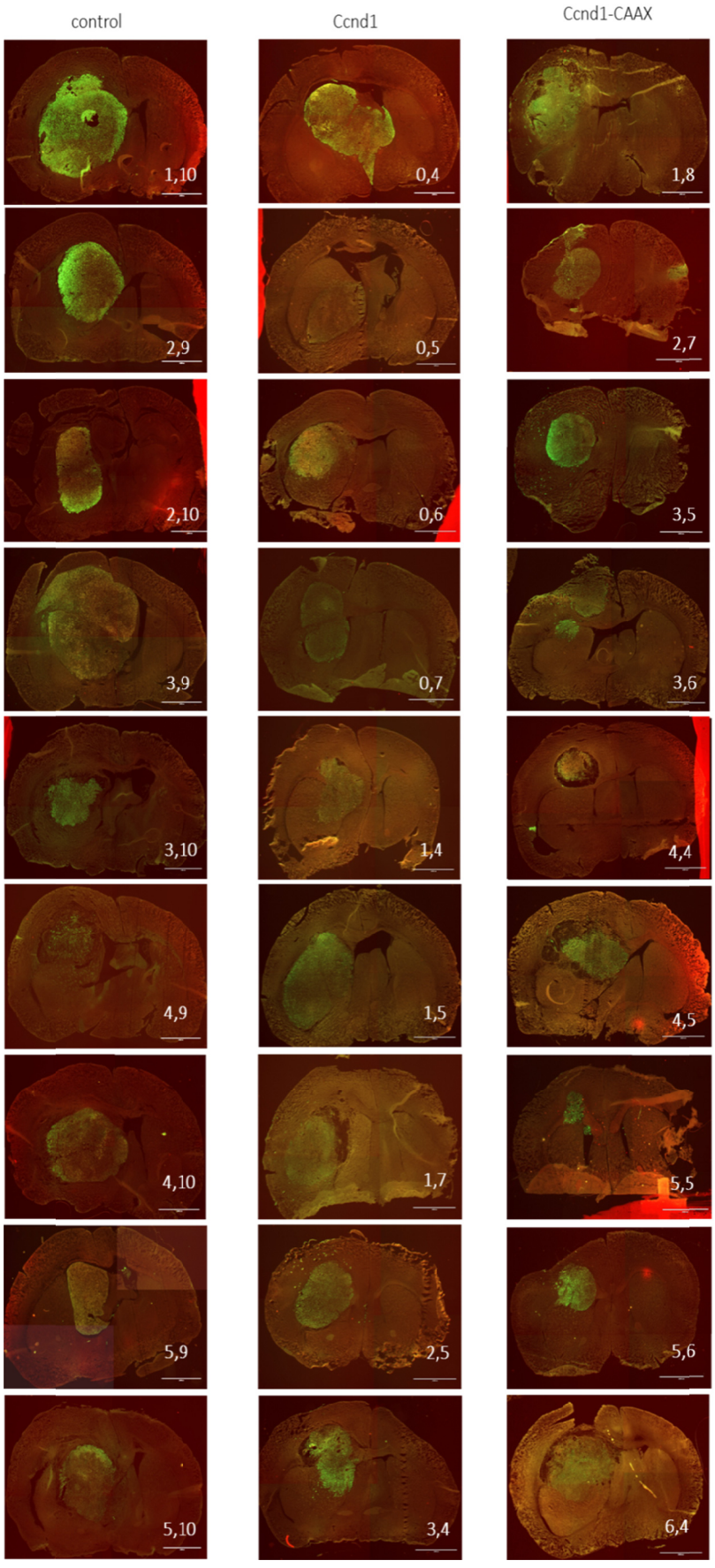

Figure 20. *Representative images of mice brain tumors by intracranial injection of tumoral cells.* To detect tumor cells (green), serial slides of the brain were immunostained with a rabbit anti-GFP conjugated with Alexa Fluor-488 (from Invitrogen). The mouse brain (red) was contrasted with a secondary anti-mouse Alexa Fluor-594 (from Invitrogen).

CHAPTER 2 – ROLE OF RAL GTPASES IN GLIOBLASTOMA GROWTH AND DISSEMINATION

STUDY OF THE EXPRESSION OF RAL GTPASES IN PRIMARY HUMAN GLIOBLASTOMA CELLS

In order to characterize the importance of Ral GTPases in GBM growth and dissemination, first we have analyzed the expression levels of Ral A and Ral B proteins in primary cultures from human GBM and grade II astrocytoma biopsies (Figure 21A). Most GBM samples showed increased Ral B amount, displaying higher levels than the low-grade astrocytoma samples. Ral A level was also increased in some GBM samples. An analysis of the data included in the GlioVis database (TCGA LGG_GBM dataset) shows that transcriptional expression of both Ral A and Ral B GTPases also increases in GBM samples in comparison with astrocytoma (Figure 21B). At least for Ral B, these data were considerably consistent indicating that the transcript and protein levels of this GTPase were enriched in GBM cells.

In addition, we analyzed whether the increase in Ral B amount also implied an augmentation of the GTPase activity. By specifically pulling down the active form of the GTPase (Ral B-GTP), we determined that the increment in total Ral B protein correlated with a raise of the active form (Figure 21C). Hence, our results suggest that primary GBM cells show an elevated level of Ral B activity.

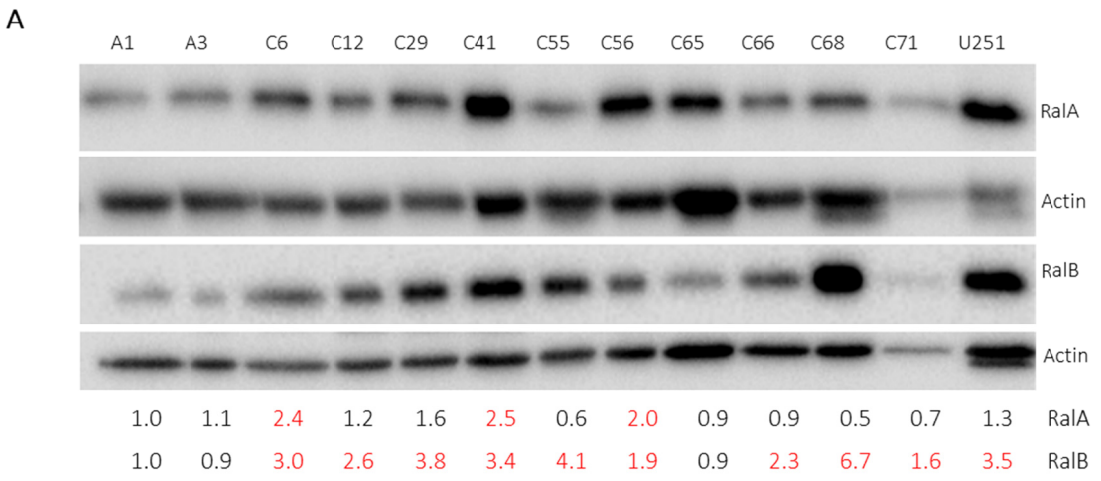

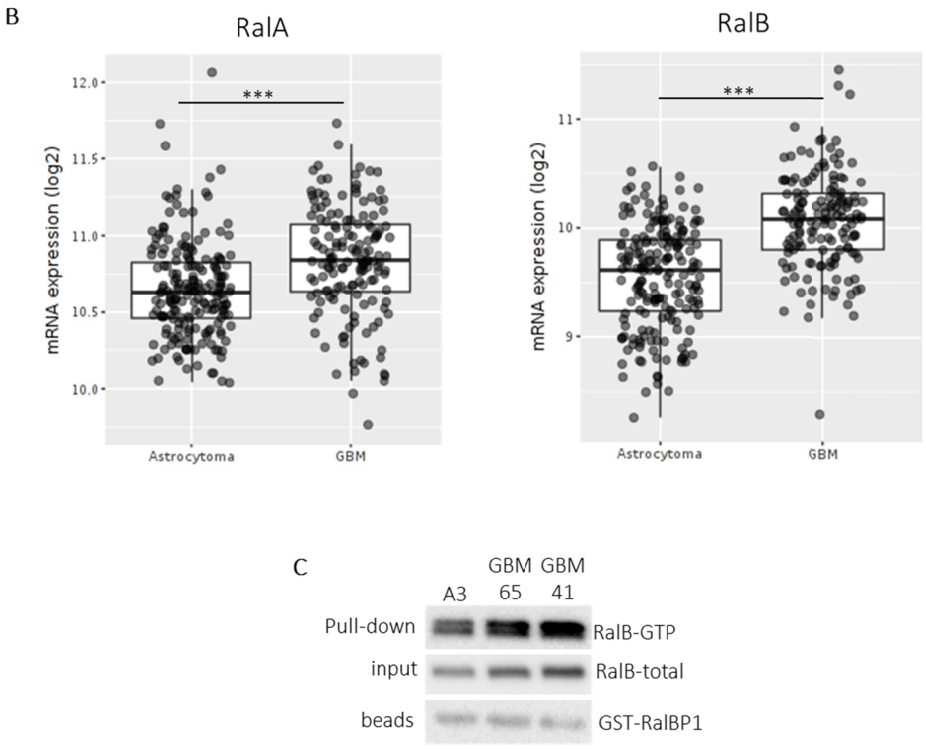

Figure 21. *Ral B is upregulated in glioblastomas*. **A)** Immunoblot to detect the levels of Ral A and Ral B in different primary glioblastoma cells (C), low grade gliomas (A) and in a glioblastoma cell line (U251-MG). Actin staining was used as loading control. Quantifications are relative to actin. **B)** Ral A and Ral B mRNA expression levels in GlioVis database (515 low grade astrocytoma and 152 glioblastoma samples). **C)** Ral B-GTP pulldown in different primary GBM cells. Active Ral B-GTP was affinity purified with Ral BP-beads from cell lysates. Ral B-GTP and total Ral B were detected by immunoblotting. Ral BP-beads were used as loading controls.

BIOLOGICAL EFFECTS OF THE DOWNREGULATION OF RAL GTPASES IN PRIMARY GLIOBLASTOMA CELLS

To test the importance of Ral GTPases on GBM growth and development, Ral A and Ral B GTPases were downregulated by using interference RNA in three different primary GBM cell cultures: GBM65, GBM6 and GBM41. Growth and viability of knockdown cells were determined by counting total and dead (trypan blue-positive) cells. Downregulation of Ral GTPases reduced growth without affecting cell viability (**Figure 22**). Intriguingly, Ral downregulation produced morphological changes: larger size and a more elongated cell shape (**Figure 22A**). The double knockdown showed the same level of growth reduction and viability than single knockdowns (**Figure 22B and C**). Thus, the inhibition of only one of the Ral GTPases may be enough to reduce cell growth.

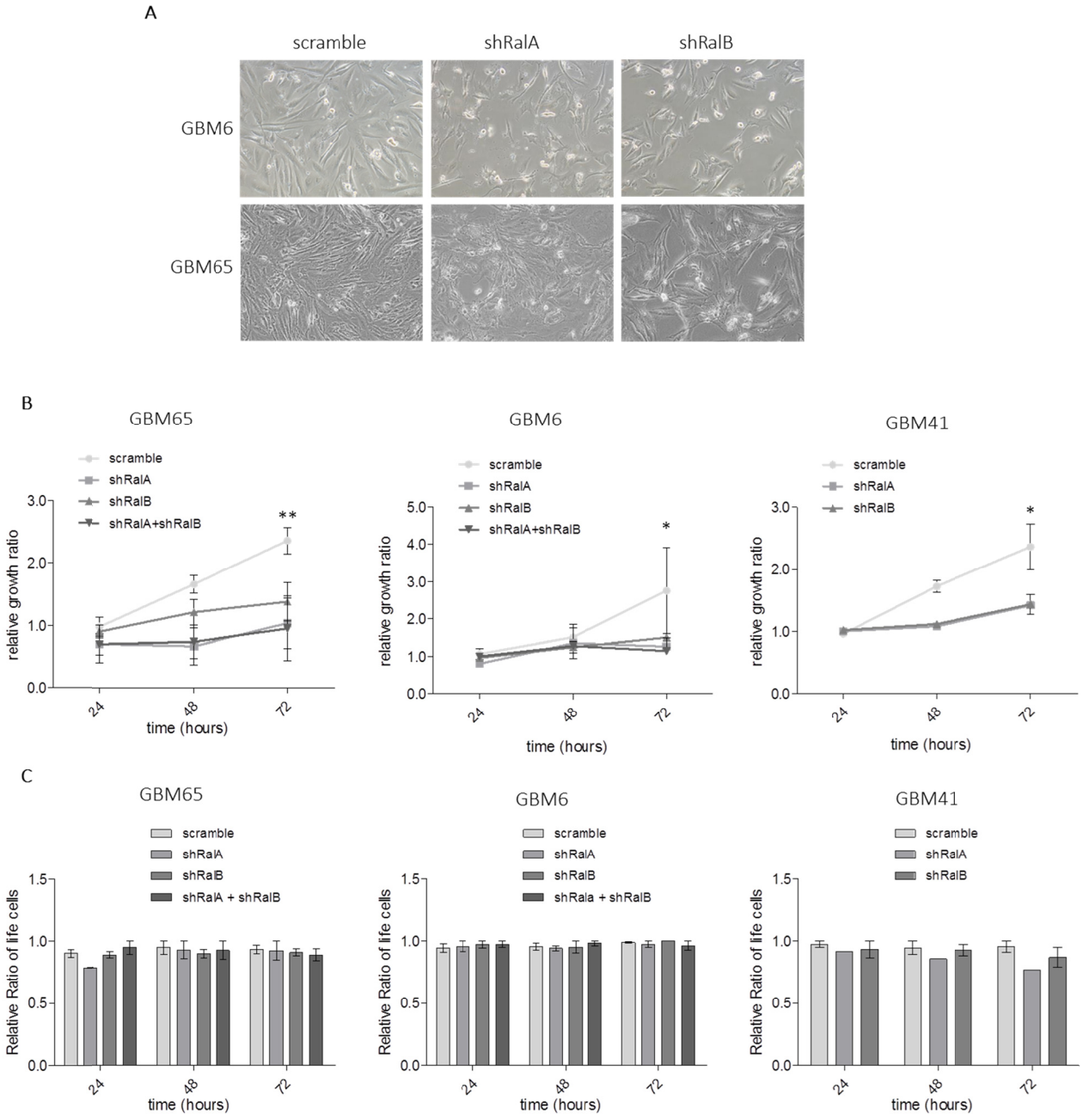

Figure 22. *Knockdown of Ral GTPases promotes a reduction of cell growth without affecting cell viability*. Primary GBM cells were infected with interference RNA against Ral A (shRalA) or Ral B (shRalB) or the combination of both. Infection with scramble was used as a control. Three days after infection, cells were seeded and counted every 24 h during 3 days. **A)** Representative images of GBM6 and GBM65 cells were taken after 4 days of infection. **B)** Graphics representing growth of knockdown GBM cells. Data is represented as mean ± SEM (n=3). Significance was determined by one way ANOVA and Tukey-HSD post-test (*p<0.05; **p<0.01). **C)** Bar diagrams showing cell viability. Dead cells were determined by counting trypan blue-positive cells. Relative viability is represented as mean ± SEM (n=3). No significant differences were found.

IMPORTANCE OF RAL GTPASES IN GLIOBLASTOMA GROWTH AND INVASION

One of the main roles of Ral GTPases is the regulation of anchorage-independent growth, a property of transformed cells that is very important for tumor formation. To test this distinctive function, a soft agar colony assay was performed for different GBM cell cultures infected with scramble or interference RNA against Ral A or Ral B. One month after seeding, cell colonies were counted by MTT staining. Most knockdown cells did not produce colonies under non-adherent growth conditions (Figure 23A), with a reduction of over 80% in colony formation (Figure 23B).

Several studies have proposed that GBM stem cells (GSCs) may account for the initiation, progression and recurrence of GBM (Chen, Li, et al. 2012; Ignatova et al. 2002; Singh et al. 2003, 2004). To analyze if Ral GTPases may have a role in the growth of GSCs, primary GBMs were cultured as tumorspheres (see methods), conditions wherein mainly tumor stem cells proliferate. Single or double knockdowns of Ral GTPases showed a huge reduction in the number of tumorspheres formed (Figure 23C and D), suggesting that downregulation of Ral GTPases also reduces GSC growth.

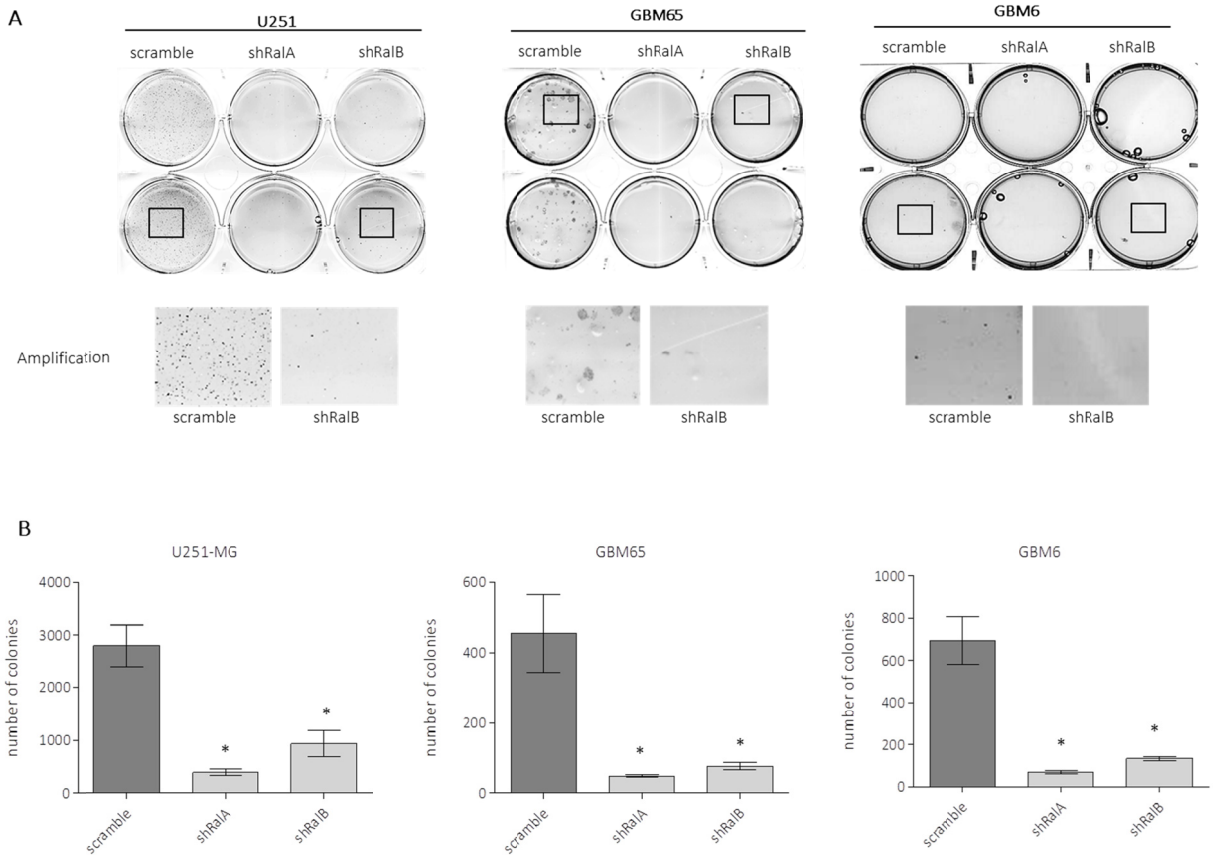

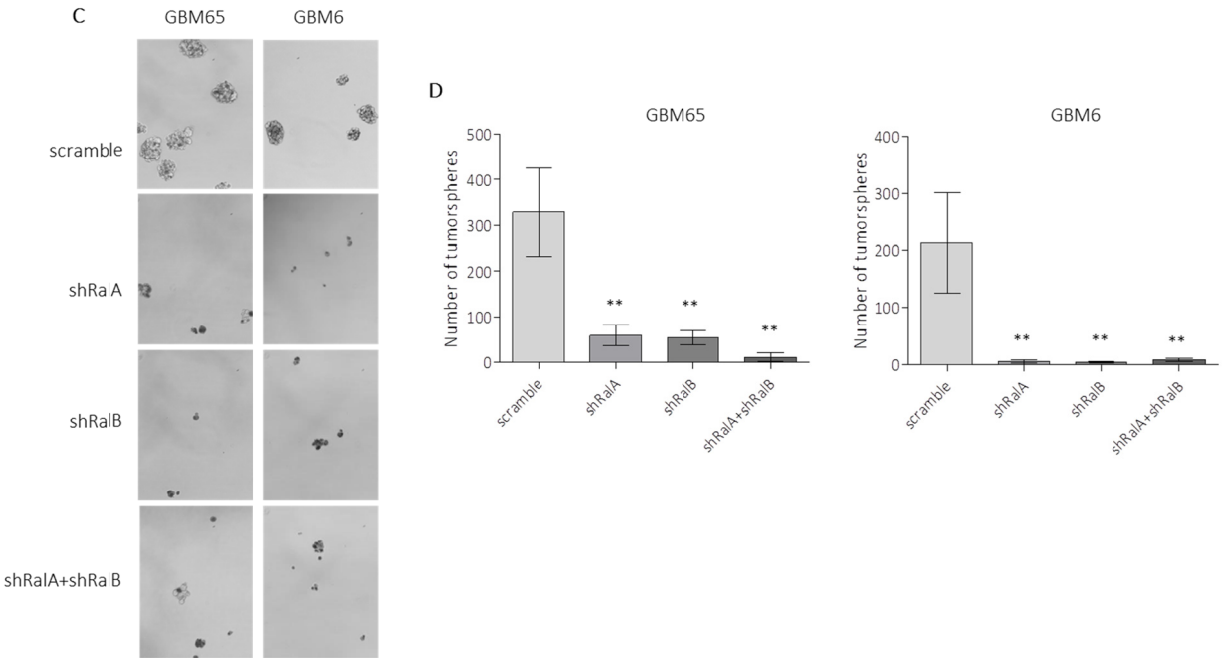

Figure 23. *Ral GTPases can affect non-adherent growth and tumorsphere formation*. **A)** U251-MG cell line, GBM65 and GBM6 were infected with interference RNA against Ral A or Ral B and seeded in a soft agar layer. After 1 month, the growing colonies were stained by the MTT reaction and the plates were scanned. Representative images of the plates in A. **B)** Diagram representing number of colonies observed in A. Colonies were quantified with the imageJ program. Values represent mean ± SEM (n=4). Significance was calculated by one-way ANOVA and Tukey-HSD post-test (*p≤0.05). **C)** Representative images of tumorsphere formation. GBM65 and GBM6 were infected with interference RNA against Ral A and Ral B or both and cells were seeded under special conditions in order to form tumorspheres. After 48 h, tumorspheres were precipitated and stained with trypan blue. **D)** Diagrams representing number of colonies observed in C. Colonies were quantified with the imageJ program. Values represent mean ± SEM (n=3). Significance was calculated by one-way ANOVA and Tukey-HSD post-test (**p≤0.01).

Another important characteristic of aggressive cancer cells is their ability to migrate and invade other surrounding tissues. To test the importance of Ral GTPases in this function, GBM primary cells were infected with scramble or with RNA interference against Ral A or Ral B, and an invasion assay was performed using transwells. Cells with low levels of Ral GTPases show a decrease in invasion capacity in comparison with control cells, suggesting that Ral A and Ral B could play a positive role in GBM cell motility and invasion (**Figure 24A and B**). In summary, all these results indicate that Ral GTPases are required for GBM growth and invasion.

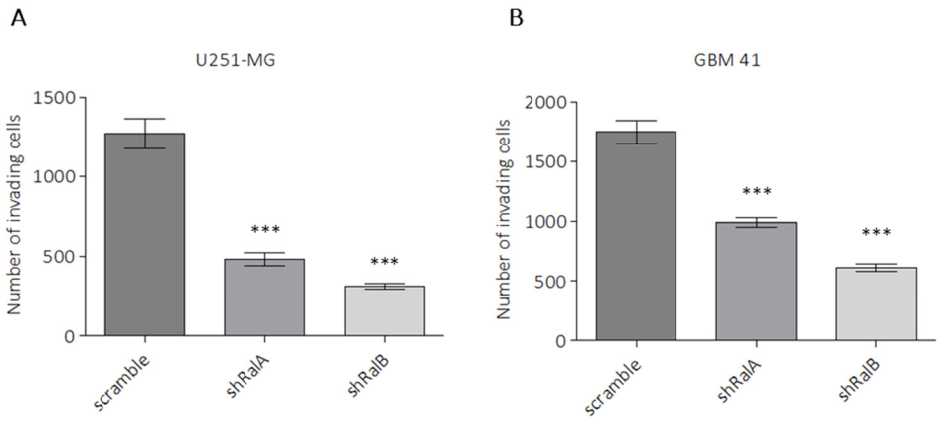

Figure 24. *Ral GTPases positively regulate the invasion capacity of glioblastoma cells*. **A)** U251-MG cell line and **B)** GBM 41 cells were infected with scramble or shRNA against Ral A or Ral B. Forty-eight hours later, cells were seeded in 24-well transwell filters previously coated with matrigel, and allowed to invade for seven hours. Values are expressed as mean ± SEM (n=3). Significance was determined by one-way ANOVA and Tukey-HSD post-test (***p<0.001).

RAL DOWNREGULATION PROMOTES SENESCENCE IN PRIMARY GLIOBLASTOMA CELLS

Our data showed that downregulation of Ral GTPases reduces cell proliferation without affecting viability. Thus, from these results the possibility arises that Ral GTPases may be regulating cell senescence. This is a process by which cells cease to divide, they can no longer proliferate but they remain metabolically active. Senescence can be triggered by a DNA damage response, reactive oxygen species and activation of oncogenes.

To test if downregulation of Ral GTPases could induce senescence in GBM cells, an X-Gal assay was performed. Five days after downregulation of Ral GTPases, cells were fixed and incubated in the presence of X-gal solution, and blue senescent cells were counted (**Figure 25A**). Ral GTPase Knockdown produced an increase in the number of positive senescent cells in comparison with controls **(Figure 25B)**. Interestingly, Ral B knockdown had a stronger effect than Ral A in all GBM cultures tested.

Typically, senescent cells are arrested in G1 phase of the cell cycle and show an increment of CDK inhibitors (CKI) such as p16, p21 and p27. To test the existence of a cell cycle arrest, a BrdU incorporation assay was performed in primary GBM cultures. Five days post-infection with interference RNAs, cells were seeded and treated with BrdU overnight, and the accumulation of

BrdU was tested by IF and the CKI levels by western blot. Downregulation of Ral GTPases significantly decreased the number of BrdU-positive cells compared with the controls (**Figure 25C**), and significantly increased CKI levels (**Figure 25D**). These data corroborate the induction of senescence when Ral GTPases are downregulated in GBM cells.

Characteristically, cancer cells show genomic instability due to defects in the control of DNA damage response pathways and to replicative stress. DNA damage induced by different stresses is a key upstream event in different pathways that promote growth arrest and cell senescence (von Kobbe 2018). Consequently, we have evaluated the levels of DNA damage in Ral GTPase-knockdown GBM cells. We have analyzed by IF the levels of phosphoserine 139 H2A.X (γ-H2A.X), a marker of double strand breaks. GBM6 cells showed more DNA damage at basal levels when compared to GBM65 (**Figure 25E**). Both primary cultures showed an increased number of positive cells when Ral B was downregulated. This result suggests that the accumulation of DNA damage in Ral B-deficient cells may be an inducer of senescence.

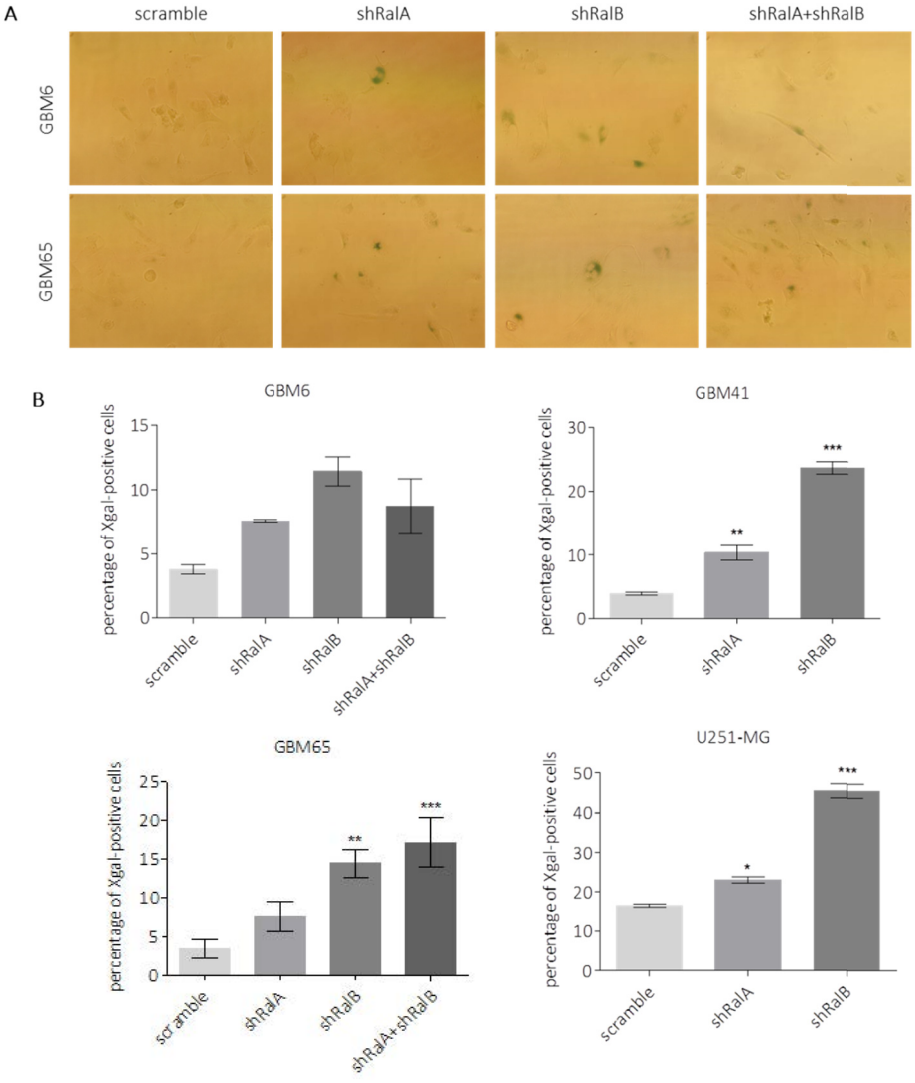

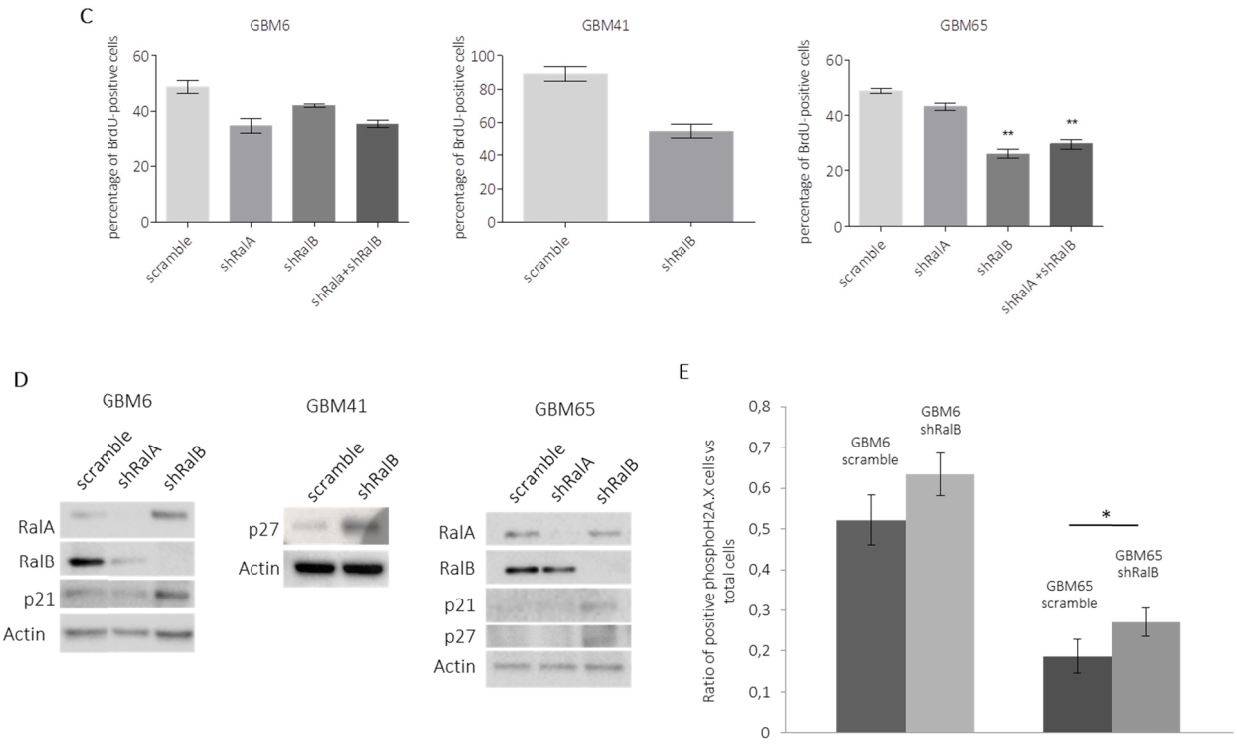

Figure 25. *Downregulation of the Ral GTPase activity promotes senescence in glioblastoma cells.* Ral GTPases Ral A and Ral B were downregulated by RNA interference, shRalA and shRalB respectively. Scramble RNA was used as a control. GBM cells were infected by lentiviral vectors harboring the shRNAs. Five days after infection cells were processed for senescence analyses. **A)** Representative images of X-gal senescence assay. Blue cells indicate positive senescence cells. **B)** Quantification of senescence assay in A as percentage of positive cells versus total cells. Values represent mean ± SEM except for GBM6 that is mean ± SD. Significance was determined by one-way ANOVA and Tukey post-test except for GBM6 ($p \leq 0.05$, *; $p \leq 0.01$, **; $p \leq 0.001$, ***) (GBM6 n=2; GBM41 n=3; GBM65 n=7; U251 n=3). **C)** Quantification of BrdU incorporation assay. Values represent the percentage of BrdU-positive nuclei. The number of total nuclei was determined by counting nuclei stained with Hoechst. We show the mean ± SD (n=2). **D)** Western Blot to determine the levels of CKIs in primary GBM cell culture extracts. **E)** Determination of DNA damage levels. Cells positive for γ-H2A.X staining (more than five foci) were counted. Graph represents the ratio of positive cells versus total cells. The confidence intervals of proportions are shown.

RAL GTPASES AS THERAPEUTIC TARGETS TO TREAT GLIOBLASTOMA

In order to test the possible use of Ral GTPase inhibitors for GBM treatment, we have compared the effect of Ral inhibition with that of Temozolomide (TMZ). The oral treatment with TMZ is the main chemotherapy for GBM. The therapeutic benefit of TMZ depends on its ability to alkylate DNA. However, some tumor cells are able to repair the DNA damage induced by TMZ by expressing the protein MGMT, a DNA alkyltransferase. In some tumors the epigenetic methylation of MGMT gene prevents the expression of this protein and as a consequence

tumors are more sensitive to this drug. Thus, we first studied the sensitivity to TMZ of our primary GBM cells. The methylation of MGMT promoter was analyzed by pyrosequencing. While the GBM6 strain has the MGMT promoter methylated the GBM65 strain does not (**Figure 26A**), and consequently only the GBM65 strain expressed the MGMT protein (**Figure 26B**). In agreement with these results, we have observed that TMZ treatment to primary GBM cultures only reduced cell viability in the case of GBM6 (**Figure 26C**). Furthermore, viability of GBM6 tumorspheres was also affected by TMZ (**Figure 26D and E**).

Once we established the sensitivity to TMZ of our primary cultures, we compared the effects of TMZ and Ral GTPase downregulation on growth and viability. Primary GBM cells were infected with scramble or interference RNA against Ral B, and treated or not with TMZ. As we observed before, a reduction of Ral B activity reduces proliferation in both primary cultures and thus, we would expect it to be favorable for the treatment of both tumor types, sensitive and non-sensitive to TMZ. In the case of TMZ-sensitive tumors, lack of Ral B enhanced the treatment of TMZ (**Figure 26F**). For the TMZ non-sensitive tumors, the reduction of Ral B activity still causes a decrease in cell proliferation (**Figure 26G**). Hence, inhibition of Ral B activity may be a potential new therapy for GBM, at least in those cases wherein tumors are insensitive to TMZ.

A

Sample	MGMT-promoter status	Percentage of methylation
U251-MG	Methylated	45
U87-MG	Methylated	74
GBM6	Methylated	50
GBM65	Un-methylated	1.5

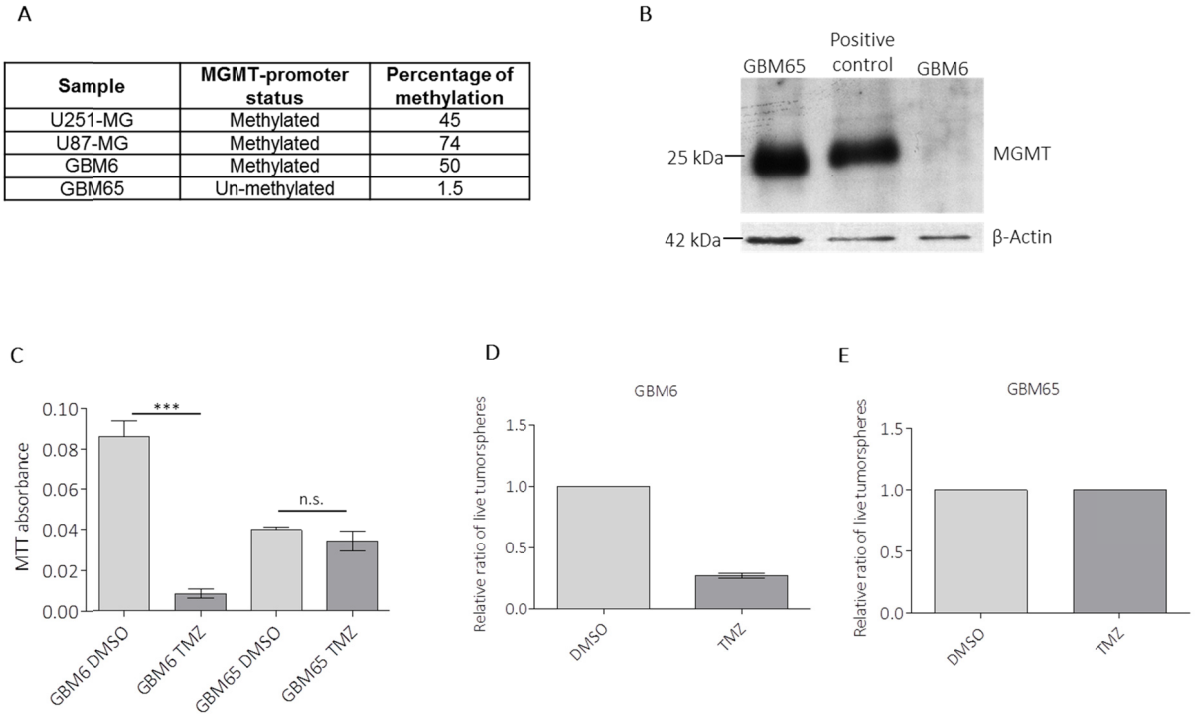

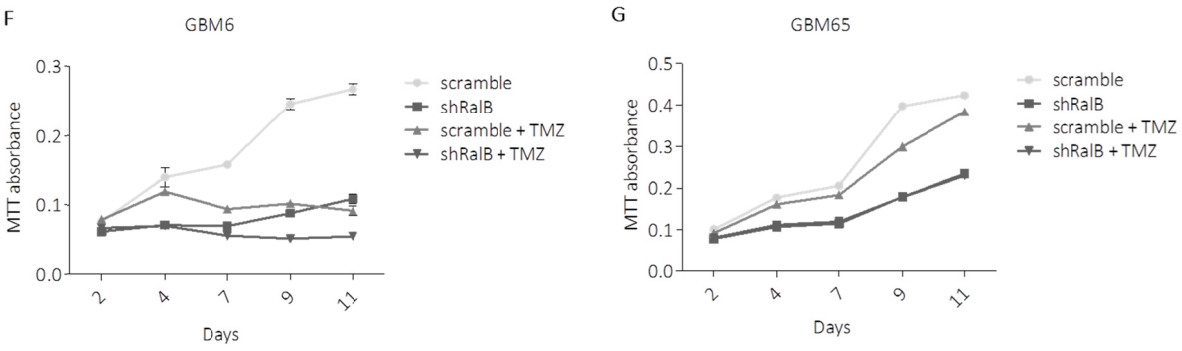

Figure 26. *Effects of the treatment of primary glioblastoma cells with Temozolomide and Ral B inhibition.* **A)** The methylation status of the MGMT promoter was resolved in primary GBM samples and cell lines by pyrosequencing after bisulfite treatment. Values represent the percentage of methylated sites in the MGMT promoter. **B)** The expression of MGMT was determined in GBM6 and GBM65 by western blot. Actin was used as a loading control. **C)** Primary GBM cells were treated with the alkylating drug Temozolomide 100 µM (TMZ) and cell growth was determined by MTT staining after 10 days of treatment (n=4). Significance was determined by one-way ANOVA and Tukey-HSD post-test ($p \leq 0.001$, ***). **D** and **E)** Tumorspheres of GBM6 and GBM65 were treated with TMZ. After 10 days of treatment, tumorspheres were stained with trypan blue and counted. Values represent the ratio of live versus total tumorspheres (mean ± SD; n=2). **F** and **G)** GBM6 or GBM65 cells Infected with scramble or shRalB were treated with TMZ or placebo. Growth was analyzed by MTT at different time points. Values represent mean ± SEM (n=3).

EFFECTS OF RAL GTPASE INHIBITORS

Our results suggest that Ral GTPases may be good candidates as new targets in the treatment of GBM. For this, it would be highly desirable to develop specific pharmacological inhibitors of these proteins. In fact, some Ral GTPase inhibitors has been previously described (Yan et al. 2014). RBC8 and BQU57 are selective inhibitors of Ral A and Ral B, without direct inhibition of Ras or RhoA activity. These inhibitors bind to a site on the GDP-bound form of Ral (inactive state) inhibiting the binding of the Ral GTPases to their effectors. We performed some experiments to check if these inhibitors could reproduce the effects we had observed with interference RNAs against Ral GTPases. In one experiment, senescence assays were carried out with cells treated with BQU57 at 10 µM or 20 µM for one week (**Figure 27**). Treated cells showed increased levels of senescence in comparison with controls, confirming the results with shRNAs against Ral GTPases. However in our hands, multiple experiments to measure senescence, proliferation and viability in the presence of RBC8 or BQU57 were inconclusive because results were not repetitive.

This may be due to the inherent instability of these compounds (Dan Theodorescu, personal communication). Hence, we cannot conclude that RBC8 and BQU57 inhibitors are useful chemotherapeutic drugs for GBM treatment.

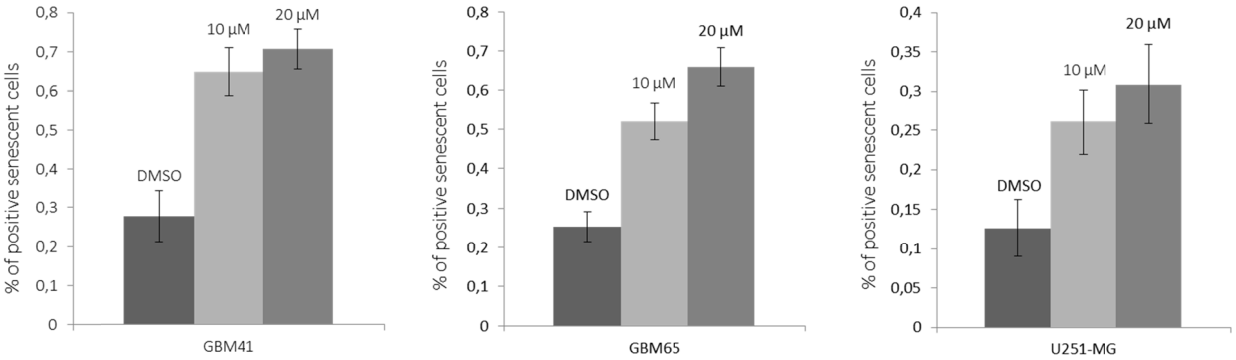

Figure 27. *BQU57 treatment increases senescence in glioblastoma cells*. GBM41, GBM65 and U251-MG cells were treated for over a week with the Ral GTPase inhibitor BQU57. Afterwards, cells were seeded in a new plate and treated with X-GAL to stain senescent cells. All cell cultures treated with BQU57 were more senescent than controls treated with DMSO. Values are percentages of positive senescent cells (mean ± SD). Error bars show the confidence interval of proportions (α=0.05, n≥150 counted cells).

CHAPTER 3 - SIGNALING PATHWAYS ACTIVATED BY CYTOPLASMIC CYCLIN D1

CYTOPLASMIC CYCLIN D1 IS ABLE TO INDUCE SIGNALING PATHWAYS

Results in other chapters of this thesis and previous results of our research group suggest that cytoplasmic Ccnd1 plays a role as a mediator of cell signaling. To advance this hypothesis, and in collaboration with Dr Isabel Mejía and Dr Lluis Fajas (University of Lausanne), we have carried out the analysis of changes in the kinoma induced by expression of cytoplasmic Ccnd1. This analysis is based on the use of peptide microarrays from PamGene Technology, a collection of peptides displayed on a solid surface (in our case called "PamChips"). The assay principle of the "PamChips" is similar to an ELISA protocol: peptides are linked to the surface of the chip, and this chip can directly be incubated with a variety of different biological samples (in our case the chips were incubated with cell lysates of KOD1 iMEFs transfected with Ccnd1-CAAX or with the inactive mutant Ccnd1K112E-CAAX). After several washing steps, an antibody against phoshoserines and phosphothreonines is applied. This antibody is fluorescently tagged and can be detected with a fluorescence scanner (PamStation).

In our approach, we have used a Ccnd1-CAAX allele to accumulate Ccnd1 in cell membranes outside the nucleus, and the inactive form of the same allele Ccnd1K112E-CAAX as a control (Figure 28A). First, KOD1 iMEFS were electroporated with farnesylated Ccnd1 or with the inactive allele and the level of expression of the proteins was checked by western blot. The extracts of samples with an adequate (similar) level of expression of Ccnd1 alleles were loaded in a serine-threonine kinase (STK) PamChip (Figure 28B). The experiment was independently repeated three times with duplicated samples. Principal component analysis shows a significant clustering of samples according to the Ccnd1 allele expressed (Figure 29A). Thirty peptides were significantly more phosphorylated in the samples with Ccnd1-CAAX than in the Ccnd1K112E-CAAX control (Figure 29B). Interestingly, and not unexpected, 60% of the peptides belong to proteins related to the cell membrane and 30% to the cytoplasm.

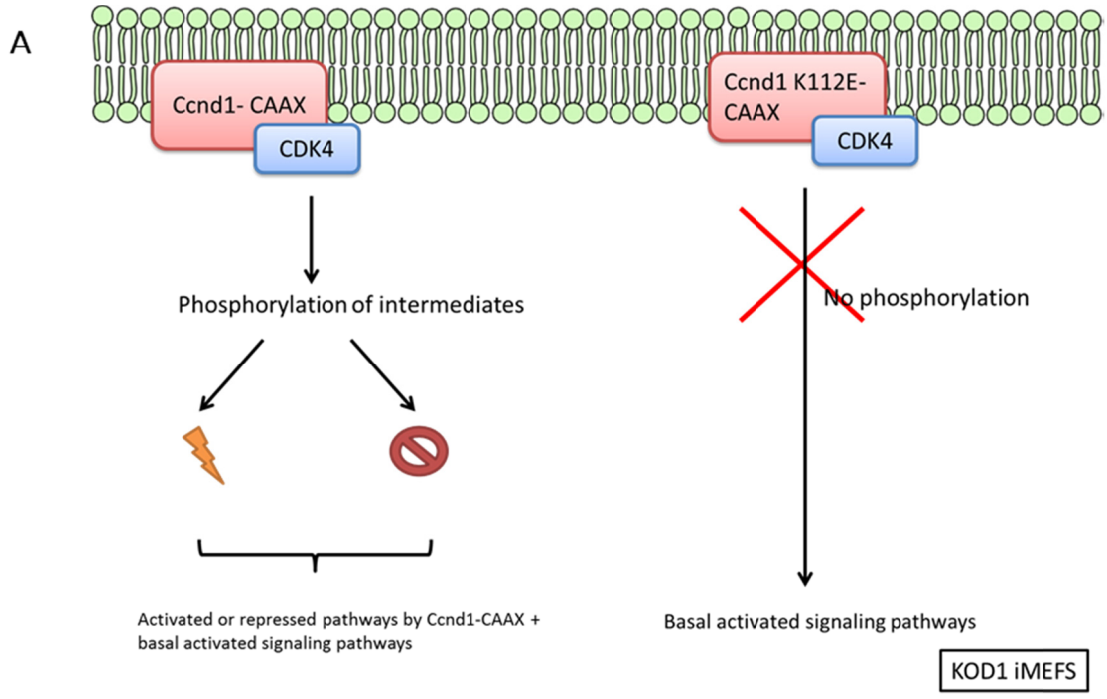

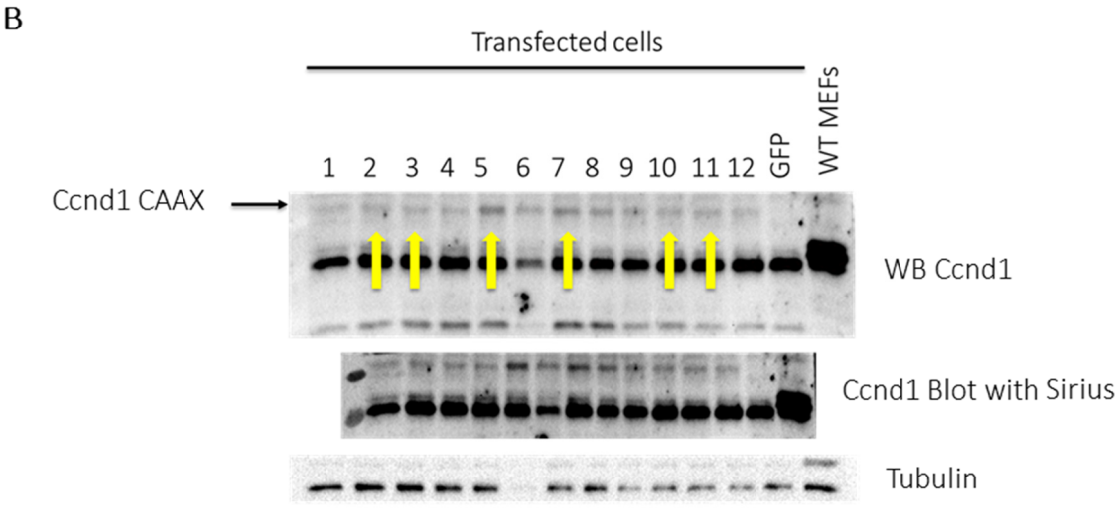

1 NEON 1	EG CAAX 1
2 NEON 1	EG CAAX 1'
3 NEON 1	EG K112E 1
4 NEON 1	EG K112E 1'
5 NEON 2	EG CAAX 2
6 NEON 2	EG CAAX 2'
7 NEON 2	EG K112E 2
8 NEON 2	EG K112E 2'
9 NEON 3	EG CAAX 3
10 NEON 3	EG CAAX 3'
11 NEON 3	EG K112E 3
12 NEON 3	EG K112E 3'

Figure 28. *Sample preparation for the experiments*. **A)** Experimental design for the Pamgene experiment. **B)** Western Blot of the electroporated cells against Ccdn1 and tubulin as a loading control. Yellow arrows indicate the selected samples to perform the experiment. The blue table below indicates which sample was loaded in each well of the western blot. EG CAAX refers to the normal farnesylated allele of cyclin D1 while EG K112E refers to the inactive allele. The number of the biological replicate is also indicated.

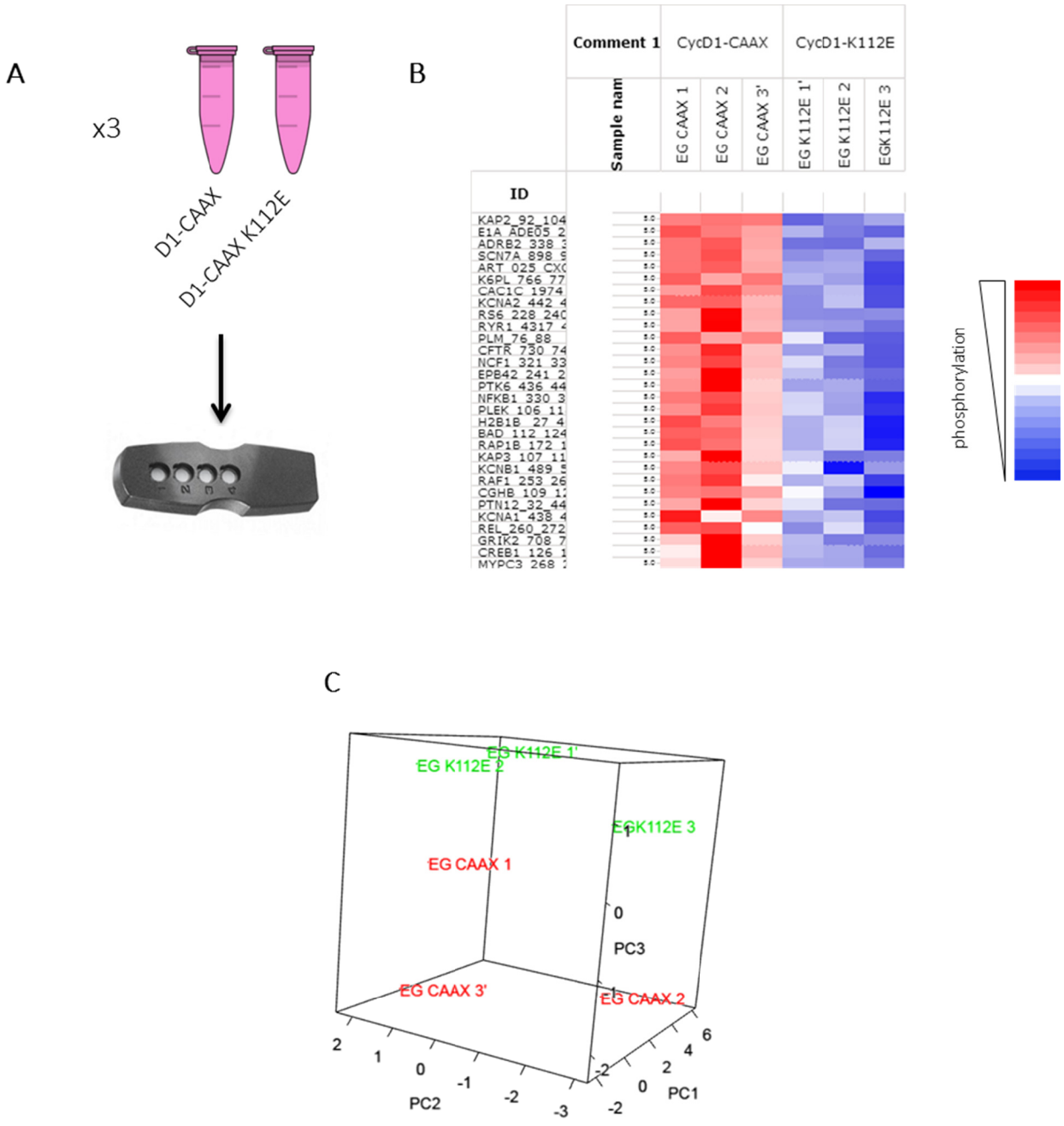

Figure 29. *PamGene Results*. **A)** Three samples from each condition were analyzed in the STK PamChip. **B)** Table showing the 30 first most significant of the total 128 peptides analyzed in the chip. Red reflects the most increased phosphorylation peptides, in blue the decrease of phosphorylation of the same peptides. **C)** Principal Components Analysis.

Kinase activity profiling with PamChip peptide microarrays can be used to study signal transduction in cell lysates. Putative "upstream" kinases that phosphorylate peptides on the microarray may be identified using PTM databases such as HPRD, PhosphoSitePlus or databases with in-silico predictions such as PhosphoNET, which contains predictions for a relatively large number of kinases. In our case, all 112 analyzed peptides were submitted to a STK upstream application of the PamGene Software (Figure 30A). Among the putative "upstream" kinases the best scored were:

1- The CHK2 serine/threonine-protein kinase is required for checkpoint-mediated cell cycle arrest, activation of DNA repair and apoptosis in response to the presence of DNA double-strand breaks.
2- The MSK1 serine/threonine-protein kinase is required for the mitogen or stress-induced phosphorylation of the transcription factors CREB1 and ATF1, and for the regulation of the transcription factors RELA, STAT3 and ETV1/ER81. This kinase contributes to gene activation by histone phosphorylation and functions in the regulation of inflammatory genes.
3- The PKG2 protein binds to and inhibits the activation of several receptor tyrosine kinases. This membrane-bound protein is a regulator of intestinal secretion, bone growth and renin secretion.
4- The PKA Cα, catalytic subunit of protein kinase A, which exists in its inactive form as a tetrameric holoenzyme with two regulatory subunits and two catalytic subunits. cAMP causes the dissociation of the inactive holoenzyme into a dimer of regulatory subunits (bound to four cAMP) and two free monomeric catalytic subunits. Four different regulatory subunits and three catalytic subunits have been identified in humans. cAMP-dependent phosphorylation of proteins by protein kinase A is important to many cellular processes, including differentiation, proliferation, and apoptosis among others.

In addition to analyzing the data with the Pamgene software, we have also used the Gene Ontology (GO) software to find signal transduction pathways (GO-reactome pathways) that might be affected by cytoplasmic Ccnd1. In this case, we have only used the 30 peptides with the highest phosphorylation enrichment in the presence of Ccnd1-CAAX. The score and probability analyses highlighted two signaling factors: the PKA pathway and Sodium-Ion transport channels (Figure 30B). These results open a whole new array of possibilities to be explored in the future.

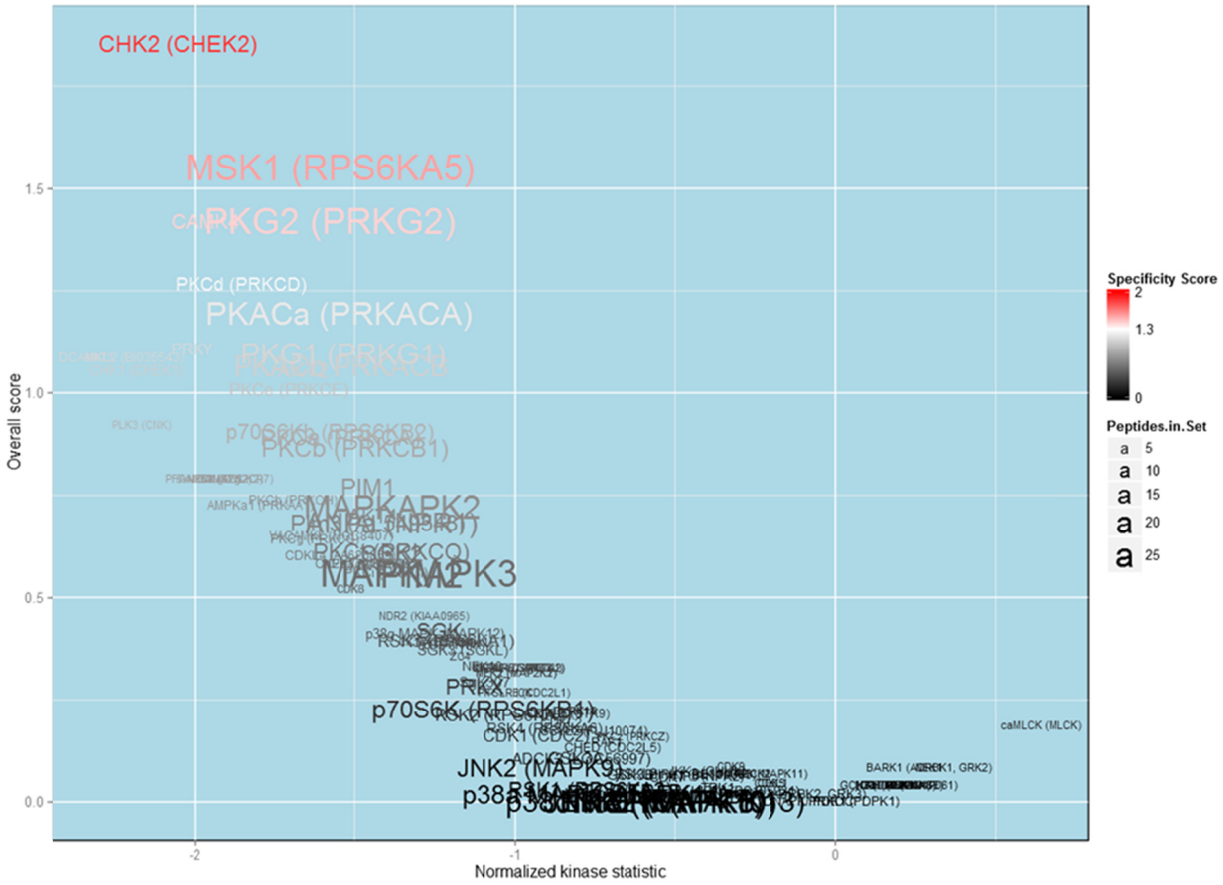

Reactome pathways	Homo sapiens (REF) #	upload_1 (▽ Hierarchy NEW!) #	expected	Fold Enrichment	+/-	raw P value	FDR
Rap1 signalling	15	2	.02	99.98	+	2.30E-04	2.80E-02
PKA activation	17	2	.02	88.22	+	2.88E-04	3.16E-02
↳PKA-mediated phosphorylation of CREB	18	3	.02	> 100	+	2.77E-06	2.02E-03
↳Calmodulin induced events	26	3	.03	86.52	+	7.55E-06	2.07E-03
↳CaM pathway	26	3	.03	86.52	+	7.55E-06	2.36E-03
↳Ca-dependent events	28	3	.04	80.34	+	9.27E-06	2.26E-03
↳PLC beta mediated events	44	3	.06	51.13	+	3.30E-05	5.16E-03
↳G-protein mediated events	45	3	.06	49.99	+	3.52E-05	5.13E-03
↳Opioid Signalling	81	3	.11	27.77	+	1.88E-04	2.42E-02
↳Signal Transduction	2667	14	3.56	3.94	+	2.02E-06	2.21E-03
↳DAG and IP3 signaling	32	3	.04	70.30	+	1.35E-05	2.95E-03
↳Intracellular signaling by second messengers	271	4	.36	11.07	+	4.58E-04	3.72E-02
PKA activation in glucagon signalling	17	2	.02	88.22	+	2.88E-04	3.01E-02
↳Integration of energy metabolism	109	4	.15	27.52	+	1.47E-05	2.92E-03
CD209 (DC-SIGN) signaling	21	2	.03	71.41	+	4.25E-04	3.58E-02
Constitutive Signaling by AKT1 E17K in Cancer	24	2	.03	62.49	+	5.45E-04	4.26E-02
↳Disease	1023	7	1.36	5.13	+	3.17E-04	3.02E-02
DARPP-32 events	24	2	.03	62.49	+	5.45E-04	4.12E-02
CREB phosphorylation through the activation of Ras	27	2	.04	55.54	+	6.79E-04	4.96E-02
↳Neuronal System	361	6	.48	12.46	+	7.39E-06	3.24E-03
Glucagon-like Peptide-1 (GLP1) regulates insulin secretion	42	3	.06	53.56	+	2.89E-05	5.28E-03
↳Regulation of insulin secretion	80	4	.11	37.49	+	4.51E-06	2.47E-03
Voltage gated Potassium channels	43	3	.06	52.32	+	3.09E-05	5.21E-03
↳Potassium Channels	99	3	.13	22.72	+	3.33E-04	3.04E-02
Cardiac conduction	139	4	.19	21.58	+	3.70E-05	5.07E-03
↳Muscle contraction	204	5	.27	18.38	+	7.55E-06	2.76E-03
Signaling by Receptor Tyrosine Kinases	440	5	.59	8.52	+	2.73E-04	3.15E-02
Transport of small molecules	716	6	.95	6.28	+	3.17E-04	3.16E-02
Developmental Biology	1038	7	1.38	5.06	+	3.47E-04	3.04E-02
Unclassified	10452	1	13.94	.07	-	2.15E-07	4.71E-04

Figure 30. *Volcano plot representing the upstream putative kinases involved in Ccnd1 signaling*. **A)** Final ranking score is plotted as a function of the associated Normalized Kinase Statistic. The text color indicates specificity score, the text size the number of peptides that were used to represent the corresponding kinase. **B)** GO analysis of the 30 most significant peptides in reactome pathways.

SIGNALING PATHWAYS ACTIVATED BY CYCLIN D1 IN GLIOBLASTOMA

Taking into account that cyclin D1 may play a role as a signaling regulator, we sought to characterize this role of Ccnd1 in GBM. For this, we used The Proteome Profiler Human Phospho-Kinase Array Kit (R&Dsystems) that is a membrane-based sandwich immunoassay. The arrays allow the measurement of up to 119 phosphorylated proteins from a single sample. This system uses captured antibodies spotted in duplicate on nitrocellulose membranes, requires no specialized equipment, and eliminates the need for multiple western blot experiments.

GBM6 cells infected with scramble or with shRNA against Ccnd1 were processed for analysis. Proteins phosphorylated at specific residues are captured by specific antibodies and then detected with a biotinylated antibody that binds any phospho-protein and that is finally visualized with a chemiluminescent detection reagent (Figure 31A). The signal produced is proportional to the level of phosphorylation in the bound analyte. The experiment was performed independently twice. Phosphorylation of some proteins was reduced after downregulation of Ccnd1, indicating that Ccnd1 may have a role in regulating some signaling pathways in primary GBM. The affected proteins were MSK1, CREB, P70S6Kinase, SRC, HCK, CHK2 and WNK1 (Figure 31B). Interestingly, the transcription factor CREB1 is the downstream target of PKA kinase. Consistently, the phosphorylated form of CREB1 was reduced in the absence of Ccnd1 and increased by overexpression of Ccnd1 (Pamgene experiment). Hence, the results obtained in this chapter suggest that Ccnd1 may regulate PKA activity. These are preliminary results and we do not know the relevance of these data yet. In any case, these results strongly suggest an important role of cyclin D1 in signaling, outside of its better characterized role as a cell cycle regulator.

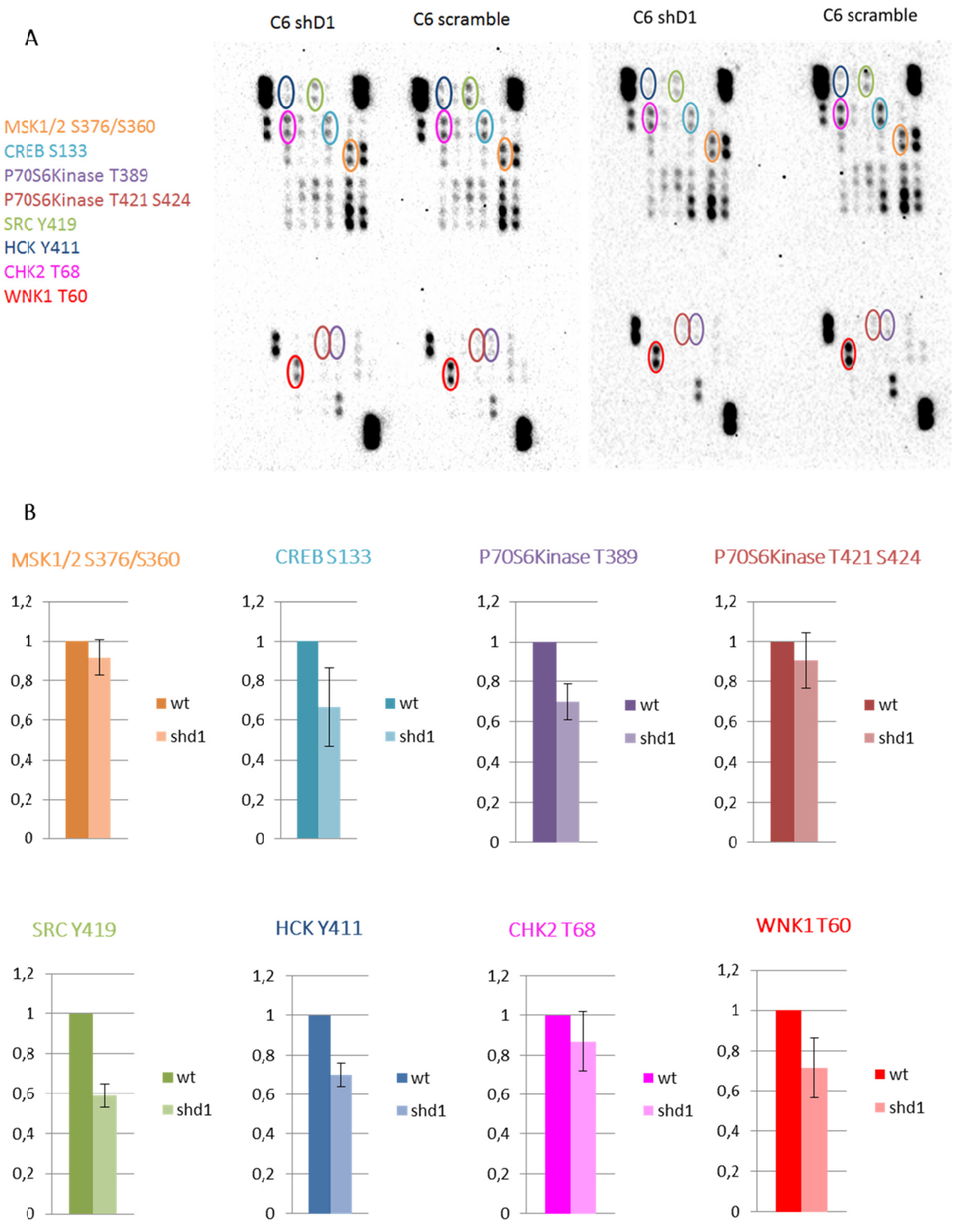

Figure 31. *Cyclin D1-dependent signaling was analyzed in glioblastoma primary cells*. **A)** The Human Phospho-Kinase Array was used to detect multiple phosphorylated kinases in GBM6 primary cell culture infected with scramble shRNA or with a shRNA against Ccnd1 (shD1). Template showing the location of kinase antibodies spotted onto the Human Phospho-Kinase Array kit and relevant kinases were indicated by colored circles. **B)** Quantification of mean spot pixel densities of the indicated kinases (mean ± SD) (n=2).

DISCUSSION

GBM is the most common brain tumor in adults. At present this tumor is practically incurable and patients show a poor survival rate after diagnosis despite the surgery, radiotherapy and chemotherapy received (Furnari et al. 2007). GBM cells present an incontrollable proliferation and a high capacity of invading surrounding tissues by migration that makes the complete surgical resection impossible (Zong et al. 2012). Thus, GBM therapy requires new anti-tumor agents capable of inhibiting GBM proliferation and migration and promoting cell death (Hanahan and Weinberg 2011; Paw et al. 2015). The results from this thesis support the idea that Ccnd1 and Ral GTPases could be potential targets for GBM treatment. Cyclin D1-CDK4 inhibitor Palbociclib has already been approved by FDA as a treatment to reduce proliferation in triple negative breast cancer (Finn and Slamon 2015). However, our work suggests a new strategy in the use of Ccnd1-CDK4 inhibitors. The inhibition of Ccnd1-associated activity is particularly efficient avoiding tumor dissemination, and this issue is very relevant in tumors such as GBM. Regarding Ral GTPases, we have shown that the inhibition of these proteins in GBM cells promotes senescence, and consequently arrests proliferation, but unfortunately at the moment there are no reliable inhibitors available.

CYTOPLASMIC CYCLIN D1 REGULATES GLIOBLASTOMA DISSEMINATION

Different works have shown that Ccnd1 functionally interacts with cytoplasmic targets involved in the regulation of cell adhesion and invasion such as filamin A, Pacsin, Rgl2 and Pxn (Fernández et al. 2011; Noel P. Fusté et al. 2016; Meng et al. 2011; Zhong et al. 2010). In these previous studies, Ccnd1 has been localized in the cytoplasm and membranes of cultured fibroblasts and various tumor cells, and here we demonstrate this localization specifically for GBM cells. Also, cytoplasmic Ccnd1 has been observed in cells at the invasive fronts of solid tumors, suggesting an important role of cytoplasmic Ccnd1 in tumor invasion (Noel P Fusté et al. 2016). In a hematological cancer, the presence of cytoplasmic Ccnd1 has been correlated with the invasive blastoid variant of mantle cell lymphoma (Body et al. 2017). We propose that cytoplasmic Ccnd1-CDK4 regulates GBM cell dissemination in the brain. In mouse models, we have observed that Ccnd1 is cytoplasmic mainly in evaded GBM cells but not in the tumor mass, and that the imposed accumulation of Ccnd1 at the cell membranes significantly increases the number of evaded cells away from the tumor mass. These results strongly suggest that cytoplasmic Ccnd1-associated activity could contribute to GBM dispersion *in vivo*.

We have demonstrated that the role of Ccnd1 in the regulation of GBM cell invasion is RB1 independent. Consequently, the invasive capacity of GBM cells is still sensitive to Palbociclib treatment in the absence of RB1. This is in agreement with the regulation of cell motility and invasion by Ccnd1 in mouse fibroblasts, which is also RB1 independent (Li, Wang, et al. 2006). Beyond this, it seems that the regulation of GBM cell invasion by Ccnd1 is unconnected to the proliferative status. In our xenograft experiments most GBM tumors expressing membrane-associated Ccnd1 show cell dissemination; still, their proliferation ratio is the same as in tumors expressing WT Ccnd1.

Our genetic data also suggest that Pxn is a downstream target of Ccnd1-CDK4 in human GBM cells. Interestingly, overexpression of Pxn is associated with high-grade gliomas and PXN seems to behave as an oncogene in glioma progression (Sun et al. 2017). Also, a positive correlation between GBM invasiveness and Pxn phosphorylation at tyrosine 118 has been reported (Arscott et al. 2013). Here, we contribute with genetic approaches to demonstrate that phosphorylation of Pxn at S83 and S178 is required for efficient invasion and inefficient spreading of GBM cells. Conceivably, these phosphorylations triggered by Ccnd1 expression could constitute an initial step in the induction of GBM invasion. Unfortunately, we have not found specific antibodies

against these phospho-sites in humans, but we have observed that expression of Ccnd1 activated downstream targets of Pxn such as FAK and Rac1. Of note, the importance of these downstream targets in GBM invasion has also been reported by different authors (Arato-Ohshima and Sawa 1999; Jaraíz-Rodríguez et al. 2017; Jones, Machado, and Merlo 2001; Kwiatkowska et al. 2012; Riemenschneider et al. 2005; Salhia et al. 2005).

We have observed that the expression of a dominant-negative allele of the small GTPase Ral A reduced the invasion efficiency of primary GBM cells, and that the hyperactivation of Ral GTPases suppresses the deleterious effect of Ccnd1 knockdown on invasiveness. Ral GTPases are regulators of exocyst formation and the secretory pathways, and are involved in the control of cell growth and invasion (Bodemann and White 2008). Furthermore, Ral activation specially contributes to Ras-driven growth transformation, and is increased in many different types of cancer (Gentry et al. 2014). Unexpectedly, very few studies exist about the importance of Ral GTPases in GBM. Other authors have shown that the knockdown of Ral B decreases the invasiveness of human GBM cell lines (Song et al. 2015), as our results corroborate. In addition we have extended the role of Ral GTPases in growth and invasion to primary GBM (see below).

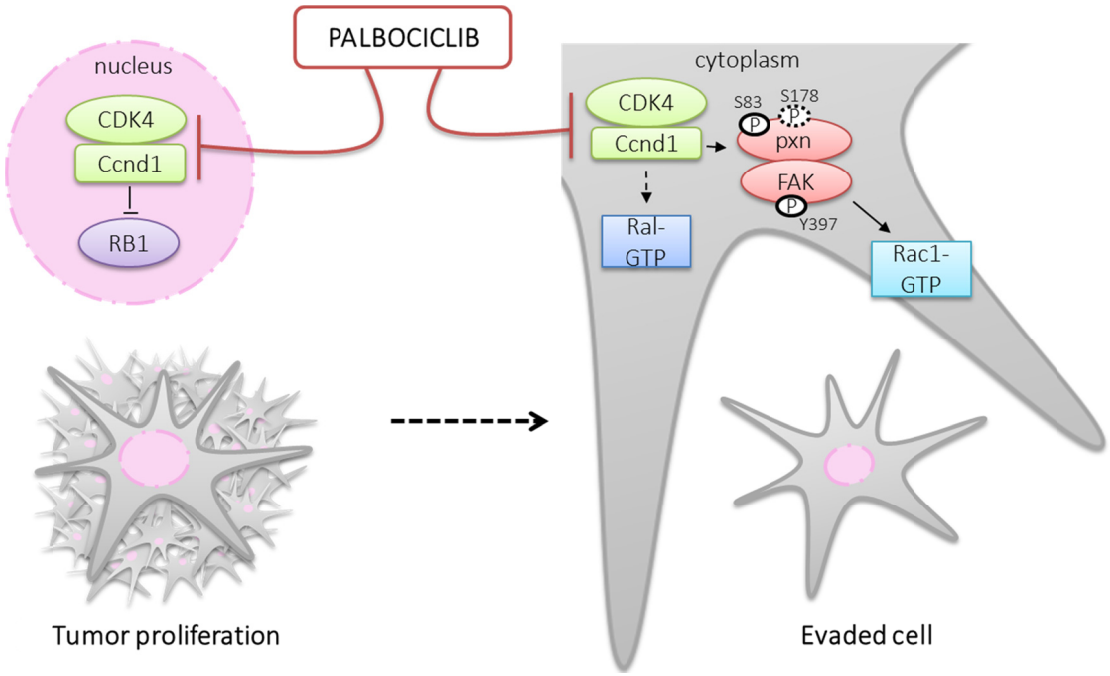

Figure 32. *Diagram of the cyclin D1-CDK4 regulatory network in GBM cells.*

We believe that cytoplasmic Ccnd1-CDK4 promotes cell evasion in GBM through activation of the Pxn-FAK-Rac1 axis and Ral GTPases (**Figure 32**), and conclude that chemical inhibition of Ccnd1-CDK4 activity could be a promising treatment against GBM dissemination in combination with other anti-proliferative drugs. Also, inhibitors of the downstream pathways, Pxn-FAK-Rac1 and Ral GTPases, may also be taken into consideration against GBM dissemination.

ROLE OF RAL GTPASES IN GLIOBLASTOMA GROWTH AND DISSEMINATION

In the first part of this work, we have established that Ral GTPases are downstream effectors of cytoplasmic Ccnd1 in the regulation of GBM cell invasion. Because there is little information in the literature about the role of Ral GTPases in GBM, we studied this further. We have determined that primary GBM cells show an increment in Ral B expression and activity in comparison with low grade gliomas. In some samples, also Ral A level was increased. Increased expression and activation of Ral GTPases in tumor samples compared with normal tissues are observed in different cancer types (Yan and Theodorescu 2017). Frequently, both Ral GTPases are activated in tumors, although in specific lung and melanoma samples only increased Ral A activity is detected (Guin et al. 2013; Zipfel et al. 2010). Ral GTPases together with PI3K and Raf kinases are the three main effectors downstream Ras signaling. However, it is unlikely that Ral activation is related to Ras status in GBM because Ras and Raf mutations are not frequent in GBM while PI3K pathway is often altered (Brennan et al. 2013), and because in other tumors (melanoma and bladder cancer) Ral GTPase activation is not correlated with Ras and Raf status (Saito et al. 2013; Zipfel et al. 2010).

Our data demonstrate that both Ral A and Ral B are required for GBM anchorage-dependent growth. The downregulation of only one of the Ral GTPases was sufficient to cause growth reduction of primary GBM cells, although these cells remained viable. In fact, the knockdown of both Ral GTPases at the same time produced a similar effect to knocking down only one. Note that the knock-out of either Ral A or Ral B does not affect growth of mouse embryonic fibroblasts (MEFs) (Peschard et al. 2012), and slightly reduces the growth of some cancer cells, such as bladder tumor cells, when growing in low serum conditions (Oxford et al. 2005). Contrary to GBM, in MEFs and bladder cancer cells, it is required the downregulation of both, Ral A and Ral B, activities to significantly reduce growth. Hence, growth of GBM cells is particularly sensitive to Ral availability.

In addition to the effect on anchorage-dependent growth, we have shown that the knockdown of either Ral A or Ral B is enough to impair anchorage-independent and tumorsphere growth, as well as the invasive capacity of primary GBM cells. This is in agreement with previous studies that have described the involvement of Ral GTPases (mainly Ral A and to a lesser extent Ral B) in anchorage-independent and tumor stem cell growth in different tumors (Martin et al. 2011; Moghadam et al. 2017). Moreover, other authors (Song et al. 2015) have described that the

downregulation of Ral B decreases the migratory and invasive capacities of two GBM cell lines. Our results suggest that Ral A and Ral B have overlapping functions in the control of growth and invasion in GBM cells. Similarly, both Ral paralogs have overlapping effects in lung and melanoma cancer cells (Peschard et al. 2012). By contrast, other works have demonstrated that Ral A is mainly involved in the control of anchorage-independent growth while Ral B regulates survival and invasion (Chien and White 2003; Falsetti et al. 2007; Lim et al. 2006; Oxford et al. 2005). These differences in the functional specificity of Ral A and Ral B may be explained by the specific downstream effectors present in the different cancer cell types. For instance, Ral A requires association with their effectors Ral BP1 and Exo84 to induce anchorage-independent growth in colorectal cancer cells, whereas Ral B is associated with Ral BP1 and Sec5 to undertake the same function (Martin et al. 2011).

The elevated expression and activity of Ral B in primary GBM cells, and the fact that Ral B (also Ral A) activity is required for growth and invasion of these cells, suggest that inhibition of Ral activity may be a powerful therapeutic strategy. Consistent with this idea, we have shown that downregulation of Ral B augmented the sensitivity to TMZ of primary GBM cells. This is not surprising as Ral B activity regulates tumor cell survival. Ral B effector Sec5 recruits and activates the TBK1 kinase, restricting the apoptotic response and promoting survival of different human cell lines (Chien et al. 2006). However, we have shown that knockdown of Ral B (and to a lesser extent Ral A) in primary GBM cells does not affect cell viability but induces a senescence response, with reduced incorporation of BrdU and accumulation of the p21 and p27 cell cycle inhibitors. Similarly, Tecleab and co-workers (Tecleab, Zhang, and Sebti 2014) have described that the downregulation of Ral B does not induce apoptosis, but instead promotes growth arrest and accumulation of p53 and p21 in lung-cancer cell lines. These authors have shown that a reduction in Ral B levels leads to DNA-damage/ATM activation that in turns phosphorylates and stabilizes p53, which induces the expression of p21 and growth arrest. They propose that Ral B activity may be blocking the DNA damage response in cancer cells. In agreement with this, we have observed that primary GBM cells have high levels of DNA damage. Therefore, it is possible that Ral B, and to a lesser degree Ral A, may prevent the DNA damage response in primary GBM cells too.

Ral GTPases have multiple downstream effectors such as RBPL1 and different exocyst components. The involvement of these downstream effectors in senescence is unknown. Interestingly, GBM overexpress Ral BP1, and this overexpression is associated with higher tumor grade and poor survival (Wang, Wang, et al. 2013). Moreover, Ral BP1 knockdown supresses invasiveness, induces proliferation arrest, increases chemosensitivity to TMZ and enhances

autophagic flux in GBM cells (Wang, Qian, et al. 2013; Zhang et al. 2017). These effects are similar to those induced by Ral B-deficiency, and thus it suggests that Ral BP1 could be the downstream effector of Ral B in controlling a senescence response. However, this question remains open for future investigations.

In this work, we have demonstrated that Ral GTPases play an important role in tumorigenesis of human GBM. In primary GBM cells, Ral GTPases are involved in the control of adherent and non-adherent cell growth processes, and the avoidance of senescence. We have also described that Ral GTPases are important for GBM invasion. Our data suggest that Ral GTPase inhibitors could be used as a new therapeutic strategy for GBM treatment. We have tried to analyze the efficiency of the new Ral-inhibitors BQU57 and RBC8 (Yan et al. 2014). Unfortunately, we have been unable to confirm the efficiency of these inhibitors in primary GBM cells because, even though we have used inhibitors from different sources and designs, the experiments did not produce repetitive results. This is likely due to the chemical instability of these molecules (D. Theodorescu, personal communication). Consistent with this, there are no other studies in the literature that have reported the use of these inhibitors. Regardless of this inconvenience, our results indicate that the inhibiton of Ral GTPases may be of great relevance in GBM treatment.

SIGNALING PATHWAYS ACTIVATED BY CITOPLASMIC CYCLIN D1

Kinases involved in cell signaling are the most intensively studied protein-targets in pharmacology research, as seen from the increasing number of kinase-targeting inhibitors in clinical trials. In this scenario, cyclin D1-associated activity is not considered relevant as a regulatory target of cell signaling. In contrast, Ccnd1 has always been placed as a final downstream effector in many cell signaling pathways. Thus, different signaling factors promote the expression, stabilization and activity of Ccnd1 (Musgrove 2006). However, preliminary results from this thesis make cytoplasmic Ccnd1 a possible regulator of cell signaling cascades.

Our analyses have shown that by expressing membrane-associated Ccnd1 (Ccnd1-CAAX) several signaling pathways could be altered. Among these, those related to the checkpoint protein kinase CHK2, the mitogen or stress-induced kinase MSK1, the cGMP-dependent protein kinase 2 KGP2, the Calcium/calmodulin-dependent protein kinase type IV CamK4 and the cAMP-dependent protein kinase PKA. Interestingly, three of these pathways MSK1, CamK4 and PKA share the downstream target CREB1 that is phosphorylated at serine 133. Importantly, we have also determined that GBM cells lacking Ccnd1 present lower levels of phosphorylated CREB.

In addition to phosphoCREB1, among the 30 phosphopeptides enriched in the Ccnd1-CAAX sample, there also appear KAP2 and KAP3 proteins, components of the PKA regulatory pathway. PKA regulates Ccnd1 transcriptionally (Lamb et al. 2000) and also phosphorylates Ccnd1 in the cyclin box (Lamb et al. 2000; Sewing and Mueller 1994). However, no data exist in the other direction, a possible regulation of PKA activity by Ccnd1. KAP2 and KAP3 are the regulatory subunits of the PKA enzyme complex (Ohno et al. 1994). Classical activation of PKA involves binding of cAMP to the regulatory subunits of the complex, which in turn promotes auto-phosphorylation of these subunits. This modification induces a conformational reorganization releasing the catalytic subunits of the complex in their active form.

We have observed that knocking down Ccnd1 in GBM cells produced diminished levels of phosphorylated Src. This tyrosine kinase participates in the regulation of several cellular processes such as cell adhesion (Mitra and Schlaepfer 2006). Cell adhesion to the extracellular matrix, via transmembrane integrin αβ heterodimers, leads to integrin activation and the recruitment of the focal adhesion complex. Interestingly, Src, Pxn and FAK are components of this complex that regulates the activity of different small GTPases such as Rac1. Previously, our group has demonstrated that Ccnd1 promotes cell motility by phosphorylating paxillin, which

leads to FAK phosphorylation and to Rac1 activation (**Figure 33**). Src forms a complex with FAK that could operate through AKT or vimentin and promote the activation of Rac1, consequently raising the migration and invasion of the cells. Thus, our data are consistent with the possibility that Ccnd1 could modulate Src activity.

In summary, we have obtained some evidences that cytoplasmic Ccnd1 may have a role in signaling transduction pathways, opening a whole new perspective in the functionality of cytoplasmic cyclin D1 that needs to be researched in the future.

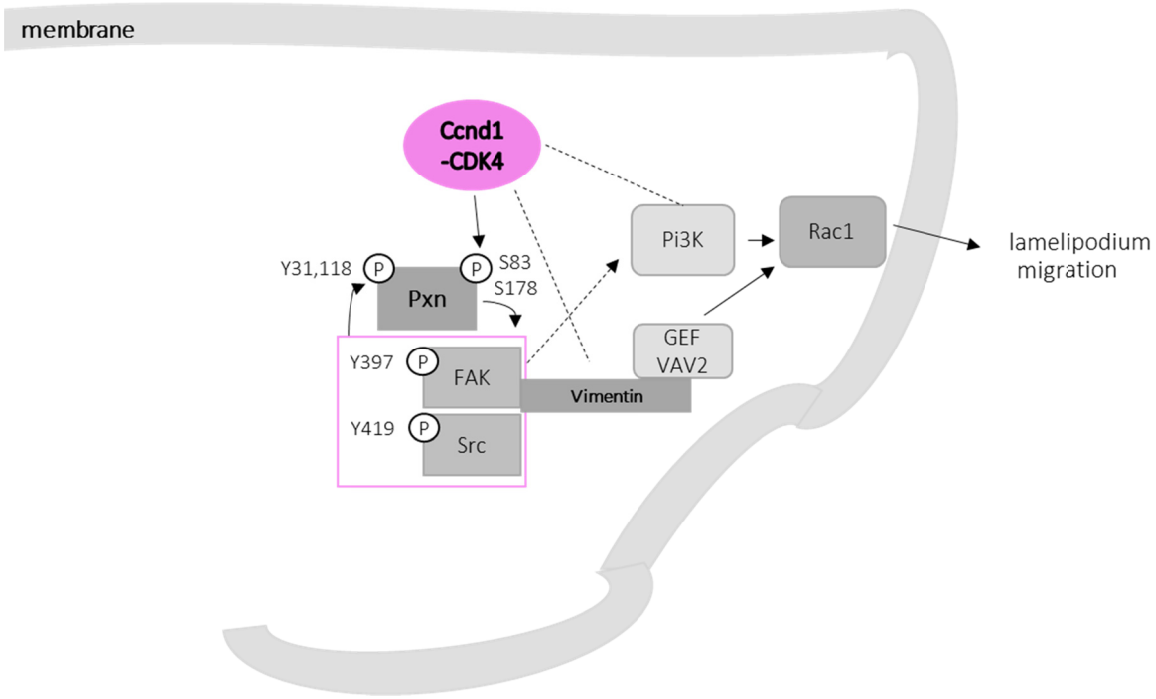

Figure 33. *Cyclin D1-CDK4/Pxn/FAK/Src/vimentin cell signaling hypothesized diagram.*

CONCLUSIONS

First. Besides its nuclear functions, Ccnd1 performs cytoplasmic functions in GBM cells controlling GBM dissemination.

Second. Ccnd1 regulates the efficiency of cell invasion and adhesion of primary GBM cells independently of RB1.

Third. Ccnd1 promotes the invasive capacity of human GBM cells through the paxillin-FAK-Rac1 and Ral GTPase pathways.

Forth. Ccnd1-CDK4 complex could be a new target for GBM dissemination inhibition.

Fifth. The Ral B GTPase is upregulated in primary GBM cells.

Sixth. Ral GTPases promote cell growth and invasion in primary GBM cells and are required for the proliferation of GBM stem cells.

Seventh. Ral B and to a lesser extent Ral A activities have a role in avoiding senescence of primary GBM cells.

Eighth. Inhibition of Ral GTPases could be a treatment to impede GBM growth. MGMT status is not important for Ral GTPase inhibition of GBM growth.

Ninth. Cyclin D1 could modulate the activation of the transcriptional factor CREB1 through the regulation of PKA-dependent signaling.

Tenth. Signaling through the Ccnd1-Pxn-Rac1 pathway could be mediated by FAK-SRC complex.

REFERENCES

Adamson, Cory et al. 2009. "Glioblastoma Multiforme Oncogenomics and Signaling Pathways." *Clinical Medicine: Oncology* 3:39–52.

Alao, John P. 2007. "The Regulation of Cyclin D1 Degradation: Roles in Cancer Development and the Potential for Therapeutic Invention." *Molecular Cancer* 6.

Alao, JohnP et al. 2006. "The Cyclin D1 Proto-Oncogene Is Sequestered in the Cytoplasm of Mammalian Cancer Cell Lines." *Molecular Cancer* 5(1):7.

Arato-Ohshima, T. and H. Sawa. 1999. "Over-Expression of Cyclin D1 Induces Glioma Invasion by Increasing Matrix Metalloproteinase Activity and Cell Motility." *International Journal of Cancer* 83(3):387–92.

Arscott, W. Tris et al. 2013. "Ionizing Radiation and Glioblastoma Exosomes: Implications in Tumor Biology and Cell Migration." *Translational Oncology* 6(6):638–48.

Ausubel, F. M. 1987. *Current Protocols in Molecular Biology*. Vol. 1.

Bartkova, J., J. Lukas, M. Strauss, and J. Bartek. 1995. "Cyclin D1 Oncoprotein Aberrantly Accumulates in Malignancies of Diverse Histogenesis." *Oncogene* 10(4):775–78.

Barton, Kelly L. et al. 2013. "PD-0332991, a CDK4/6 Inhibitor, Significantly Prolongs Survival in a Genetically Engineered Mouse Model of Brainstem Glioma" edited by M. M. Alonso. *PLoS ONE* 8(10):e77639.

Beier, Dagmar et al. 2007. "CD133+ and CD133- Glioblastoma-Derived Cancer Stem Cells Show Differential Growth Characteristics and Molecular Profiles." *Cancer Research* 67(9):4010–15.

Bendris, Nawal, Bénédicte Lemmers, and Jean Marie Blanchard. 2015. "Cell Cycle, Cytoskeleton Dynamics and beyond: The Many Functions of Cyclins and CDK Inhibitors." *Cell Cycle* 14(12):1786–98.

Benzeno, S. et al. 2006. "Identification of Mutations That Disrupt Phosphorylation-Dependent Nuclear Export of Cyclin D1." *Oncogene* 25(47):6291–6303.

Beroukhim, Rameen et al. 2010. "The Landscape of Somatic Copy-Number Alteration across Human Cancers." *Nature* 463(7283):899–905.

Besson, Arnaud, Mark Gurian-West, Anja Schmidt, Alan Hall, and James M. Roberts. 2004. "P27Kip1 Modulates Cell Migration through the Regulation of RhoA Activation." *Genes & Development* 18(8):862–76.

Bienvenu, Frédéric et al. 2010. "Transcriptional Role of Cyclin D1 in Development Revealed by a Genetic-Proteomic Screen." *Nature* 463(7279):374–78.

Blumenthal, Deborah T. et al. 2016. "Clinical Utility and Treatment Outcome of Comprehensive Genomic Profiling in High Grade Glioma Patients." *Journal of Neuro-Oncology* 130(1):211–19.

Bodemann, Brian O. and Michael A. White. 2008. "Ral GTPases and Cancer: Linchpin Support of the Tumorigenic Platform." *Nature Reviews Cancer* 8(2):133–40.

Body, Simon et al. 2017. "Cytoplasmic Cyclin D1 Controls the Migration and Invasiveness of Mantle Lymphoma Cells." *Scientific Reports* 7(1):13946.

Bollard, Julien et al. 2017. "Palbociclib (PD-0332991), a Selective CDK4/6 Inhibitor, Restricts Tumour Growth in Preclinical Models of Hepatocellular Carcinoma." *Gut* 66(7):1286–96.

Brennan, Cameron W. et al. 2013. "The Somatic Genomic Landscape of Glioblastoma." *Cell* 155(2):462–77.

de Bruyn, K. M. et al. 2000. "RalGEF2, a Pleckstrin Homology Domain Containing Guanine Nucleotide Exchange Factor for Ral." *The Journal of Biological Chemistry* 275(38):29761–66.

Camonis, Jacques H. and Michael A. White. 2005. "Ral GTPases: Corrupting the Exocyst in Cancer Cells." *Trends in Cell Biology* 15(6):327–32.

Casimiro, Mathew C., Marco Velasco-Velázquez, Charmina Aguirre-Alvarado, and Richard G. Pestell. 2014. "Overview of Cyclins D1 Function in Cancer and the CDK Inhibitor Landscape: Past and Present." *Expert Opinion on Investigational Drugs* 23(3):295–304.

Cen, Ling et al. 2012. "P16-Cdk4-Rb Axis Controls Sensitivity to a Cyclin-Dependent Kinase Inhibitor PD0332991 in Glioblastoma Xenograft Cells." *Neuro-Oncology* 14(7):870–81.

Ceriani, Michela et al. 2007. "Functional Analysis of RalGPS2, a Murine Guanine Nucleotide Exchange Factor for RalA GTPase." *Experimental Cell Research* 313(11):2293–2307.

Chakrabarty, A., L. R. Bridges, and S. Gray. 1996. "Cyclin D1 in Astrocytic Tumours: An Immunohistochemical Study." *Neuropathology and Applied Neurobiology* 22(4):311–16.

Chen, Jian, Yanjiao Li, et al. 2012. "A Restricted Cell Population Propagates Glioblastoma Growth after Chemotherapy." *Nature*.

Chen, Jian, Renée M. McKay, and Luis F. Parada. 2012. "Malignant Glioma: Lessons from Genomics, Mouse Models, and Stem Cells." *Cell* 149(1):36–47.

Chen, Xiao-Wei, Mayumi Inoue, Shu C. Hsu, and Alan R. Saltiel. 2006. "RalA-Exocyst-Dependent Recycling Endosome Trafficking Is Required for the Completion of Cytokinesis." *The Journal of Biological Chemistry* 281(50):38609–16.

Cheung, T. H. et al. 2001. "Alteration of Cyclin D1 and CDK4 Gene in Carcinoma of Uterine Cervix." *Cancer Letters* 166(2):199–206.

Chien, Yuchen et al. 2006. "RalB GTPase-Mediated Activation of the IκB Family Kinase TBK1 Couples Innate Immune Signaling to Tumor Cell Survival." *Cell*.

Chien, Yuchen and Michael A. White. 2003. "RAL GTPases Are Linchpin Modulators of Human Tumour-Cell Proliferation and Survival." *EMBO Reports* 4(8):800–806.

Clark, Amy S. et al. 2016. "Palbociclib (PD0332991)-a Selective and Potent Cyclin-Dependent Kinase Inhibitor: A Review of Pharmacodynamics and Clinical Development." *JAMA Oncology* 2(2):253–60.

Cuddapah, Vishnu Anand, Stefanie Robel, Stacey Watkins, and Harald Sontheimer. 2014. "A Neurocentric Perspective on Glioma Invasion." *Nature Reviews Neuroscience* 15(7):455–65.

Deakin, N. O. and C. E. Turner. 2008. "Paxillin Comes of Age." *Journal of Cell Science* 121(15):2435–44.

Delgado-López, P. D., E. M. Corrales-García, J. Martino, E. Lastra-Aras, and M. T. Dueñas-Polo. 2017. "Diffuse Low-Grade Glioma: A Review on the New Molecular Classification, Natural History and Current Management Strategies." *Clinical and Translational Oncology* 19(8):931–44.

Dickson, C. et al. 1995. "Amplification of Chromosome Band 11q13 and a Role for Cyclin D1 in Human Breast Cancer." *Cancer Letters* 90(1):43–50.

Dickson, M. A. 2014. "Molecular Pathways: CDK4 Inhibitors for Cancer Therapy." *Clinical Cancer Research* 20(13):3379–83.

Dickson, Mark A. et al. 2013. "Phase II Trial of the CDK4 Inhibitor PD0332991 in Patients with Advanced CDK4-Amplified Well-Differentiated or Dedifferentiated Liposarcoma." *Journal of Clinical Oncology : Official Journal of the American Society of Clinical Oncology* 31(16):2024–28.

Diehl, J. Alan, Frederique Zindy, and Charles J. Sherr. 1997. "Inhibition of Cyclin D1 Phosphorylation on Threonine-286 Prevents Its Rapid Degradation via the Ubiquitin-Proteasome Pathway." *Genes and Development*.

Digman, Michelle A., Claire M. Brown, Alan R. Horwitz, William W. Mantulin, and Enrico Gratton. 2008. "Paxillin Dynamics Measured during Adhesion Assembly and Disassembly by Correlation Spectroscopy." *Biophysical Journal* 94(7):2819–31.

Drobnjak, M., I. Osman, H. I. Scher, M. Fazzari, and C. Cordon-Cardo. 2000. "Overexpression of Cyclin D1 Is Associated with Metastatic Prostate Cancer to Bone." *Clinical Cancer Research : An Official Journal of the American Association for Cancer Research* 6(5):1891–95.

de Dueñas, E. Martínez et al. 2018. "Preclinical and Clinical Development of Palbociclib and Future Perspectives." *Clinical and Translational Oncology*, 1–9.

Falsetti, S. C. et al. 2007. "Geranylgeranyltransferase I Inhibitors Target RalB To Inhibit Anchorage-Dependent Growth and Induce Apoptosis and RalA To Inhibit Anchorage-Independent Growth." *Molecular and Cellular Biology*.

Feig, Larry A., Takeshi Urano, and Sharon Cantor. 1996. "Evidence for a Ras/Ral Signaling Cascade." *Trends in Biochemical Sciences* 21(11):438–41.

Fernández-Hernández, Rita et al. 2013. "Cyclin D1 Localizes in the Cytoplasm of Keratinocytes during Skin Differentiation and Regulates Cell-Matrix Adhesion." *Cell Cycle (Georgetown, Tex.)* 12(15):2510–17.

Fernández, R. M. H., M. Ruiz-Miró, X. Dolcet, M. Aldea, and E. Garí. 2011. "Cyclin D1 Interacts and Collaborates with Ral GTPases Enhancing Cell Detachment and Motility." *Oncogene* 30(16):1936–46.

Finn, R. S. and D. J. Slamon. 2015. “Targeting CDK 4-6 Pathway.” *Breast*.

Finn, Richard S. et al. 2016. “Palbociclib and Letrozole in Advanced Breast Cancer.” *New England Journal of Medicine* 375(20):1925–36.

Finn, Richard S. et al. 2015. “The Cyclin-Dependent Kinase 4/6 Inhibitor Palbociclib in Combination with Letrozole versus Letrozole Alone as First-Line Treatment of Oestrogen Receptor-Positive, HER2-Negative, Advanced Breast Cancer (PALOMA-1/TRIO-18): A Randomised Phase 2 Study.” *The Lancet. Oncology* 16(1):25–35.

Frisch, S. M., K. Vuori, E. Ruoslahti, and P. Y. Chan-Hui. 1996. “Control of Adhesion-Dependent Cell Survival by Focal Adhesion Kinase.” *The Journal of Cell Biology* 134(3):793–99.

Fry, David W. et al. 2004. “Specific Inhibition of Cyclin-Dependent Kinase 4/6 by PD 0332991 and Associated Antitumor Activity in Human Tumor Xenografts.” *Molecular Cancer Therapeutics* 3(11):1427–38.

Furnari, Frank B. et al. 2007. “Malignant Astrocytic Glioma: Genetics, Biology, and Paths to Treatment.” *Genes and Development* 21(21):2683–2710.

Fusté, Noel P. et al. 2016. “Characterization of Cytoplasmic Cyclin D1 as a Marker of Invasiveness in Cancer.” *Oncotarget* 7(19):26979–91.

Fusté, Noel P. et al. 2016. “Cytoplasmic Cyclin D1 Regulates Cell Invasion and Metastasis through the Phosphorylation of Paxillin.” *Nature Communications* 7.

Gentry, Leanna R., Timothy D. Martin, David J. Reiner, and Channing J. Der. 2014. “Ral Small GTPase Signaling and Oncogenesis: More than Just 15minutes of Fame.” *Biochimica et Biophysica Acta (BBA) - Molecular Cell Research* 1843(12):2976–88.

Gilbertson, Richard J. and Jeremy N. Rich. 2007. “Making a Tumour’s Bed: Glioblastoma Stem Cells and the Vascular Niche.” *Nature Reviews Cancer* 7(10):733–36.

Guin, Sunny et al. 2013. “Contributions of KRAS and RAL in Non-Small-Cell Lung Cancer Growth and Progression.” *Journal of Thoracic Oncology*.

Guin, Sunny and Dan Theodorescu. 2015. “The RAS-RAL Axis in Cancer: Evidence for Mutation-Specific Selectivity in Non-Small Cell Lung Cancer.” *Acta Pharmacologica Sinica* 36(3):291–97.

Győrffy, Balázs et al. 2015. “Effects of RAL Signal Transduction in KRAS- and BRAF-Mutated Cells and Prognostic Potential of the RAL Signature in Colorectal Cancer.” *Oncotarget* 6(15):13334–46.

Hagel, Margit et al. 2002. “The Adaptor Protein Paxillin Is Essential for Normal Development in the Mouse and Is a Critical Transducer of Fibronectin Signaling.” *Molecular and Cellular Biology* 22(3):901–15.

Hanahan, Douglas and Robert A. Weinberg. 2011. “Hallmarks of Cancer: The next Generation.” *Cell* 144(5):646–74.

Henry, D. O. et al. 2000. “Ral GTPases Contribute to Regulation of Cyclin D1 through Activation of NF-KappaB.” *Molecular and Cellular Biology* 20(21):8084–92.

Hofer, F., S. Fields, C. Schneider, and G. S. Martin. 1994. “Activated Ras Interacts with the Ral Guanine Nucleotide Dissociation Stimulator.” *Proceedings of the National Academy of Sciences of the United States of America* 91(23):11089–93.

Holland, Eric C. 2001. “Gliomagenesis: Genetic Alterations and Mouse Models.” *Nature Reviews Genetics* 2(2):120–29.

Hoppe, Adam D. and Joel A. Swanson. 2004. “Cdc42, Rac1, and Rac2 Display Distinct Patterns of Activation during Phagocytosis.” *Molecular Biology of the Cell* 15(8):3509–19.

Huang, Zhi, Da-Peng Yan, and Bao-Xue Ge. 2008. “JNK Regulates Cell Migration through Promotion of Tyrosine Phosphorylation of Paxillin.” *Cellular Signalling* 20(11):2002–12.

Hynes, Richard O. 2002. “Integrins: Bidirectional, Allosteric Signaling Machines.” *Cell* 110(6):673–87.

Ignatova, Tatyana N. et al. 2002. “Human Cortical Glial Tumors Contain Neural Stem-like Cells Expressing Astroglial and Neuronal Markers in Vitro.” *GLIA*.

Ishibe, Shuta, Dominique Joly, Zhen-Xiang Liu, and Lloyd G. Cantley. 2004. “Paxillin Serves as an ERK-Regulated Scaffold for Coordinating FAK and Rac Activation in Epithelial Morphogenesis.” *Molecular Cell* 16(2):257–67.

Jaraíz-Rodríguez, Myriam et al. 2017. “A Short Region of Connexin43 Reduces Human Glioma Stem Cell Migration, Invasion, and Survival through Src, PTEN, and FAK.” *Stem Cell Reports* 9(2):451–63.

Jiang, W. et al. 1992. “Amplification and Expression of the Human Cyclin D Gene in Esophageal Cancer.” *Cancer Research* 52(10):2980–83.

Jones, G., J. Machado, and A. Merlo. 2001. “Loss of Focal Adhesion Kinase (FAK) Inhibits Epidermal Growth Factor Receptor-Dependent Migration and Induces Aggregation of Nh(2)-Terminal FAK in the Nuclei of Apoptotic Glioblastoma Cells.” *Cancer Research* 61(13):4978–81.

Kashatus, David F. 2013. “Ral GTPases in Tumorigenesis: Emerging from the Shadows.” *Experimental Cell Research* 319(15):2337–42.

Kato, J., H. Matsushime, S. W. Hiebert, M. E. Ewen, and C. J. Sherr. 1993. “Direct Binding of Cyclin D to the Retinoblastoma Gene Product (PRb) and PRb Phosphorylation by the Cyclin D-Dependent Kinase CDK4.” *Genes and Development* 7(3):331–42.

Kato, Shumei et al. 2015. “Cyclin-Dependent Kinase Pathway Aberrations in Diverse Malignancies: Clinical and Molecular Characteristics.” *Cell Cycle* 14(8):1252–59.

Khatib, Z. A. et al. 1993. “Coamplification of the CDK4 Gene with MDM2 and GLI in Human Sarcomas.” *Cancer Research* 53(22):5535–41.

Kikuchi, A., S. D. Demo, Z. H. Ye, Y. W. Chen, and L. T. Williams. 1994. “RalGDS Family Members Interact with the Effector Loop of Ras P21.” *Molecular and Cellular Biology* 14(11):7483–91.

Kleihues, P. and H. Ohgaki. 1999. “Primary and Secondary Glioblastomas: From Concept to Clinical Diagnosis.” *Neuro-Oncology* 1(1):44–51.

Kleihues, Paul, Peter C. Burger, and Bernd W. Scheithauer. 1993. “The New WHO Classification of Brain Tumours.” Pp. 255–68 in *Brain Pathology*. Vol. 3.

Knudsen, K. E., J. Alan Diehl, C. A. Haiman, and E. S. Knudsen. 2006. “Cyclin D1: Polymorphism, Aberrant Splicing and Cancer Risk.” *Oncogene* 25(11):1620–28.

von Kobbe, Cayetano. 2018. “Cellular Senescence: A View throughout Organismal Life.” *Cellular and Molecular Life Sciences*.

Kozar, Katarzyna et al. 2004. “Mouse Development and Cell Proliferation in the Absence of D-Cyclins Activate, and Provide Substrate Specificity for Their Cata- Lytic Partners, CDKs. These Cyclin-CDK Complexes Phosphorylate Critical Cellular Substrates, Thereby Allowing Cell Cycle Progr.” *Cell* 118:477–91.

Kumar, Abbas, Fausto, Aster. 2010. *Robbins and Cotran Pathologic Basis of Disease*.

Kwiatkowska, Aneta et al. 2012. “The Small GTPase RhoG Mediates Glioblastoma Cell Invasion.” *Molecular Cancer* 11(1):65.

Lamb, J., M. H. Ladha, C. McMahon, R. L. Sutherland, and M. E. Ewen. 2000. “Regulation of the Functional Interaction between Cyclin D1 and the Estrogen Receptor.” *Mol Cell Biol*.

Lee, Bo Yun et al. 2006. “Senescence-Associated β-Galactosidase Is Lysosomal β-Galactosidase.” *Aging Cell*.

Leonard, J. P. et al. 2012. “Selective CDK4/6 Inhibition with Tumor Responses by PD0332991 in Patients with Mantle Cell Lymphoma.” *Blood* 119(20):4597–4607.

Li, Wusheng, Kai Li, Li Zhao, and Huawei Zou. 2014. “Bioinformatics Analysis Reveals Disturbance Mechanism of MAPK Signaling Pathway and Cell Cycle in Glioblastoma Multiforme.” *Gene* 547(2):346–50.

Li, Xiao-Yan et al. 2011. “Snail1 Controls Epithelial-Mesenchymal Lineage Commitment in Focal Adhesion Kinase-Null Embryonic Cells.” *The Journal of Cell Biology* 195(5):729–38.

Li, Zhiping, Xuanmao Jiao, et al. 2006. “Cyclin D1 Induction of Cellular Migration Requires P27(KIP1).” *Cancer Research* 66(20):9986–94.

Li, Zhiping, Chenguang Wang, et al. 2006. “Cyclin D1 Regulates Cellular Migration through the Inhibition of Thrombospondin 1 and ROCK Signaling.” *MOLECULAR AND CELLULAR BIOLOGY* 26(11):4240–56.

Li, Zhiping, Chenguang Wang, George Prendergast, and Richard G. Pestell. 2014. “Cyclin D1 Functions in Cell Migration.” *Cell Cycle* 5(21):2440–42.

Liang, Dong et al. 2015. “Elevated Expression of UHRF1 Predicts Unfavorable Prognosis for Patients with Hepatocellular Carcinoma.” *International Journal of Clinical and Experimental Pathology* 8(8):9416–21.

Lim, Kian-Huat et al. 2005. “Activation of RalA Is Critical for Ras-Induced Tumorigenesis of Human Cells.” *Cancer Cell* 7(6):533–45.

Lim, Kian-Huat et al. 2006. “Divergent Roles for RalA and RalB in Malignant Growth of Human Pancreatic Carcinoma Cells.” *Current Biology* 16(24):2385–94.

Louis, David N. et al. 2007. “The 2007 WHO Classification of Tumours of the Central Nervous System.” *Acta Neuropathologica* 114(2):97–109.

Malumbres, Marcos. 2014. “Cyclin-Dependent Kinases.” *Genome Biology* 15(6):1–10.

Marampon, Francesco et al. 2008. “Nerve Growth Factor Regulation of Cyclin D1 in PC12 Cells through a P21RAS Extracellular Signal-Regulated Kinase Pathway Requires Cooperative Interactions between Sp1 and Nuclear Factor-KappaB.” *Molecular Biology of the Cell* 19(6):2566–78.

Martin, Timothy D., Jonathan C. Samuel, Elizabeth D. Routh, Channing J. Der, and Jen Jen Yeh. 2011. “Activation and Involvement of Ral GTPases in Colorectal Cancer.” *Cancer Research*.

Martínez-Sáez, Elena et al. 2016. “PeIF4E as an Independent Prognostic Factor and a Potential Therapeutic Target in Diffuse Infiltrating Astrocytomas.” *Cancer Medicine* 5(9):2501–12.

McLendon, Roger et al. 2008. “Comprehensive Genomic Characterization Defines Human Glioblastoma Genes and Core Pathways.” *Nature* 455(7216):1061–68.

Meng, Hui et al. 2011. “PACSIN 2 Represses Cellular Migration through Direct Association with Cyclin D1 but Not Its Alternate Splice Form Cyclin D1b.” *Cell Cycle* 10(1):73–81.

Michaud, Karine et al. 2010. “Pharmacologic Inhibition of Cyclin-Dependent Kinases 4 and 6 Arrests the Growth of Glioblastoma Multiforme Intracranial Xenografts.” *Cancer Research* 70(8):3228–38.

Mitra, Satyajit K. and David D. Schlaepfer. 2006. “Integrin-Regulated FAK-Src Signaling in Normal and Cancer Cells.” *Current Opinion in Cell Biology*.

Moghadam, Adel Rezaei et al. 2017. “Ral Signaling Pathway in Health and Cancer.” *Cancer Medicine* 6(12):2998–3013.

Moreno-Bueno, Gema et al. 2003. “Cyclin D1 Gene (CCND1) Mutations in Endometrial Cancer.” *Oncogene* 22(38):6115–18.

Morokoff, Andrew, Wayne Ng, Andrew Gogos, and Andrew Kaye. 2015. “Molecular Subtypes, Stem Cells and Heterogeneity: Implications for Personalised Therapy in Glioma.” *Journal of Clinical Neuroscience* 22(8):1219–26.

Motokura, Toru et al. 1991. “A Novel Cyclin Encoded by a Bcl1-Linked Candidate Oncogene.” *Nature* 350(6318):512–15.

Musgrove, Elizabeth A. 2006. “Cyclins: Roles in Mitogenic Signaling and Oncogenic Transformation.” *Growth Factors*.

Musgrove, Elizabeth A., C. Elizabeth Caldon, Jane Barraclough, Andrew Stone, and Robert L. Sutherland. 2011. “Cyclin D as a Therapeutic Target in Cancer.” *Nature Reviews Cancer* 11(8):558–72.

Naidu, Rakesh, Norhanom Abdul Wahab, Man Mohan Yadav, and Methil Kannan Kutty. 2002. “Expression and Amplification of Cyclin D1 in Primary Breast Carcinomas: Relationship with Histopathological Types and Clinico-Pathological Parameters.” *Oncology Reports* 9(2):409–16.

Narasimha, Anil M. et al. 2014. “Cyclin D Activates the Rb Tumor Suppressor by Mono-Phosphorylation.” *ELife*.

Neumeister, Peter et al. 2003. “Cyclin D1 Governs Adhesion and Motility of Macrophages □ V.” *Molecular Biology of the Cell* 14.

Nomura, Naoko, Motohiro Nomura, Nobuhisa Mizuki, and Jun-Ichiro Hamada. 2008. “Rac1 Mediates Phorbol 12-Myristate 13-Acetate-Induced Migration of Glioblastoma Cells via Paxillin.” *Oncology Reports* 20(4):705–11.

Ohno, K., T. Kitahara, N. Takeda, T. Kubo, and H. Kiyama. 1994. “Gene Regulation of Cyclic Amp-Dependent Protein Kinase Subunits (Cα,β; RIα, β and RIIα,β) in Rat Facial Motoneurons after Nerve Transection.” *Neuroscience*.

Ostrom, Quinn T., Haley Gittleman, Lindsay Stetson, Selene M. Virk, and Jill S. Barnholtz-Sloan. 2015. “Epidemiology of Gliomas.” *Cancer Treatment and Research* 163:1–14.

Oxford, Gary et al. 2005. “RalA and RalB: Antagonistic Relatives in Cancer Cell Migration.” *Cancer Research*.

Ozawa, Tatsuya et al. 2014. “Most Human Non-GCIMP Glioblastoma Subtypes Evolve from a Common Proneural-like Precursor Glioma.” *Cancer Cell* 26(2):288–300.

Parylo, S., A. Vennepureddy, V. Dhar, P. Patibandla, and A. Sokoloff. 2018. “Role of Cyclin-Dependent Kinase 4/6 Inhibitors in the Current and Future Eras of Cancer Treatment.” *Journal of Oncology Pharmacy Practice* 107815521877090.

Paw, Ivy, Richard C. Carpenter, Kounosuke Watabe, Waldemar Debinski, and Hui Wen Lo. 2015. "Mechanisms Regulating Glioma Invasion." *Cancer Letters* 362(1):1–7.

Pedraza, Neus, Tània Cemeli, Ma Ventura Monserrat, Eloi Garí, and Francisco Ferrezuelo. 2017. "Regulation of Small GTPase Activity by G1 Cyclins." *Small GTPases* 1–7.

Peschard, Pascal et al. 2012. "Genetic Deletion of RALA and RALB Small GTPases Reveals Redundant Functions in Development and Tumorigenesis." *Current Biology : CB* 22(21):2063–68.

Pestell, Richard G. 2013. "New Roles of Cyclin D1." *The American Journal of Pathology* 183(1):3–9.

Peterson, S. N. et al. 1996. "Identification of a Novel RalGDS-Related Protein as a Candidate Effector for Ras and Rap1." *The Journal of Biological Chemistry* 271(47):29903–8.

Qie, Shuo and J. Alan Diehl. 2016. "Cyclin D1, Cancer Progression, and Opportunities in Cancer Treatment." *Journal of Molecular Medicine* 94(12):1313–26.

Raub, T. J. et al. 2015. "Brain Exposure of Two Selective Dual CDK4 and CDK6 Inhibitors and the Antitumor Activity of CDK4 and CDK6 Inhibition in Combination with Temozolomide in an Intracranial Glioblastoma Xenograft." *Drug Metabolism and Disposition* 43(9):1360–71.

Ridley, A. J., H. F. Paterson, C. L. Johnston, D. Diekmann, and A. Hall. 1992. "The Small GTP-Binding Protein Rac Regulates Growth Factor-Induced Membrane Ruffling." *Cell* 70(3):401–10.

Riemenschneider, Markus J., Wolf Mueller, Rebecca A. Betensky, Gayatry Mohapatra, and David N. Louis. 2005. "In Situ Analysis of Integrin and Growth Factor Receptor Signaling Pathways in Human Glioblastomas Suggests Overlapping Relationships with Focal Adhesion Kinase Activation." *The American Journal of Pathology* 167(5):1379–87.

Rosse, C. et al. 2006. "RalB Mobilizes the Exocyst To Drive Cell Migration." *Molecular and Cellular Biology* 26(2):727–34.

Saito, R. et al. 2013. "Downregulation of Ral GTPase-Activating Protein Promotes Tumor Invasion and Metastasis of Bladder Cancer." *Oncogene*.

Salhia, Bodour et al. 2005. "Inhibition of Rho-Kinase Affects Astrocytoma Morphology, Motility, and Invasion through Activation of Rac1." *Cancer Research* 65(19):8792–8800.

Sanai, Nader, Arturo Alvarez-Buylla, and Mitchel S. Berger. 2005. "Neural Stem Cells and the Origin of Gliomas." *The New England Journal of Medicine* 353(8):811–22.

Sanidas, Ioannis et al. 2019. "A Code of Mono-Phosphorylation Modulates the Function of RB." *Molecular Cell*.

Scherer, H. J. 1938. "Structural Development in Gliomas." *The American Journal of Cancer* 34(3):333–51.

Schröder, Lisette B. W. and Kerrie L. McDonald. 2015. "CDK4/6 Inhibitor PD0332991 in Glioblastoma Treatment: Does It Have a Future?" *Frontiers in Oncology* 5:259.

Sewing, A. and R. Mueller. 1994. "Protein Kinase A Phosphorylates Cyclin D1 at Three Distinct Sites within the Cyclin Box and at the C-Terminus." *Oncogene*.

Shao, H. and D. A. Andres. 2000. "A Novel RalGEF-like Protein, RGL3, as a Candidate Effector for Rit and Ras." *The Journal of Biological Chemistry* 275(35):26914–24.

Sheppard, K. E. and G. A. McArthur. 2013. "The Cell-Cycle Regulator CDK4: An Emerging Therapeutic Target in Melanoma." *Clinical Cancer Research* 19(19):5320–28.

Sherr, Charles J. 2016. "A New Cell-Cycle Target in Cancer — Inhibiting Cyclin D–Dependent Kinases 4 and 6." *New England Journal of Medicine* 375(20):1920–23.

Sherr, Charles J. and James M. Roberts. 1999. "CDK Inhibitors: Positive and Negative Regulators of G1-Phase Progression." *Genes and Development* 13(12):1501–12.

Shirakawa, Ryutaro et al. 2009. "Tuberous Sclerosis Tumor Suppressor Complex-like Complexes Act as GTPase-Activating Proteins for Ral GTPases." *The Journal of Biological Chemistry* 284(32):21580–88.

Shirakawa, Ryutaro and Hisanori Horiuchi. 2015. "Ral GTPases: Crucial Mediators of Exocytosis and Tumourigenesis." *Journal of Biochemistry* 157(5):285–99.

Sicinska, Ewa et al. 2003. "Requirement for Cyclin D3 in Lymphocyte Development and T Cell Leukemias." *Cancer Cell* 4(6):451–61.

Sicinski, Piotr et al. 1995. “Cyclin D1 Provides a Link between Development and Oncogenesis in the Retina and Breast.” *Cell* 82(4):621–30.

Sicinski, Piotr et al. 1996. “Cyclin D2 Is an FSH-Responsive Gene Involved in Gonadal Cell Proliferation and Oncogenesis.” *Nature* 384(6608):470–74.

Singh, Shalini and David J. Solecki. 2015. “Polarity Transitions during Neurogenesis and Neuronal Migration in the Developing Central Nervous System.” *Frontiers in Cellular Neuroscience*.

Singh, Sheila K. et al. 2003. “Identification of a Cancer Stem Cell in Human Brain Tumors.” *Cancer Research*.

Singh, Sheila K. et al. 2004. “Identification of Human Brain Tumour Initiating Cells.” *Nature*.

Song, X. et al. 2015. “Involvement of RalB in the Effect of Geranylgeranyltransferase I on Glioma Cell Migration and Invasion.” *Clinical and Translational Oncology* 17(6):477–85.

Spiczka, K. S. and C. Yeaman. 2008. “Ral-Regulated Interaction between Sec5 and Paxillin Targets Exocyst to Focal Complexes during Cell Migration.” *Journal of Cell Science* 121(17):2880–91.

Stiles, CD and DH Rowitch. 2008. “Glioma Stem Cells: A Midterm Exam.” *Neuron* 58(6):832–46.

Sumrejkanchanakij, Piyamas, Mimi Tamamori-Adachi, Yuko Matsunaga, Kazuhiro Eto, and Masa-Aki Ikeda. 2003. “Role of Cyclin D1 Cytoplasmic Sequestration in the Survival of Postmitotic Neurons.” *Oncogene* 22(54):8723–30.

Sun, Li-Hua et al. 2017. “Overexpression of Paxillin Correlates with Tumor Progression and Predicts Poor Survival in Glioblastoma.” *CNS Neuroscience & Therapeutics* 23(1):69–75.

Tecleab, Awet, Xiaolei Zhang, and Said M. Sebti. 2014. “Ral GTPase Down-Regulation Stabilizes and Reactivates P53 to Inhibit Malignant Transformation.” *Journal of Biological Chemistry*.

van Triest, Miranda and Johannes L. Bos. 2004. “Pull-down Assays for Guanoside 5’-Triphosphate-Bound Ras-like Guanosine 5’-Triphosphatases.” *Methods in Molecular Biology (Clifton, N.J.)* 250(1):97–102.

Tsubouchi, Asako et al. 2002. “Localized Suppression of RhoA Activity by Tyr31/118-Phosphorylated Paxillin in Cell Adhesion and Migration.” *The Journal of Cell Biology* 159(4):673–83.

Turner, C. E., J. R. Glenney, and K. Burridge. 1990. “Paxillin: A New Vinculin-Binding Protein Present in Focal Adhesions.” *The Journal of Cell Biology* 111(3):1059–68.

Veikkola, T., M. Karkkainen, L. Claesson-Welsh, and K. Alitalo. 2000. “Regulation of Angiogenesis via Vascular Endothelial Growth Factor Receptors.” *Cancer Research* 60(2):203–12.

Velasco-Velázquez, Marco A. et al. 2011. “Examining the Role of Cyclin D1 in Breast Cancer.” *Future Oncology* 7(6):753–65.

Verhaak, Roel G. W. et al. 2010. “Integrated Genomic Analysis Identifies Clinically Relevant Subtypes of Glioblastoma Characterized by Abnormalities in PDGFRA, IDH1, EGFR, and NF1.” *Cancer Cell* 17(1):98–110.

Wang, Junyu et al. 2012. “Knockdown of Cyclin D1 Inhibits Proliferation, Induces Apoptosis, and Attenuates the Invasive Capacity of Human Glioblastoma Cells.” *Journal of Neuro-Oncology* 106(3):473–84.

Wang, Qi, Jun Qian, et al. 2013. “Knockdown of RLIP76 Expression by RNA Interference Inhibits Invasion, Induces Cell Cycle Arrest, and Increases Chemosensitivity to the Anticancer Drug Temozolomide in Glioma Cells.” *Journal of Neuro-Oncology* 112(1):73–82.

Wang, Qi, Jun-Yu Wang, et al. 2013. “RLIP76 Is Overexpressed in Human Glioblastomas and Is Required for Proliferation, Tumorigenesis and Suppression of Apoptosis.” *Carcinogenesis* 34(4):916–26.

Webb, Donna J. et al. 2004. “FAK–Src Signalling through Paxillin, ERK and MLCK Regulates Adhesion Disassembly.” *Nature Cell Biology* 6(2):154–61.

Weiner, M. P. et al. 1994. “Site-Directed Mutagenesis of Double-Stranded DNA by the Polymerase Chain Reaction.” *Gene* 151(1–2):119–23.

Weller, Michael et al. 2015. “Glioma.” *Nature Reviews Disease Primers* 1.

Weller, Michael, Timothy Cloughesy, James R. Perry, and Wolfgang Wick. 2013. “Standards of Care for Treatment of Recurrent Glioblastoma-Are We There Yet?” *Neuro-Oncology* 15(1):4–27.

Wick, Wolfgang et al. 2012. “Temozolomide Chemotherapy Alone versus Radiotherapy Alone for Malignant Astrocytoma in the Elderly: The NOA-08 Randomised, Phase 3 Trial.” *The Lancet Oncology* 13(7):707–15.

Wiedemeyer, W. R. et al. 2010. "Pattern of Retinoblastoma Pathway Inactivation Dictates Response to CDK4/6 Inhibition in GBM." *Proceedings of the National Academy of Sciences* 107(25):11501–6.

Xing, Xiang-Bin et al. 2013. "The Prognostic Value of P16 Hypermethylation in Cancer: A Meta-Analysis" edited by J. Tost. *PLoS ONE* 8(6):e66587.

Xiong, Yue, Tim Connolly, Bruce Futcher, and David Beach. 1991. "Human D-Type Cyclin." *Cell* 65(4):691–99.

Yan, Chao et al. 2014. "Discovery and Characterization of Small Molecules That Target the GTPase Ral." *Nature* 515(7527):443–47.

Yan, Chao and Dan Theodorescu. 2017. "RAL GTPases: Biology and Potential as Therapeutic Targets in Cancer." *Pharmacological Reviews*.

Yoon, Hyunho, Joshua P. Dehart, James M. Murphy, and Ssang-Taek Steve Lim. 2015. "Understanding the Roles of FAK in Cancer: Inhibitors, Genetic Models, and New Insights." *The Journal of Histochemistry and Cytochemistry : Official Journal of the Histochemistry Society* 63(2):114–28.

Zhang, Chenran et al. 2017. "RLIP76 Depletion Enhances Autophagic Flux in U251 Cells." *Cellular and Molecular Neurobiology* 37(3):555–62.

Zhao, J. H., H. Reiske, and J. L. Guan. 1998. "Regulation of the Cell Cycle by Focal Adhesion Kinase." *The Journal of Cell Biology* 143(7):1997–2008.

Zhao, Jihe and Jun-Lin Guan. 2009. "Signal Transduction by Focal Adhesion Kinase in Cancer." *Cancer and Metastasis Reviews* 28(1–2):35–49.

Zheng, Hongwu et al. 2008. "P53 and Pten Control Neural and Glioma Stem/Progenitor Cell Renewal and Differentiation." *Nature* 455(7216):1129–33.

Zheng, Liduan et al. 2013. "MicroRNA-9 Suppresses the Proliferation, Invasion and Metastasis of Gastric Cancer Cells through Targeting Cyclin D1 and Ets1." edited by A. H. Corvalan. *PloS One* 8(1):e55719.

Zhong, Zhijiu et al. 2010. "Cyclin D1/Cyclin-Dependent Kinase 4 Interacts with Filamin A and Affects the Migration and Invasion Potential of Breast Cancer Cells." *Cancer Research* 70(5):2105–14.

Zhu, Yuan and Luis F. Parada. 2002. "The Molecular and Genetic Basis of Neurological Tumours." *Nature Reviews Cancer* 2(8):616–26.

Zipfel, P. A. et al. 2010. "Ral Activation Promotes Melanomagenesis." *Oncogene*.

Zong, Hui, Roel G. W. Verhaak, and Peter Canolk. 2012. "The Cellular Origin for Malignant Glioma and Prospects for Clinical Advancements." *Expert Review of Molecular Diagnostics* 12(4):383–94.

ANNEX

PUBLICATIONS

- Cytoplasmic cyclin D1 regulates cell invasion and metastasis through the phosphorylation of paxillin.

Fusté NP*, Fernández-Hernández R*, **Cemeli T**, Mirantes C, Pedraza N, Rafel M, Torres-Rosell J, Colomina N, Ferrezuelo F, Dolcet X, Garí E.

*Authors contributed equally to this work

Nat Commun. 2016 May 16;7:11581. doi: 10.1038/ncomms11581.

- Characterization of cytoplasmic cyclin D1 as a marker of invasiveness in cancer.

Fusté NP*, Castelblanco E*, Felip I*, Santacana M, Fernández-Hernández R, Gatius S, Pedraza N, Pallarés J, **Cemeli T**, Valls J, Tarres M, Ferrezuelo F, Dolcet X, Matias-Guiu X, Garí E.

*Authors contributed equally to this work

Oncotarget. 2016 May 10;7(19):26979-91. doi: 10.18632/oncotarget.8876.

- Regulation of small GTPase activity by G1 cyclins.

Pedraza N, **Cemeli T**, Monserrat MV, Garí E, Ferrezuelo F.

Small GTPases. 2019 Jan;10(1):47-53. doi: 10.1080/21541248.2016.1268665. Epub 2017 Jan 27. Review.

- Barley β-glucan accelerates wound healing by favoring migration versus proliferation of human dermal fibroblasts.

Fusté NP*, Guasch M*, Guillen P*, Anerillas C, **Cemeli T**, Pedraza N, Ferrezuelo F, Encinas M, Moralejo M, Garí E.

*Authors contributed equally to this work

Carbohydr Polym. 2019 Apr 15;210:389-398. doi: 10.1016/j.carbpol.2019.01.090. Epub 2019 Jan 28.

- Cytoplasmic cyclin D1 regulates glioblastoma dissemination.

Cemeli T, Guasch-Vallés M, Nàger M, Felip I, Cambray S, Santacana M, Gatius S, Pedraza N, Dolcet X, Ferrezuelo F, Schuhmacher AJ, Herreros J, Garí E.

J Pathol. 2019 Apr 7. doi: 10.1002/path.5277. [Epub ahead of print]